

South Dakota State University

# Open PRAIRIE: Open Public Research Access Institutional Repository and Information Exchange

---

Electronic Theses and Dissertations

---

2021

## Advanced Analytical Techniques for the Analysis of Therapeutics of Toxic Inhalation Agents and Pharmacokinetic Investigation

Subrata Bhadra

South Dakota State University, [subrata\\_bhadra@outlook.com](mailto:subrata_bhadra@outlook.com)

Follow this and additional works at: <https://openprairie.sdstate.edu/etd2>

 Part of the [Analytical Chemistry Commons](#)

---

### Recommended Citation

Bhadra, Subrata, "Advanced Analytical Techniques for the Analysis of Therapeutics of Toxic Inhalation Agents and Pharmacokinetic Investigation" (2021). *Electronic Theses and Dissertations*. 197.  
<https://openprairie.sdstate.edu/etd2/197>

This Dissertation - Open Access is brought to you for free and open access by Open PRAIRIE: Open Public Research Access Institutional Repository and Information Exchange. It has been accepted for inclusion in Electronic Theses and Dissertations by an authorized administrator of Open PRAIRIE: Open Public Research Access Institutional Repository and Information Exchange. For more information, please contact [michael.biondo@sdstate.edu](mailto:michael.biondo@sdstate.edu).

ADVANCED ANALYTICAL TECHNIQUES FOR THE ANALYSIS OF  
THERAPEUTICS OF TOXIC INHALATION AGENTS AND PHARMACOKINETIC  
INVESTIGATION

BY

SUBRATA BHADRA

A dissertation submitted in partial fulfillment of the requirements for the

Doctor of Philosophy

Major in Chemistry

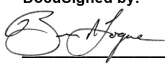
South Dakota State University

2021

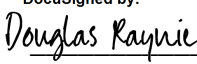
## DISSERTATION ACCEPTANCE PAGE

Subrata Bhadra

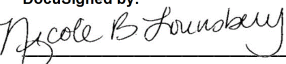
This dissertation is approved as a creditable and independent investigation by a candidate for the Doctor of Philosophy degree and is acceptable for meeting the dissertation requirements for this degree. Acceptance of this does not imply that the conclusions reached by the candidate are necessarily the conclusions of the major department.

DocuSigned by:  
  
13B40923B119476... 9/27/2021 | 07:21 PDT

Brian Logue  
Advisor Date

DocuSigned by:  
  
6515BC2773FA4A3... 9/27/2021 | 07:32 PDT

Douglas Raynie  
Department Head Date

DocuSigned by:  
  
E3BEAA596D57438... 9/28/2021 | 06:25 PDT

Nicole Lounsbery, PhD  
Director, Graduate School Date

This dissertation is dedicated to my loving parents, Sunil Kumar Bhadra and Hasi Rani Bhadra, younger brothers (Subir and Suman), and my life partner, Shuvra Chakraborty. I am always grateful for your encouragement, unconditional love, prayer, and continuous support. This PhD marathon would never have been completed without you all.

## ACKNOWLEDGEMENTS

I would like to express my heartfelt appreciation to my advisor, Dr. Brian A. Logue, for his timely assistance, guidance, encouragement, and constructive feedbacks throughout my journey at South Dakota State University. You are truly a great mentor! I am forever grateful to you for considering me as a member of your LARGE group, believing in me, and guiding me through the entire doctoral journey. My special thanks go to the LARGE research group, my advisory committee members, the Department of Chemistry and Biochemistry and all the faculty members and the staffs for their assistance and their active participation in shaping my success at SDSU. I am also grateful to Drs. Randy Jackson and Nesta Bortey-Sam for helping me to understand the sensor-related activities, Dr. Amanda Appel for guiding me during LC-MS/MS work, Dr. Erica Manandhar for sharing her experience about DMTS, and Drs. Frederick Ochieng and Obed Gyamfi for making my stay a memorable one at SDSU. I would also like to thank the collaborators, especially Drs. Gary A. Rockwood and Vikhyat Bebartha for sending the animal samples, and Dr. Gerry R. Boss for providing the aquohydroxocobinamide needed in this project. Lastly, my sincere gratitude goes to the funding agencies that have supported my research works and made the completion of my degree possible.

## TABLE OF CONTENTS

ABBREVIATIONS .....	ix
LIST OF FIGURES .....	xiii
LIST OF TABLES .....	xv
ABSTRACT.....	xvi
Chapter 1. Introduction .....	1
1.1. Overall Significance.....	1
1.2. Project Objectives .....	1
1.3. Toxic Inhalation Agents .....	2
1.4. Pathogenesis of TIAs .....	4
1.5. Exposure to CN, H <sub>2</sub> S, and MT.....	5
1.6. Hydrogen Cyanide.....	6
1.6.1. Overview .....	6
1.6.2. Sources and use of CN.....	6
1.6.3. Major CN exposure events .....	7
1.6.4. Current treatments and limitations .....	7
1.6.4.1. Sodium nitrite.....	8
1.6.4.2. Sodium thiosulfate .....	9
1.6.4.3. Hydroxocobalamin.....	9
1.7. Hydrogen Sulfide .....	10
1.7.1. Sources and Applications .....	10
1.7.2. Toxicity.....	10
1.7.3. Recent H <sub>2</sub> S exposure events .....	11
1.8. Methanethiol.....	11
1.8.1. Sources and Applications .....	11
1.8.2. Toxicity.....	12
1.9. Potential Antidotes Against CN, H <sub>2</sub> S and MT Poisoning.....	12
1.9.1. Dimethyl trisulfide.....	13
1.9.2. 3-Mercaptopyruvate.....	13
1.9.3 Sodium tetrathionate.....	14

1.9.4 Cobinamide.....	15
Chapter 2. Analysis of Potential Cyanide Antidote, Dimethyl Trisulfide, in Whole Blood by Dynamic Headspace Gas Chromatography-Mass Spectroscopy .....	17
2.1. Abstract .....	17
2.2. Introduction .....	18
2.3. Experimental .....	22
2.3.1. Materials .....	22
2.3.2. Biological samples.....	23
2.3.3. Preparation of DMTS standards and samples.....	24
2.3.4. DHS-GC-MS analysis of DMTS.....	25
2.3.5. Calibration, quantification, and limit of detection.....	26
2.3.6. Selectivity and stability .....	28
2.3.7. Matrix effect .....	30
2.4. Results and discussion.....	30
2.4.1. GC-MS analysis of DMTS .....	30
2.4.2. Dynamic range, limit of detection, and sensitivity.....	34
2.4.3. Accuracy and Precision .....	36
2.4.4. Matrix effect and storage stability .....	36
2.4.5. Pharmacokinetic study of DMTS-treated animals.....	38
2.5. Conclusions .....	41
2.6. Acknowledgement.....	41
Chapter 3: Analysis of the Soil Fumigant, Dimethyl Disulfide, in Swine Blood by Dynamic Headspace Gas Chromatography–Mass Spectroscopy .....	43
3.1. Abstract .....	43
3.2. Introduction .....	44
3.3. Experimental .....	48
3.3.1. Materials .....	49
3.3.2. Biological samples.....	50
3.3.3. Sample preparation for DHS-GC-MS analysis .....	51
3.3.4. DHS-GC-MS analysis .....	52

3.3.5. Calibration, quantification, and limit of detection.....	53
3.3.6. Accuracy and precision .....	54
3.3.7. Recovery and matrix effect.....	55
3.3.8. Selectivity and stability .....	56
3.4. Results and discussion.....	59
3.4.1. GC-MS analysis of DMDS.....	59
3.4.2. Dynamic range, limit of detection, and sensitivity .....	61
3.4.3. Accuracy and Precision .....	62
3.4.4. Matrix effect and recovery .....	63
3.4.5. DMDS storage stability .....	64
3.4.6. Analysis of DMDS in treated animals.....	68
3.5. Conclusions .....	70
3.6. Acknowledgement.....	70

Chapter 4: Analysis of aminotetrazole cobinamide, a next-generation antidote for cyanide, hydrogen sulfide and methanethiol poisoning, in swine plasma by liquid chromatography-tandem mass spectrometry .....	72
4.1. Abstract .....	72
4.2. Introduction .....	73
4.3. Experimental .....	76
4.3.1. Reagents and standards.....	76
4.3.2 Biological samples.....	77
4.3.3 Sample preparation for LC-MS/MS analysis .....	78
4.3.4. LC-MS/MS analysis .....	78
4.3.5. Calibration, quantification, and limit of detection.....	80
4.3.6. Accuracy and precision .....	81
4.3.7. Matrix effect and recovery .....	82
4.3.8. Stability.....	82
4.4. Results and Discussion.....	84
4.4.1. LC-MS/MS analysis of CbiAT.....	84
4.4.2. Dynamic range and limit of detection .....	86
4.4.3. Accuracy and Precision .....	87

4.4.4. Matrix effect, recovery, and storage stability .....	88
4.4.5. Method application and pharmacokinetics .....	89
4.5. Conclusions .....	92
4.6. Acknowledgments .....	93
Chapter 5. Conclusions, Broader Impacts, and Future Works.....	94
5.1. Conclusions .....	94
5.2. Broader impacts.....	94
5.3. Future work .....	95
References.....	96

## ABBREVIATIONS

3-MP: 3-mercaptopyruvate

3-MST: 3- mercaptopyruvate sulfurtransferase

AALAC: Association for the Assessment and Accreditation of Laboratory Animal Care

ACN: Acetonitrile

AHCbi: Aquohydroxocobinamide

APR: Antidotal potency ratio

A<sub>s</sub>: Asymmetry factor

ATM: 5-amino-1H-tetrazole monohydrate

ATM: 5-amino-1H-tetrazole

ATP: Adenosine triphosphate

AUC: Area under the curve

Cbi: Cobinamide

CbiAT: Aminotetrazole cobinamide

CE: Collision energy

CIS: Cooled injection system

CN: Cyanide

CWAs: Chemical warfare agents

CXP: Collision cell exit potential

Cyt c: Cytochrome c

DI: Deionized

DHS: Dynamic headspace

DMDS: Dimethyl disulfide

DMDS-d<sub>6</sub>: Dimethyl disulfide-d<sub>6</sub>

DMTS-d<sub>6</sub>: Dimethyl trisulfide-d<sub>6</sub>

DMTS: Dimethyl trisulfide

DP: Declustering potential

ECM: Extracellular matrix

EDTA: Ethylenediaminetetraacetic acid

EI: Electron impact

EPA: U.S. Environmental protection agency

ESI: Electron spray ionization

FDA: Food and Drug Administration

FID: Flame ionization detector

FT: Freeze thaw

GC: Gas chromatography

GoF: Goodness-of-fit

HCN: Hydrogen cyanide

HPLC: High performance liquid chromatography

HQC: High quality control

HS: Headspace

IACUC: Institutional animal care and use committee

IM: Intramuscular

IV: Intravenous

IS: Internal standard

LC: Liquid chromatography

LD: Lethal dose

LLOQ: Lower limit of quantification

LOD: Limit of detection

LQC: Low quality control

MAP: Mean arterial pressure

MITC: Methyl isothiocyanate

MPS: MultiPurpose sampler

MQC: Medium quality control

MRM: Multiple reaction monitoring

MS: Mass spectrometry

MS/MS: Tandem mass spectroscopy

MT: Methanethiol

N: Theoretical plate

NIH: U.S. National Institute of Health

NO: Nitric Oxide

PDMS: Polydimethylsiloxane

PRA: Percent residual accuracy

PTFE: Polytetrafluoroethylene

PTV: Programmable temperature vaporization

QC: Quality control

R<sub>s</sub>: Resolution

RSCs: Reduced sulfur compounds

RSD: Relative standard deviation

RT: Room temperature

SBSE: Stir bar sorptive extraction

SCN: Thiocyanate

SEM: Standard error of the mean

SIM: Selective ion monitoring

S/N: Signal-to-noise

SPME: Solid phase microextraction

TC: Tube conditioner

TDU: Thermal desorption unit

T<sub>f</sub>: Tailing factor

UHP: Ultra-high purity

ULOQ: Upper limit of quantification

USAMRICD: United States Army Medical Research Institute of Chemical Defense

VOCs: Volatile organic chemicals

UV: Ultraviolet

## LIST OF FIGURES

<b>Figure 1.1.</b> Aqueous solubility and particle size-based site of injury of TIAs in the respiratory tract [1]. .....	4
<b>Figure 1.2.</b> Reaction showing the conversion of CN to SCN and the formation of DMDS as a byproduct of this reaction. ....	13
<b>Figure 1.3.</b> Reaction showing the formation of nontoxic SCN from CN by the donation of singlet sulfur from the 3-MP molecule. ....	14
<b>Figure 1.4.</b> A two-step reaction of STT with 2 moles of CN.....	15
<b>Figure 1.5.</b> Reaction showing the interaction between CbiAT and CN, where the central cobalt ion detaches two aminotetrazole ligands, resulting in the formation of dicyanocobinamide, Cbi(CN) <sub>2</sub> .....	16
<b>Figure 2.1.</b> SIM mode GC-MS chromatograms of A) DMTS-spiked blood (0.5 μM) and non-spiked blood at m/z of 126 (quantification ion, upper trace) and m/z of 111 (qualification ion, lower trace), and B) IS-spiked blood (2 μM) and non-spiked blood at m/z of 132 (quantification ion, upper trace) and at m/z of 114 (qualification ion, lower trace). ....	32
<b>Figure 2.2.</b> Representative GC-MS chromatograms of the blood of DMTS-treated and untreated rats (m/z 126). ....	39
<b>Figure 2.3.</b> Blood concentration-time behavior of DMTS following IM administration of DMTS solution to rats. Each value is expressed as mean ± SEM (n = 5). ....	40
<b>Figure 3.1.</b> GC-MS chromatograms (in SIM mode) of A) DMDS-spiked (0.5 μM) and non-spiked blood at m/z of 94 (quantification ion, upper trace) and m/z of 79 (qualification ion, lower trace), and B) IS-spiked (2 μM) and non-spiked blood at m/z of 100 (quantification ion, upper trace) and at m/z of 82 (qualification ion, lower trace).....	61
<b>Figure 3.2.</b> Evaluation of DMDS stability studies (with IS correction) during storage at 4, -30 and -80 °C, over 90-day period tested. ....	67
<b>Figure 3.3.</b> Representative GC-MS chromatograms of DMDS (10.46 μM) in the blood of DMTS-treated and untreated swine (m/z of 94). ....	69

**Figure 4.1.** ESI(+) mass spectra of CbiAT with identification of the abundant ions. Insets: Structure of CbiAT with abundant fragments indicated. AT represents 5-amino-1H-tetrazole..... 85

**Figure 4.2.** LC-MS-MS chromatogram of CbiAT-spiked plasma (20  $\mu$ M) and non-spiked plasma. Transitions 1196.5/1028.6 and 1196.5/989.7 represent quantification and identification MRM, respectively. .... 86

**Figure 4.3.** Representative LC-MS/MS chromatogram at an MRM transition of 1196.5/1028.6 m/z (CbiAT quantification MRM transition) from the plasma of CbiAT-treated and untreated (prior to CbiAT treatment) swine. .... 91

**Figure 4.4.** Plasma concentration-time behavior of CbiAT following IM administration of CbiAT to swine. Error bars represent standard error of the mean (n=3). Inset: Representation of CbiAT elimination constant ( $K_E$ ) by log concentration-time graph. .... 92

## LIST OF TABLES

<b>Table 2.1:</b> Comparison of some important features of published and the current method for the analysis of DMTS from biological matrices. ....	33
<b>Table 2.2:</b> Curve equations and related values. ....	35
<b>Table 2.3:</b> Intra- and inter-assay accuracy and precision for analysis of DMTS in spiked rabbit blood. ....	36
<b>Table 2.4:</b> Slopes obtained from non-IS corrected and IS-corrected calibration curves of DMTS. ....	37
<b>Table 3.1:</b> List of approved DMDS containing soil fumigants. ....	47
<b>Table 3.2:</b> Freeze-thaw sample preparation. ....	57
<b>Table 3.3:</b> Calibration curve equations and goodness-of-fit analysis. ....	62
<b>Table 3.4:</b> Intra- and interassay accuracy and precision for analysis of DMDS in spiked swine blood. ....	63
<b>Table 4.1:</b> MRM transitions, and optimized declustering potentials (DPs), entrance potentials (EPs), collision energies (CEs), and collision cell exit potentials (CXPs) for CbiAT analysis by LC-MS/MS. ....	79
<b>Table 4.2:</b> Calibration curve equations prepared on three consecutive days with related goodness-of-fit parameters. ....	87
<b>Table 4.3:</b> The intra- and interassay accuracies and precisions for analysis of CbiAT from spiked swine plasma. ....	88

## ABSTRACT

ADVANCED ANALYTICAL TECHNIQUES FOR THE ANALYSIS OF  
THERAPEUTICS OF TOXIC INHALATION AGENTS AND PHARMACOKINETIC  
INVESTIGATION

SUBRATA BHADRA

2021

Toxic inhalation agents (TIAs), (i.e., cyanide (CN) and reduced sulfur compounds (RSCs)), including hydrogen sulfide (H<sub>2</sub>S) and methanethiol (MT)) are extremely poisonous upon exposure. Many TIAs act by inhibiting mitochondrial cytochrome c oxidase, resulting in cellular hypoxia, cytotoxic anoxia, apnea, respiratory failure, cardiovascular collapse, seizure and potentially death. CN is generated in structural fires and cigarette smoke as well as in mining, electroplating and polymer processing, whereas H<sub>2</sub>S and MT are found in petroleum, oil and natural gas, waste treatment facilities and decaying organic matter. All are common occupational gas exposure hazards in chemical industries and for first responders, including firefighters, and can be used as suicide, homicide, or chemical warfare agents. Despite many TIAs being on the potential terrorist threat's list and common occupational exposure hazards, there are no FDA-approved intramuscular or oral antidotes for these compounds which are effective in a mass-casualty event. Dimethyl trisulfide (DMTS) has recently gained prominence as a promising next generation CN antidote. DMTS converts CN to less toxic thiocyanate (SCN) forming dimethyl disulfide (DMDS), a relatively toxic compound as a major breakdown product. Another potential antidote, aminotetrazole cobinamide (CbiAT), which is a prodrug of

cobinamide (Cbi), can directly bind and detoxify CN, H<sub>2</sub>S and MT. Both DMTS and CbiAT have significant advantages over current treatments, but there is no method available for the analysis of CbiAT in any biological matrices and the methods available for DMDS and DMTS analysis have significant disadvantages. Hence, in this study, an extremely simple and rapid dynamic headspace (DHS) gas chromatography–mass spectroscopy (GC-MS) method was developed for the analysis of DMTS and DMDS from whole blood. The dynamic ranges for DMTS (0.2 – 50 µM) and DMDS (0.1 – 200 µM) were wide and the limits of detection (LODs) (40 and 30 nM, respectively) were excellent. Inter- and intraassay accuracies were within 100±15%, and the precision of <10% relative standard deviation (RSD) was excellent. The method performed well during pharmacokinetic analysis of DMTS and DMDS from the blood treated with DMTS. Although preliminary, pharmacokinetic results from DMTS-treated rats showed impressive results, i.e., C<sub>max</sub> and t<sub>max</sub> of 0.89±0.09 µM and 10 min, respectively, indicating rapid absorption and distribution of DMTS as well as slow elimination (t<sub>1/2</sub> = 10.5 hr). The DMDS method was used to analyze the level of formation of DMDS in swine blood after DMTS treatment and found almost 50% conversion of DMTS to DMDS, which indicated about 6.7 times lower blood DMDS concentration than its LD<sub>50</sub> value (i.e., 33.7 mg/kg). Understanding the level of formation of DMDS along with the availability of the methods will allow the further development of DMTS as a potential CN countermeasure. Additionally, a liquid chromatography tandem mass spectrometry (LC-MS/MS) method was developed for the analysis of CbiAT in plasma. The method produced an LOD of 0.3 µM with a wide dynamic range from 2 – 500 µM. Inter- and intraassay accuracies (100±12% and 100±19%, respectively) and precision (<12% and <9% RSD, respectively)

were good. The developed method was used to analyze CbiAT from treated swine and the preliminary pharmacokinetic parameters showed impressive results, most notably quick absorption, and distribution ( $C_{\max}$  and  $t_{\max}$  of 44.7  $\mu\text{M}$  and 4 h, respectively) and slow elimination ( $t_{1/2} = 23.7$  h). This method can be used for the further development of CbiAT as a potential antidote for CN, H<sub>2</sub>S and MT poisoning. Overall, multiple methods were developed and validated for the analysis of CN, H<sub>2</sub>S and MT countermeasures in biological matrices that have significant advantages over current analytical approaches and can be used to perform DMTS and CbiAT drug development studies.

## Chapter 1. Introduction

### 1.1. Overall Significance

Cyanide ( $\text{CN}^-$  and HCN, inclusively represented as CN) and reduced sulfur compounds (RSCs, i.e., hydrogen sulfide ( $\text{H}_2\text{S}$ ) and methanethiol (MT)), each known as a toxic inhalation agent (TIA), are widely used in chemical, pharmaceutical, polymer and agrochemical industries. RSCs are also found in nature, including in hot springs and volcanoes. They are a common cause of occupational gas exposure hazards and are also used as chemical warfare agents or potential terrorist agents. Exposure to these agents can cause serious risk to human health (i.e., hypoxia, cytotoxic anoxia, cardiac arrhythmias, bronchospasm, respiratory paralysis, coma, and death) and the environment. There is no approved antidote for RSCs and approved antidotes for CN poisoning have serious limitations. Therefore, there is a critical need to develop novel therapeutics, which each require highly sensitive analytical methods for pharmacokinetic and toxicokinetic investigations.

### 1.2. Project Objectives

This research work covers three main objectives: 1) analysis of potential cyanide antidote, dimethyl trisulfide, in whole blood by dynamic headspace gas chromatography–mass spectroscopy, 2) analysis of the soil fumigant, dimethyl disulfide, in swine blood by dynamic headspace gas chromatography–mass spectroscopy, and 3) analysis of aminotetrazole cobinamide, a next-generation antidote for cyanide, hydrogen sulfide and methanethiol poisoning, in swine plasma by liquid chromatography-tandem mass spectrometry. Chapter 2 describes a rapid and highly sensitive gas chromatography–mass

spectroscopy (GC-MS) method for a highly promising next generation CN antidote, dimethyl trisulfide (DMTS), in blood and preliminary pharmacokinetic profile of DMTS in rat blood. Chapter 3 addresses a GC-MS method for a relatively toxic soil fumigant and the major breakdown product of DMTS, dimethyl disulfide (DMDS), and preliminary correlation between the formation of DMDS in blood following DMTS administration. Chapter 4 focuses on determination of aminotetrazole cobinamide (CbiAT), which is effective against CN, H<sub>2</sub>S and MT poisoning and the analysis of the compound in swine plasma obtained from a CbiAT pharmacokinetic study. Chapter 5 describes conclusions, broader impacts and suggested future works.

### **1.3. Toxic Inhalation Agents**

The most common route of toxic exposure is inhalation, although it can happen via ingestion or direct skin or eye contact [1]. Inhalation of toxic gases and vapors as well as liquids or solids in the form of mists and aerosols can directly affect respiratory tract resulting in irritation, bronchiolitis, and pulmonary edema, and in severe cases, they may cause systemic toxicity [1, 2]. Toxic inhalation agents (TIAs) are gases and vapors that are detrimental to health and can be deadly when someone is exposed. Examples of TIAs include CN, H<sub>2</sub>S, MT, mustard gas, sarin, cyclosarin, nerve gas, ammonia, phosgene, diphosgene, carbon monoxide, methyl isocyanate, methane, formaldehyde, ozone, chlorine, hydrogen chloride, and hydrogen fluoride [2, 3]. Exposure to these chemicals can happen in several ways, but because of industrialization, the most common cause is occupational exposure where mishandling of chemicals, inadequate ventilation or improper protective equipment is the root cause of fatalities in chemical, pharmaceutical or plastic industries

[1]. Other major sources of exposure are: (1) structural fire smoke, which typically contains carbon monoxide and HCN, (2) mixing of household chemicals or gas leakage (i.e., methane or carbon monoxide exposure), and (3) acts of terrorism using TIAs, e.g., phosgene, CN, H<sub>2</sub>S, MT, chlorine, nerve agents and sulfur mustard) [1, 2, 4]. Because of their ease of production, low manufacturing cost and high reactivity, TIAs are commonly used in chemical industries for the synthesis of many compounds of pharmaceutical and agricultural importance. These are also used for the production of plastics, synthetic fibers and polymers, gold mining, insecticides, antiseptics, and dyes and pigments [5].

The demand for TIAs is increasing worldwide, therefore, industrial, mining workers, and custodians are frequently becoming the victims of these chemicals. Fatalities have been reported almost every year because of the accidental leakage of TIAs in industries and densely populated areas, and even unregulated storage and transportation have also been playing role for many mass-casualties [6-9]. There are many incidences where military groups have deliberately released TIAs on the battlefields to kill and injured adversary troops [10]. In 1984, a major industrial disasters occurred in Bhopal, India, where as many as 200,000 people (20% of the city's total population) were exposed to methyl isocyanate from explosion resulting from a leak in a storage tank [6, 11]. There are many historical incidents of exposure to TIAs other than inhalation. For example, the Jonestown massacre, in Guyana in 1978, resulted in the death of more than 900 people, including children, because of toxic CN ingestion [12]. Moreover, the first large-scale incidence of chemical terrorism or product tampering happened in the mainland of the U.S. in 1982 in Chicago, where seven people died by consumption of CN-laced Tylenol [13]. The

perpetrator collected the drugs from the store, added CN (60-100 mg per capsule) and put them back to the store [14].

#### 1.4. Pathogenesis of TIAs

Exposure to TIAs (e.g., CN, H<sub>2</sub>S or MT) can cause mild to severe damage to the respiratory tract depending on the level and duration of exposure, particle size and the water solubility of the TIA [1, 15]. Highly water soluble TIAs with comparatively greater particle size (>10 µm) generally deposit in the upper respiratory tract, whereas low solubility gases or small-sized particles (<5 µm) reach the lower part of the respiratory tract (Figure 1.1).

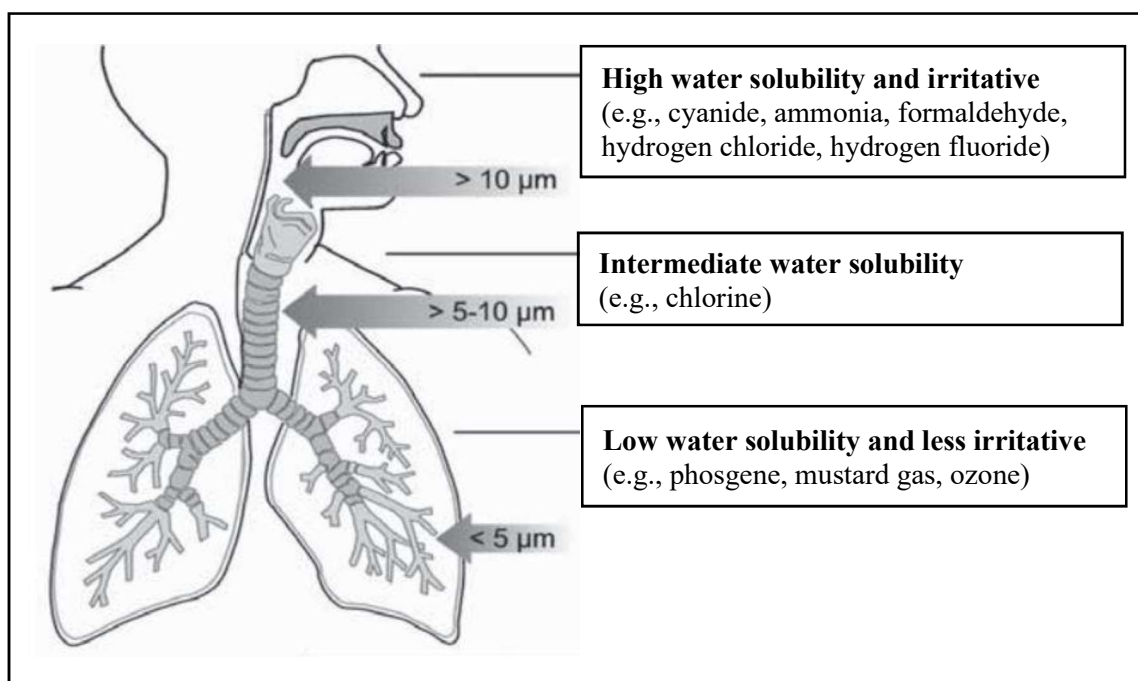


**Figure 1.1.** Aqueous solubility and particle size-based site of injury of TIAs in the respiratory tract [1].

The degree of illness depends on many factors, including victim's age, allergic response, metabolic rate, smoking history, condition of the lungs, immune response and

underlying disease [1, 16]. Mild level of exposure of TIAs generally creates watery eye, sneezing, coughing and mucous membrane irritation, whereas in prolong or severe case, it can severely damage lungs by causing pulmonary edema and asphyxiation. Even, entering into the systemic circulation, they can terminate the oxidative phosphorylation process binding with cytochrome c oxidase, and causing cellular hypoxia, cardiac arrest, and even death in some cases [16-19].

### **1.5. Exposure to CN, H<sub>2</sub>S, and MT**

Exposure to CN, H<sub>2</sub>S and MT can occur by inhalation, ingestion, or skin penetration. Once absorbed, these compounds exhibit very similar mechanisms of toxicity, therefore, they produce almost identical clinical signs and symptoms. After entering into the systemic circulation, they distribute throughout the body quickly, bind strongly with cytochrome c oxidase, and terminate the oxidative phosphorylation process [17, 20-22]. As a result, cytochrome c oxidase loses the ability to carry oxygen in the body, thereby disrupting electron transport chain, increasing cellular lactic acid concentration, lowering ATP production, and producing cellular hypoxia, hyperlactatemia, metabolic acidosis, cytotoxic anoxia, cardiac arrest and even death [7, 23-25]. These compounds can inhibit many other vital enzymes, including succinic dehydrogenase, superoxide dismutase and carbonic anhydrase, therefore inhibiting the formation of fumarate in the Krebs cycle, blocking the removal of harmful reactive oxygen species (ROS) and interrupting the interconversion of carbon dioxide and carbonic acid [26, 27].

## 1.6. Hydrogen Cyanide

### 1.6.1. Overview

Hydrogen cyanide (HCN), also known as hydrocyanic acid and prussic acid, is an extremely poisonous chemical (human LD<sub>50</sub>, 30-min inhalation = 150-173 ppm) [10]. It is lighter than air (density = 0.94), and has a boiling point of 26 °C. It is a relatively weak acid, with a pK<sub>a</sub> of 9.32, and is soluble in water, chloroform and ethanol [28].

### 1.6.2. Sources and use of CN

CN can be found in nature and is produced by fungi, bacteria, and plants [29]. It can also be produced by volcanic eruption [29], but the major sources of natural CN are cyanogenic plants, which include cassava, apples, almonds, peaches, and apricots [29-32]. Among these, cassava, a staple food in Africa, contains the highest percentage of CN (i.e., 1–1550 ppm in root, 900-2000 ppm in the peel and 20–1860 ppm in the leaves) [33]. CN can also be produced from anthropogenic sources, including mining, electroplating and polymer processing, and from burning of anthropogenic materials, (e.g., cigarettes, rubber, fibers, etc.) [34, 35].

CN is extensively used for the extraction of various metals (e.g., gold, silver, and zinc) from the soil or rocks [17, 36]. Current annual industrial need of CN is over 1.1 million tons [17]. Other industrial uses include production of polymers, fabrication of synthetic fibers, electroplating, and pest control [7, 37, 38].

### ***1.6.3. Major CN exposure events***

Because of low production cost, ease of synthesis and high toxicity, many casualties have been reported related to CN. A few of them are reported here. The Holocaust, a mass murder of Jews during 1941-1945 under the regime of Nazi, was performed in gas chambers by applying Zyklon B, which contains HCN gas. This brutal and deadliest event killed roughly one million Jews people [39, 40]. The mass-suicide event, Jonestown massacre, was happened in Guyana on November 18, 1978, where a group of followers (including over 300 children) of a cult leader, Jim Jones, drank CN-laced fruit punch. This so-called “revolutionary suicide” killed over 900 people, which is one of the deadliest mass-casualty events in American history [12, 41]. In Tianjin, China in 2015, a warehouse containing sodium cyanide (700 tons) was exploded and caused the death of 115 people. Because of this explosion, the surrounding CN level was increased as high as 365 times greater than the normal safety margin. This incidence also contaminated the river water and caused the death of thousands of fishes [42, 43].

### ***1.6.4. Current treatments and limitations***

Three U.S. Food and Drug Administration (FDA)-antidotes are currently available to detoxify CN: sodium nitrite (methemoglobin/nitric oxide generator), hydroxocobalamin (direct binding agent), and sodium thiosulfate (sulfur donor). These antidotes are commercially available as two intravenous (IV) drugs: Nithiodote<sup>®</sup> (a preparation of sodium thiosulfate and sodium nitrite mixture) and Cyanokit<sup>®</sup> (contains hydroxocobalamin) [17, 36]. An overview of their mechanism of action is provided below.

#### *1.6.4.1. Sodium nitrite*

Sodium nitrite is commercially available as Nithiodote<sup>®</sup> in combination with the sulfur donor, sodium thiosulfate, in the form of an IV preparation. It is a sterile solution containing 300 mg of sodium nitrite in a 10-mL glass vial and administered at a rate of 2.5-5 mL/min. Depending on the severity of exposure, a second dose (150 mg of sodium nitrite) is recommended at the same rate [44]. Sodium nitrite antagonizes CN poisoning via two routes: (1) indirect sequestering by generating methemoglobin, and (2) direct displacement by forming nitric oxide (NO) [45]. Indirect sequestering involves oxidation of Fe<sup>2+</sup> to Fe<sup>3+</sup> in hemoglobin, resulting in the formation of methemoglobin, which has a relatively strong affinity towards CN. By replacing the hydroxyl group at position 6 of the iron in hemoglobin, methemoglobin binds CN to form the less toxic cyanomethemoglobin and excretes this product by the regular body process [24, 45, 46]. Additionally, sodium nitrite can directly displace CN from cytochrome c oxidase by undergoing biotransformation to form NO [47]. But the major limitation is that the production of methemoglobin limits the oxygen carrying capacity and excess production of methemoglobin (>30%) causes additional health hazards, including headache, fatigue, cyanosis, hypotension, coma, and even death. It is not recommended and can be lethal for smoke-inhalation victims with high carboxyhemoglobin (<10%), as it reduces oxygen-carrying capacity of the blood [24]. Therefore, following sodium nitrite treatment, patients may need to be treated with supplemental oxygen and methylene blue to convert methemoglobin back to hemoglobin [24, 48, 49].

#### 1.6.4.2. *Sodium thiosulfate*

Sodium thiosulfate, a sulfur donor, converts CN to less toxic thiocyanate (SCN) by donating one sulfur to CN. This conversion requires rhodanese, a mitochondrial thiosulfate sulfurtransferase enzyme [50, 51]. Although, it is safer than sodium nitrite and is readily excreted from the body, its sulfur donating capability depends on less available rhodanese and its inability to quickly transverse cell walls cause delayed onset of action. Some organs, including brain and heart, have no (or very low) available rhodanese, therefore, the CN detoxification process problematic in these organs, if sodium thiosulfate is administered alone [24]. It is commercially available as an IV preparation (12.5 g/50 mL vial) and must be administered via IV over a 10-min period following sodium nitrite administration [44]. A second dose of sodium thiosulfate (6.25 g) is sometimes required depending on patient's condition. Apart from rhodanese dependency, it has short biological half-life and requires trained medical staff for administrating the drug [44, 52].

#### 1.6.4.3. *Hydroxocobalamin*

Hydroxocobalamin (available as Cyanokit<sup>®</sup>) binds directly with CN and forms a much less toxic and water-soluble cyanocobalamin (vitamin B<sub>12</sub>). The central cobalt ion (Co<sup>3+</sup>) of hydroxocobalamin has a strong affinity for CN, which replaces the hydroxyl ligand attached to it [53, 54]. Hydroxocobalamin also requires IV infusion, and has a large recommended dose (5 g over 15 min at a rate of 15 mL/min). Like Nithiodote<sup>®</sup>, it also requires the support from medical personnel to administer. Although it is safe, it requires on-site reconstitution and is expensive [44, 45]. A second dose is also recommended over a prolonged period (15 min to 2 h) for patients with severe CN poisoning [50].

Although the current FDA-approved CN antidotes are effective, but each has major limitations. Both antidotes require slow IV infusion, which necessitates the help from a trained medical staff [55, 56]. They require large dose, expensive, and depending on the level of exposure, a second dose is sometimes required [44, 57]. They may cause adverse effects, including dizziness, vomiting, confusion, hypotension, hypertension, cardiac arrhythmia, and methemoglobinemia and require special medical supervision [57-59].

## **1.7. Hydrogen Sulfide**

### ***1.7.1. Sources and Applications***

H<sub>2</sub>S is a colorless, corrosive, and flammable compound. It occurs naturally in decaying organic matter, natural gas, petroleum, waste water treatment facilities and volcanoes [60]. It is a weak acid with a pKa of 6.9, dissolves in water to form hydrosulfide (HS<sup>-</sup>) [61]. It is commonly used in chemical industries as a source of elemental sulfur for the synthesis of MT, ethanethiol and thioglycolic acid. It is also used in the pulp and paper industries to break down cellulose and lignin components [62].

### ***1.7.2. Toxicity***

H<sub>2</sub>S is a highly toxic compound and the second most common cause of occupational gas exposure hazard [22]. The LC<sub>50</sub>-value of H<sub>2</sub>S in rats is 444 ppm for 5-min of inhalation exposure [55]. Common sulfur-containing household items can produce toxic levels of H<sub>2</sub>S when mixing with acid cleaner, which can be lethal in a small or enclosed room [63-65]. Brief or low-dose exposure to H<sub>2</sub>S can cause several health problems, including fatigue, eye irritation, memory loss, dizziness and loss of appetite, whereas prolonged or high-dose

exposure can induce immediate collapse, respiratory paralysis, and even death [66]. Although H<sub>2</sub>S poses occupational, environmental, and even chemical threat, there is no currently-approved FDA approved antidote available for H<sub>2</sub>S poisoning [22].

### ***1.7.3. Recent H<sub>2</sub>S exposure events***

Many incidences and fatalities happened because of the H<sub>2</sub>S exposure in an unregulated industrial setting, including poor chemical handling and inadequate ventilation. Suicide by inhaling H<sub>2</sub>S is not that rare also [67]. An article published in 2010 [67], focused on the suicidal craze of Japanese people using homemade H<sub>2</sub>S, reported the deaths of 208 individuals between March to June in 2008. Most of the cases were happened when bath additive (containing lime sulfur) was mixed with toilet detergent, which generated toxic H<sub>2</sub>S gas.

## **1.8. Methanethiol**

### ***1.8.1. Sources and Applications***

MT, also known as methyl mercaptan, is a flammable, colorless gas and has a characteristic rotten cabbage odor. It has a low boiling point (6 °C) and is heavier than air, with a density of 1.66 (air = 1), therefore, it is mostly found in low-lying regions [68]. MT is also detected in the air around the waste treatment facilities, including sewage plants and landfills [68, 69]. It is added to natural gases to detect gas leakage, and is used in chemical industries to produce methionine, which is a dietary component of animal food, and for the manufacturing of pesticides [68, 70]. It is found in high concentrations in waste treatment

facilities, and also generated in paper, pulp, plastic, and petroleum industries as a waste product [69].

### ***1.8.2. Toxicity***

Although MT has many industrial applications, it is highly poisonous, with a LC<sub>50</sub> value in rats for 5-min of inhalation exposure of 675 ppm [71]. Prolonged and high concentration exposure to MT can lead to dizziness, vomiting, fatigue, bronchospasm, air flow obstruction, asthma, ischemic heart disease, hypotension, pulmonary and central nervous system damage, coma and even death [72-75]. Although mass exposure to MT in an industrial setting remains an ongoing risk, the Department of Homeland Security has established a safe handling practice guideline for MT and the Occupational Safety and Health Administration (OSHA) has proposed an emergency response guideline for MT, yet there is no-FDA approved antidote available for MT poisoning [68, 69].

## **1.9. Potential Antidotes Against CN, H<sub>2</sub>S and MT Poisoning**

No treatment currently exists for H<sub>2</sub>S and MT poisoning, but there are multiple CN antidotes. While these antidotes can be effective, they each have limitations. The limitations of current antidotes limit their applicability in a mass-casualty event (i.e., industrial accident, structural fire, or terrorism), where quick treatment of CN poisoning is extremely vital [57, 76]. These limitations have necessitated the search for superior countermeasures which are effective via oral or intramuscular (IM) route by untrained personnel. Recently, four antidotes (i.e., dimethyl trisulfide, cobinamide, 3-mercaptopyruvate and sodium tetrathionate) show promising results in overcoming the the

limitations of current CN antidotes. Among these, dimethyl trisulfide (DMTS) and 3-mercaptopyruvate (3-MP) are effective against CN [17, 77], sodium tetrathionate (STT) is effective against both CN and MT [76], and cobinamide (in the form of aminotetrazole cobinamide, CbiAT) can detoxify each of these poisons [22].

### 1.9.1. Dimethyl trisulfide

DMTS, a promising next generation sulfur donor, has proved very effective against CN toxicity [23, 78, 79]. DMTS converts CN to less toxic SCN and forms dimethyl disulfide (DMDS) as a breakdown product [36]. Unlike current FDA-approved sulfur donor, sodium thiosulfate, it does not require the active presence of rhodanese enzyme, is 79 times more effective, and can be administered IM [80]. In presence of rhodanese, it shows 43 times better antidotal properties than sodium thiosulfate [17]. It is highly lipophilic and can easily cross blood brain barrier and cell membranes [45]. Recent studies have shown that DMTS is about 3 times superior to sodium thiosulfate at detoxifying CN [80]. Figure 1.2 shows the reaction of DMTS with CN to detoxify CN, in presence or absence of rhodanese.

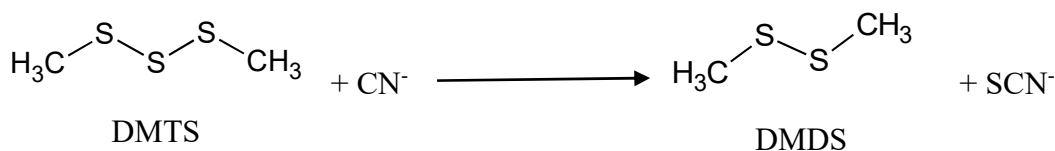


**Figure 1.2.** Reaction showing the conversion of CN to SCN and the formation of DMDS as a byproduct of this reaction.

### 1.9.2. 3-Mercaptopyruvate

Like sodium thiosulfate, 3-MP, is a sulfur donor and acts by donating one sulfur unit to CN to form the less toxic SCN [77]. The advantage of 3-MP over sodium thiosulfate

is that it does not depend on rhodanese, it instead is catalyzed by a more readily available enzyme (i.e., 3-mercaptopyruvate sulfurtransferase, 3-MST). 3-MST is available in all the vital organs, including heart, brain, lungs, liver, and kidney, and therefore, can better protect CN-exposed victims [81]. Moreover, 3-MST is available in both mitochondria and cytosol, whereas rhodanese is generally only found in mitochondria, allowing improved protection for CN intoxication [82, 83]. The disadvantages of 3-MP are poor bioavailability and instability in blood [84, 85]. Therefore, several prodrugs have been tested, among which the dimer of 3-MP (sulfanegen) has shown promising results [85, 86]. This dimer is soluble in water and nonenzymatically breaks down into two 3-MP molecules under biological conditions, making it a promising drug candidate for treating CN poisoning [86]. Figure 1.3 shows the possible reaction pathway of sulfanegen in treating CN toxicity [87].

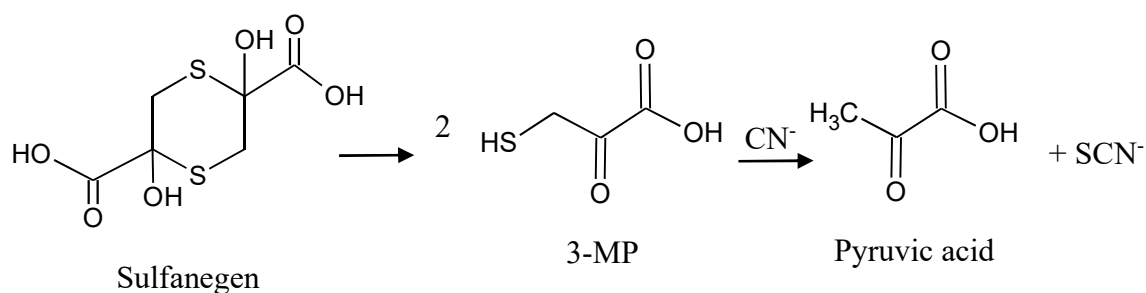


**Figure 1.3.** Reaction showing the formation of nontoxic SCN from CN by the donation of singlet sulfur from the 3-MP molecule.

### 1.9.3 Sodium tetrathionate

STT is a highly water-soluble compound, which can detoxify two CN molecules via a two-step reaction. The first step involves the direct reaction of STT with CN (known as “cyanolysis”) to form SCN. This direct interaction produces sodium thiosulfate, which can then convert a second molecule of CN to SCN in presence of rhodanese [76]. This dual

action makes STT 1.5 to 3.3 times more effective than sodium thiosulfate at detoxifying CN [76, 88]. Figure 1.4 shows the two step CN detoxification process of STT.



**Figure 1.4.** A two-step reaction of STT with 2 moles of CN.

Based on a recent study [76], STT was found to be well-tolerated by rats, mice and rabbits via IM injection and it effectively neutralized sodium cyanide. Moreover, STT rescued mice from a lethal MT gas exposure. Although, STT seems to be a promising drug candidate for both CN and MT poisoning, but only a few animal experiment [76, 89] have been performed on STT, therefore, more animal experiment need to be done to elucidate its bioavailability, safety and effectiveness.

#### 1.9.4 Cobinamide

Cbi (available as Cyanokit<sup>®</sup>), a vitamin B<sub>12</sub> analogue and the penultimate precursor of hydroxocobalamin biosynthesis. It has recently gained attention for its capability in treating multiple metabolic poisons, including CN, H<sub>2</sub>S and MT [22, 90-95]. Although its structure is similar to hydroxocobalamin, unlike hydroxocobalamin, it has two ligand binding sites instead of one. This makes it more effective than hydroxocobalamin [22]. Moreover, Cbi shows much higher affinity for ligands than hydroxocobalamin because it does not suffer from the negative *trans* effect of dimethyl-benzimidazole group on the upper binding site [55, 96]. As a result, it requires 3-10 times less Cbi dose than hydroxocobalamin to produce similar antidotal efficacy [56, 91]. In aqueous solution, Cbi is predominately present as aquohydroxocobinamide (AHCbi, [Cbi(OH)(H<sub>2</sub>O)]<sup>+</sup>), but

under acidic and basic conditions, it can also present as diaquocobinamide ( $[\text{Cbi}(\text{H}_2\text{O})_2]^{2+}$ ) and dihydroxocobinamide ( $[\text{Cbi}(\text{OH})_2]$ ), respectively [56]. Although, AHCbi has five times greater water solubility than hydroxocobalamin [96], it is not a good drug candidate for IM administration because it interacts with the macromolecules in the extracellular matrix (ECM) at the injection site, which limits its rate of absorption post-injection [97]. Recently, a prodrug of Cbi, aminotetrazole cobinamide (CbiAT), has shown very promising results for treating CN,  $\text{H}_2\text{S}$  and MT poisoning. It is safe and highly potent, allowing for quick absorption after IM administration, and effective binding of CN,  $\text{H}_2\text{S}$  and MT [22, 68, 95]. Figure 1.5 shows the reaction between CbiAT and CN, where one molecule of CbiAT detoxifies two molecules of CN. A similar mechanism is responsible for CbiAT's effectiveness against  $\text{H}_2\text{S}$  and MT poisoning.

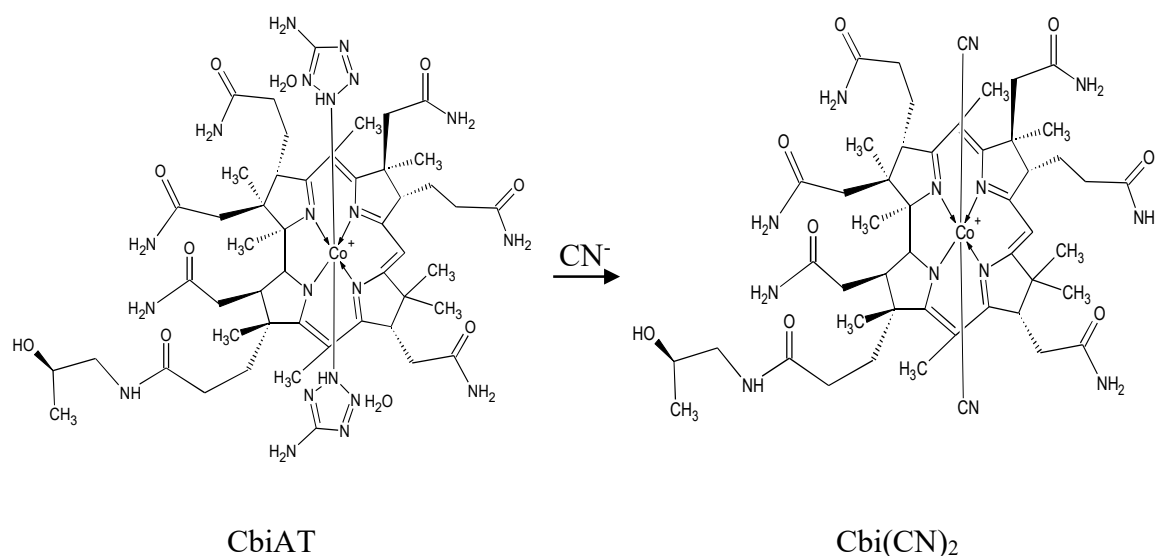


**Figure 1.5.** Reaction showing the interaction between CbiAT and CN, where the central cobalt ion detaches two aminotetrazole ligands, resulting in the formation of dicyanocobinamide,  $\text{Cbi}(\text{CN})_2$ .

## Chapter 2. Analysis of Potential Cyanide Antidote, Dimethyl Trisulfide, in Whole Blood by Dynamic Headspace Gas Chromatography-Mass Spectroscopy

### 2.1. Abstract

Cyanide is a rapidly acting and highly toxic chemical. It inhibits cytochrome c oxidase in the mitochondrial electron transport chain, resulting in cellular hypoxia, cytotoxic anoxia and even death. In order to overcome challenges associated with current cyanide antidotes, dimethyl trisulfide (DMTS), which converts cyanide to less toxic thiocyanate *in vivo*, has gained much attention recently as a promising next-generation cyanide antidote. While there are three analysis methods available for DMTS, they each have significant disadvantages. Hence, in this study, a dynamic headspace (DHS) gas chromatography–mass spectroscopy method was developed for the analysis of DMTS from rabbit whole blood. The method is extremely simple, involving only acidification of a blood sample, addition of an internal standard (DMTS-d<sub>6</sub>) and DHS-GC-MS analysis. The method produced a limit of detection of 0.04 μM for DMTS with dynamic range from 0.2-50 μM. Inter- and intraassay accuracy (100±15% and 100±9%, respectively), and precision (<10% and <9% relative standard deviation, respectively) were good. The validated method performed well during pharmacokinetic analysis of DMTS from the blood of rats treated with DMTS, producing excellent pharmacokinetic parameters for the treatment of cyanide exposure. The method produced significant advantages over current methods for analysis of DMTS and should be considered as a “gold standard” method for the further development of DMTS as a potential next-generation cyanide countermeasure.

## 2.2. Introduction

Hydrogen cyanide (HCN) is an extremely poisonous chemical with a human LD<sub>50</sub> of only 150-173 ppm via inhalation for a 30-min exposure. Because of its toxicity, HCN has been used as a chemical warfare agent, but it is more commonly found in smoke from cigarettes or fires and in food items [23, 24, 37]. Despite its serious health and safety related concerns, both forms of cyanide (HCN and CN<sup>-</sup>, inclusively represented as CN) are widely used in the chemical industry to produce polymers, to fabricate synthetic fibers, for electrolysis, to extract minerals, for electroplating, and for pest control [7, 37, 38]. Because of its industrial uses, the approximate global industrial need for cyanide is 1.1 million tons per year [7]. Cyanide exposure can occur through inhalation, ingestion and absorption through the skin. Once CN is absorbed, it quickly distributes throughout the body and moves through cells to strongly bind with cytochrome C oxidase. CN blocks the ability of oxygen to bind to cytochrome C oxidase, thereby terminating oxidative phosphorylation. As a result, glycolysis becomes the preferred method of energy production, increasing the lactic acid concentration in cells, resulting in metabolic acidosis. As a result, the toxic outcomes of CN poisoning include cellular hypoxia, cytotoxic anoxia, cardiac arrest, and death [7, 23-25].

Three antidotes have commonly been used to treat cyanide poisoning: sodium nitrite (methemoglobin/nitric oxide generator), hydroxocobalamin (direct binding agent), and sodium thiosulfate (sulfur donor). They are commercially available as Cyanokit<sup>®</sup> (hydroxocobalamin) and Nithiodote<sup>®</sup> (the combination of sodium thiosulfate and sodium nitrite), and both are administered intravenously (IV). Hydroxocobalamin has a strong affinity towards cyanide, binding it to form cyanocobalamin (Vitamin B<sub>12</sub>), which is water

soluble and readily excreted from the body [45]. Although hydroxocobalamin has a rapid onset of action and is generally considered safe, it has some limitations. It requires on-site reconstitution, is expensive, and has a large recommended dose (5 g administered by IV infusion over 15 min). It also must be administered at a rate of approximately 15 mL/min by trained personnel, which limits its acceptability in mass-exposure situations. Moreover, a second dose of 5 g is sometimes required over a prolonged period (15 min to 2 h) depending upon the severity of poisoning [44, 45, 50].

Sodium nitrite, which is often used in combination with sodium thiosulfate, antagonizes CN activity by generating methemoglobin and by forming nitric oxide (NO). It oxidizes  $\text{Fe}^{2+}$  to  $\text{Fe}^{3+}$  in hemoglobin to form methemoglobin. Methemoglobin has a strong affinity to cyanide and serves as a temporary binding site. Methemoglobin then transiently removes free cyanide as cyanomethemoglobin [24, 45]. Although methemoglobin generation is classically considered nitrite's protection mechanism, it can also undergo biotransformation to form NO, which can directly displace CN from cytochrome c oxidase, and reverse its toxicity [47]. Sodium nitrite is commercially available for IV administration (300 mg/10 mL vial at a rate of 2.5-5 mL/min) in combination with sodium thiosulfate (Nithiodote<sup>®</sup>), with a second dose (150 mg at a rate of 2.5-5 mL/min) potentially required, depending upon the severity of poisoning [44]. Unlike hemoglobin, methemoglobin cannot carry oxygen and its excess production (>30%) leads to headaches, cyanosis, fatigue, coma, and death in severe cases. Moreover, it causes hypotension and should not be used for smoke-inhalation patients with high carboxyhemoglobin (<10%) [24], which also reduces the oxygen-carrying capacity of

blood. Therefore, supplemental oxygen and methylene blue may also be administered to convert methemoglobin back to hemoglobin, following nitrite administration [24, 48, 49].

Sodium thiosulfate converts cyanide to less toxic thiocyanate in presence of rhodanese (a mitochondrial thiosulfate sulfurtransferase enzyme). The thiocyanate is subsequently excreted in urine [50, 51]. Although, sodium thiosulfate is safer than sodium nitrite, it has a delayed onset of action. Therefore, it is administered with sodium nitrite as Nithiodote<sup>®</sup> to overcome this limitation [24]. It is administered intravenously (12.5 g/50 mL vial) and requires a large dose (12.5 g administered by IV infusion over 10 min) immediately following the administration of sodium nitrite, with a second dose of 6.25 g potentially required [44]. Like hydroxocobalamin and sodium nitrite, trained medical personnel are necessary for administration, which limits the use of sodium thiosulfate in mass casualty cyanide-poisoning events.

The limitations of currently available antidotes have necessitated the search for next-generation CN antidotes. Recently, dimethyl trisulfide (DMTS) has shown impressive efficacy against cyanide toxicity and has other advantages over current treatments [23, 78, 79]. DMTS, which is found in some whole and processed foods (e.g., garlic and soy sauce), converts cyanide to thiocyanate and is 43 times more effective than thiosulfate in presence of rhodanese [45, 98-102]. In the absence of rhodanese, DMTS shows even higher relative efficacy (79 times) [45]. Animal studies have shown that DMTS is up to 3 times more effective at treating CN poisoning than sodium thiosulfate, as measured by antidotal potency ratio (APR) [80]. Because it is less dependent on rhodanese and has higher cell membrane permeability than thiosulfate, DMTS promises to be more effective as a sulfur

donor. It can also be administered intramuscularly (IM), which allows feasible use in a mass-casualty scenario [103].

Three methods of analysis of DMTS from biological samples have been published, including stir bar sorptive extraction (SBSE) GC-MS [45], headspace solid-phase microextraction (HS-SPME) GC-MS, and HPLC-UV techniques [104]. Although these methods are effective, each approach has significant disadvantages. The SBSE method features simple acidification of blood, extraction of DMTS via an SBSE stir bar, and analysis of the stir bar via thermal desorption GC-MS. While it is highly sensitive (LOD = 0.06  $\mu\text{M}$ ), this method does have the disadvantages of requiring sorptive stir bars to extract DMTS from the blood matrix, making it a relatively costly technique (even though the stir bars can be reused multiple times) and the sample preparation is relatively lengthy. The HPLC-UV method involves defibrinating blood, addition of DMDS (used as IS), precipitation of blood proteins by centrifugation ( $14,000 \times g$  at  $4^\circ\text{C}$  for 5 min), and analysis of supernatant by HPLC using C8 column and a UV detector at 215 nm. While this technique has the advantage of more straightforward and affordable sample preparation, it is 193 times less sensitive than the SBSE technique, with a reported LOD of approximately 11.56  $\mu\text{M}$  (reported as 1.46  $\mu\text{g/mL}$ ). Also, DMTS is converted to DMDS during its reaction with cyanide, so it should not be used as an IS in DMTS-treated and cyanide-exposed individuals. For increased sensitivity, the same authors used an SPME technique which featured homogenized brain samples (in aqueous polysorbate 80 or HPLC grade ethanol), extraction of DMTS via direct immersion SPME with a polydimethylsiloxane (PDMS) sorbent, and analysis via GC-MS. While the reported LOD (213 ng/g of brain, which is 1.49  $\mu\text{M}$ ) is much lower than the HPLC method, it is still about 25 times less-sensitive than

the SBSE technique. Additionally, similar to SBSE, SPME requires relatively expensive microextraction components. To overcome the limitations of current DMTS analysis methods, there is a need to develop a simple, sensitive, and less costly technique to analyze DMTS from whole blood.

Therefore, the objective of this study was to develop and validate a simple and effective DHS-GC-MS method for the detection of DMTS in rabbit whole blood which combines the advantages of each of previous published methods. The availability of such a method would accelerate further development of DMTS as a possible next-generation cyanide antidote.

## **2.3. Experimental**

### **2.3.1. Materials**

All reagents and solvents were of reagent grade unless mentioned otherwise. Methanol (LC-MS grade) and sulfuric acid (certified ACS plus) were purchased from Fisher Scientific (Fair Lawn, NJ, USA). Reverse-osmosis water was passed through a polishing unit (Lab Pro, Labconco, Kansas City, KS, USA) and had a resistivity of 18.2 M $\Omega$ -cm. DMTS and internal standard (IS) dimethyl-d<sub>6</sub> trisulfide (DMTS-d<sub>6</sub>) were purchased from Sigma-Aldrich (St. Louis, MO, USA) and US Biological Life Sciences (Salem, MA, USA), respectively. Freshly prepared DMTS stock solution in methanol (200 mM) was used for each experiment and the standard DMTS container was kept in the dark at ambient temperature. The as received IS solution was diluted in methanol to produce a stock solution of 100 mM, which was further diluted to 1 mM in DI water and stored in -30 °C freezer (Isotemp plus freezer, Fisher Scientific, NJ, USA). Thermal desorption tubes

filled with Tenax® TA sorptive material, was obtained from Gerstel Inc. (Linthicum, MD, USA). The sorbent was conditioned using a TC 2 tube conditioner and Aux-controller 163 (Gerstel Inc., MD, USA) for 8 h at 315 °C under 68 psi of ultra-high purity (UHP) 5.0 grade nitrogen gas (A-OX Welding Supply Co., Sioux Falls, SD, USA) before use for the first time. One TD tube was used for the entirety of the current study.

### ***2.3.2. Biological samples***

Rabbit whole blood (Non-sterile with EDTA), obtained from Pel-Freez Biologicals (Rogers, AR, USA), was used for method development and validation, and was kept in a –80 °C freezer (TSU series, Thermo scientific, NJ, USA) until used. Following validation, the effectiveness of the DMTS method was evaluated by analyzing blood from a DMTS pharmacokinetic study performed at United States Army Medical Research Institute of Chemical Defense (USAMRICD, Aberdeen Proving Ground, MD, USA). Male Sprague Dawley® SAS-400 rats (Charles River Laboratories, Kingston, NY, USA) implanted with jugular vein catheters were used for this study. Rats, weighing between 250–350 g, were intramuscularly (IM) administered with a proprietary formulation of DMTS to the right caudal thigh muscle. Multiple blood draws were performed from each catheterized rat. A maximum of 7 blood draws for each rat were randomly distributed among the cohorts at times: 0 (blank control), 2, 5, 10, 15, 30, 60, 90, 120, 180, 240, 300 and 360 min. Note: The total maximum blood volume drawn from each rat did not exceed 700 µL. Negative control samples were drawn from rats prior to DMTS injection. For each sample, 50 µL of blood was collected into a syringe from the jugular vein catheter, and the blood samples were prepared as below (in the “Preparation of DMTS standards and samples” section).

The prepared samples were then flash frozen and shipped to South Dakota State University (Brookings, SD, USA) on dry ice for analysis. Samples were kept at  $-80\text{ }^{\circ}\text{C}$  until analyzed. All animals were handled and housed in accordance with the Guide for the Care and Use of Laboratory Animals published by the United States National Institutes of Health (NIH Publication No. 85-23, Revised 1996). The experimental protocol was approved by Institutional Animal Care and Use Committee at USAMRICD.

### ***2.3.3. Preparation of DMTS standards and samples***

The stock solution of DMTS (200 mM in methanol) was diluted to 4, 10, 15, 20, 40, 100, 150, 200, 400, 700, and 1000  $\mu\text{M}$  with DI water to produce working standard solutions. Whenever needed, 40  $\mu\text{M}$  aqueous IS was prepared from a 1 mM stock solution in methanol and was either added directly to acidified blood (see below) or spiked (100  $\mu\text{L}$ ) into DMTS working standard solutions (1:1 mixture of DMTS:IS).

Two techniques were used to prepare blood for DHS analysis: “large volume” and “small volume” sample preparation techniques. For preparation of samples where a large volume of blood is available, 450  $\mu\text{L}$  of whole blood (i.e., rabbit blood for this study) was transferred to a 4-mL HPLC vial with 500  $\mu\text{L}$  of 0.4% sulfuric acid. The mixture was then vortexed for 10 s at  $252 \times g$  to ensure proper coagulation and denaturation of proteins. Note that acid denaturation prior to the addition of DMTS and/or IS is a crucial step in DMTS sample preparation to mitigate the quick and irreproducible degradation of DMTS in non-denatured blood. Finally, 50  $\mu\text{L}$  of a DMTS:IS mixture (for standards) or an IS solution (for samples) was added to the acidified blood (950  $\mu\text{L}$ ). The sample was then vortexed for

10 s at  $252 \times g$ , and an aliquot of the sample solution (100  $\mu\text{L}$ ) was placed in a 20-mL HS vial with a polytetrafluoroethylene-lined septum for analysis.

For the preparation of blood samples from the animal studies, where only a small volume of blood was available, 0.4% sulfuric acid (950  $\mu\text{L}$ ) was added to a 2-mL centrifuge tube along with 50  $\mu\text{L}$  of whole blood (e.g., rat blood in this study) with mixing. IS (25  $\mu\text{L}$  of 6  $\mu\text{M}$ ) was then added. The sample was mixed and flash frozen. For preparation of standards for the small volume protocol, acidified blood (25  $\mu\text{L}$ ) was spiked with 50  $\mu\text{L}$  of a mixture of DMTS:IS, and then vortexed for 10 s to ensure proper mixing. An aliquot of this preparation (900  $\mu\text{L}$ ) was placed in a 20-mL HS vial for analysis.

In both approaches, the concentrations of DMTS in the acidified blood calibration standards were 0.2, 0.5, 0.75, 1, 2, 5, 7.5, 10, 20, 35, and 50  $\mu\text{M}$ , whereas the IS concentration was fixed at 2  $\mu\text{M}$  (final concentration). When analyzing the whole blood of DMTS-treated animals, acidification and addition of the IS was performed immediately following the collection of blood to ensure minimal degradation of DMTS.

#### ***2.3.4. DHS-GC-MS analysis of DMTS***

Analysis of prepared samples was performed using DHS via a Gerstel MPS sampler (Gerstel Inc., Linthicum, MD, USA) coupled with an Agilent GC-MS (Agilent Technologies, Wilmington, DE, USA) consisting of a 6890N series gas chromatograph, and a 5975 series mass selective (MS) detector. The HS vial was initially incubated at 40  $^{\circ}\text{C}$  for 1 min, the septum was punctured using dual needles and nitrogen was delivered through the headspace of the vial to carry DMTS to the adsorptive material (Tenax<sup>®</sup> TA) where it was collected. The trapping and the incubation temperatures were set at 28 and 40

°C, respectively. The transfer heater temperature was set at 75 °C. After trapping for 10 mins, the TDU tube was inserted into the TDU and was heated from 30 °C to 280 °C at a rate of 12 °C/s. The analyte was desorbed at 275 °C and transferred to a cooled injection system (CIS) PTV-type inlet, where it was trapped at –100 °C on a CIS liner. The CIS liner was then heated to 275 °C at a rate of 12 °C/s to transfer the analyte to the GC column before returning to its initial temperature.

A DB5-MS bonded-phase column (30 m x 0.25 mm i.d., 0.25 µm film thickness; J&W Scientific, Folsom, CA, USA) was used with helium as the carrier gas at a flow rate of 1.0 mL/min and a column head pressure of 10.0 psi. The initial GC oven temperature was 30 °C and was held for 1 min, then elevated at a rate of 120 °C/min up to 250 °C, where it was held constant for 2 min, before returning to its initial temperature. The retention times for both DMTS and IS were about 3.5 min. The GC was interfaced with an MS detector with electron ionization (EI). DMTS and IS were identified and quantified using selective-ion-monitoring (SIM) mode at m/z of 126 ( $[\text{CH}_3\text{-S-S-S-CH}_3]^+$ , quantification) and 111 ( $[\text{CH}_3\text{-S-S-S}]^+$ , identification), and 132 ( $[\text{CD}_3\text{-S-S-S-CD}_3]^+$ , quantification) and 114 ( $[\text{CD}_3\text{-S-S-S}]^+$ , identification), respectively.

### ***2.3.5. Calibration, quantification, and limit of detection***

The proposed method was validated following the Food and Drug Administration (FDA) bioanalytical method validation guidelines [105-107]. Stock solutions of both DMTS (200 mM) and IS (100 mM) were prepared in methanol, which were further diluted with DI water to prepare the calibration standards (0.2, 0.5, 1, 2, 5, 10, 20, and 50 µM) and quality-control (QC) standards (0.75, 7.5, and 35 µM) for DMTS in denatured rabbit blood.

Each calibration standard was prepared in triplicate, where the concentration of IS was 2  $\mu\text{M}$ . To construct a calibration curve, the average peak area signal ratios of DMTS to IS were plotted as a function of calibrator concentrations. Peak areas of both DMTS and IS were calculated by manual integration from baseline to baseline in Agilent ChemStation software (Santa Clara, CA, USA). To evaluate the calibration behavior of DMTS, a total of six preliminary calibration curves were constructed. Both linear ( $y = mx + c$ ) and log-log ( $\log y = m \log x + \log a$ ) regressions were used, with goodness-of-fit (GOF) quantified by percent residual accuracy (PRA) [108]. PRA was used, in conjunction with the coefficient of determination ( $R^2$ ), to more effectively quantify the GOF.  $R^2$  is predominantly based on the GOF of the highest concentration 2 or 3 calibrators and doesn't accurately quantify GOF throughout the calibration range. The disadvantages of  $R^2$  are exacerbated when using a geometric series of concentrations for calibration standards and when calibration curves span 2–3 orders of magnitude, as in this study. Therefore, for a more accurate representation of the goodness-of-fit, PRA was reported in the manuscript, along with  $R^2$ . A “good” fit of the calibration model throughout the calibration range will produce a PRA of 90–100%. Preliminary studies and the validation experiment confirmed that a log-log curve fit best described the calibration behavior of DMTS, as also reported by Manandhar et al. [45].

The upper and lower limits of quantification (ULOQ and LLOQ) were investigated using two inclusion criteria: (1) calibrator precision of <10% relative standard deviation (RSD), and (2) calibrator accuracy of  $\pm 15\%$  of the nominal concentration compared to the concentration back-calculated from the calibration curve. In parallel with the calibration standards, three QCs (0.75, 7.5 and 35  $\mu\text{M}$  as low, medium, and high, respectively) were

also prepared in the same way (not included in the calibration curve) and were analyzed in quintuplicate each day for 3 days in order to calculate the intraassay (within same day) and interassay (over 3 days, within 5 calendar days) accuracy and precision. The LOD, which was defined as the lowest DMTS concentration to reproducibly produce a signal-to-noise ratio (S/N) of 3, was calculated by analyzing blood samples spiked with DMTS concentrations below the LLOQ. Noise was calculated as peak-to-peak noise in blank solutions over the retention time of DMTS.

### ***2.3.6. Selectivity and stability***

Selectivity of the method was evaluated by confirming the absence of significant signals above the baseline in the blank over the retention time of DMTS, as determined by comparing blank rabbit blood and DMTS-spiked rabbit blood samples by the procedure described earlier (see section “Calibration, quantification and limit of detection”). Resolution of the DMTS peak was also calculated as a measure of selectivity by standard methods [109].

Short- and long-term storage stability of DMTS was evaluated in triplicate using denatured rabbit blood spiked with HQC and LQC concentrations at different storage conditions over multiple time periods. For short-term stability, both QCs were evaluated in the autosampler and under multiple freeze–thaw (FT) cycles. The autosampler stability was evaluated by placing triplicates of low (0.75  $\mu\text{M}$ ) and high (35  $\mu\text{M}$ ) QCs on the autosampler of the GC at ambient temperature and analyzing them at approximately 0, 2, 5, 10, and 24 h following preparation to ensure the integrity of DMTS during the course of analysis. Because of the evaporative loss of DMTS in blood, IS was also incorporated to

track the change of analyte signal with respect to time, but it was not considered when evaluating the autosampler stability, as it would correct for the loss of DMTS in blood during the analysis. For FT analysis, four sets of LQCs and HQCs were prepared in triplicates without IS. Three sets of QCs were stored in a -80 °C freezer, while one set was analyzed on the same day after adding IS. After 24 h, all QC samples were thawed at room temperature (RT) by running tap water (about 25 °C) over the base of the sample vials. To one set of thawed QCs, IS was added, the samples were centrifuged at  $252 \times g$  for 10 s and then analyzed. The remaining two sets of QCs were placed back in the -80 °C freezer for 24 h. This freeze-thaw cycle was repeated two more times to evaluate three FT cycles.

Bench-top stability and long-term stability studies for DMTS at -20 and 4 °C have been reported by Manandhar et al. [45] and were not evaluated in this study. Manandhar et al. [45] recommended to immediately add acid to a blood sample, add IS, snap freeze, and keep samples at -80 °C in order to store blood samples for DMTS analysis, but only performed a 5-day stability study to confirm this recommended procedure. Therefore, we extended this experiment to 90 days to evaluate how long DMTS can be stored under these conditions before inaccurate results are found. For this study, triplicates of LQC and HQC concentrations of DMTS in blood were prepared for storage and analyzed after 0, 1, 2, 5, 10, 20, 30, 45, 60 and 90 days at -80 °C. Both QCs were prepared in bulk (30 mL) in 50-mL Falcon<sup>®</sup> conical tubes to minimize sample-to-sample variation in the original QC concentrations. IS was spiked before storage, and from these bulk QCs, 10 sets of LQCs and HQCs each were prepared in triplicate by simply transferring 1 mL of sample to a 4-mL HPLC vial for each replicate. One set of IS-treated QCs were analyzed on the same day (i.e., Day “0”), and the rest were snap-frozen using a dry ice–acetone bath before

storing them in a -80 °C freezer. After 24 h, another set of QCs (in triplicate) were thawed and analyzed (Day 1). The same protocol was followed for the rest of the samples. For all the stability experiments, stability of DMTS was calculated as a percentage of the initial (“Day 0”) signal. DMTS was considered stable if the signal from the stored sample was within  $\pm 10\%$  of the initial signal.

### ***2.3.7. Matrix effect***

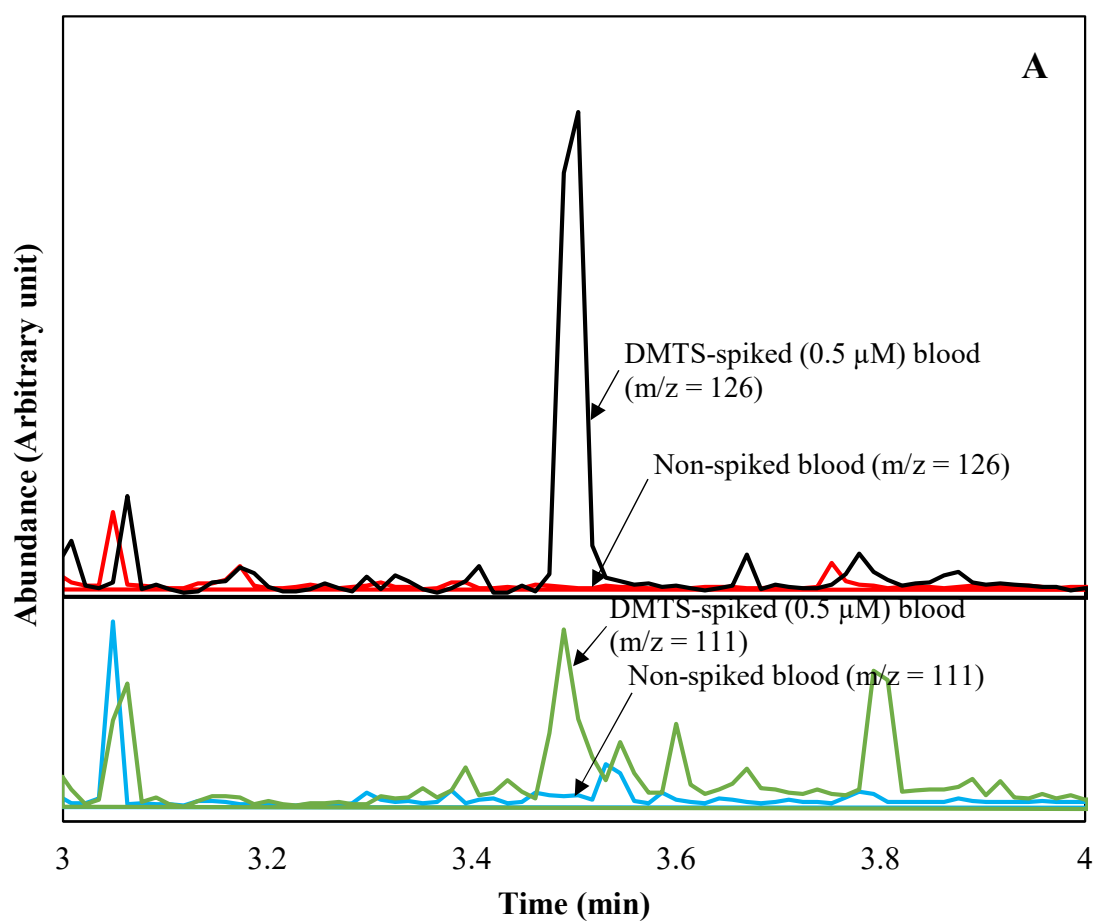
Matrix effects for the analysis of DMTS in blood were evaluated by comparing an aqueous calibration curve with a calibration curve in blood. The assessment of matrix effects reveals the direct or indirect alteration of response due to the presence of interfering substances in the blood sample. The slopes ( $m$ ) of the log-log plots for the calibration curves in blood and aqueous solution were used to evaluate and quantify (i.e.,  $m_{\text{blood}}/m_{\text{aq}}$ ) the matrix effect. The value of ( $m_{\text{blood}}/m_{\text{aq}}$ ) equal to 1 indicates no matrix effect, whereas less than 1 and greater than 1 represent suppression and enhancement effects, respectively. The effectiveness of IS to compensate the matrix effect was also evaluated by comparing the ratio of  $m_{\text{blood}}/m_{\text{aq}}$  of non-corrected curves with the IS-corrected curves.

## **2.4. Results and discussion**

### ***2.4.1. GC-MS analysis of DMTS***

The analytical method presented here features simple and quick sample preparation for the analysis of DMTS from whole blood. The sample preparation involves only 3 steps: 1) treatment of whole blood with acid (0.4%  $\text{H}_2\text{SO}_4$ ), 2) addition of IS, and 3) mixing. An aliquot of the resulting mixture is transferred to a HS vial and analyzed via DHS-GC-MS.

During DHS, the TDU tube (filled with Tenax<sup>®</sup> TA sorbent) dynamically adsorbs chemicals within the headspace vapor, including DMTS. This process allows exhaustive extraction of the DMTS from the blood. The DMTS is then thermally desorbed into the GC-MS by heating the TDU tube. The selected ion chromatograms of DMTS-spiked blood (0.5  $\mu\text{M}$ , at  $m/z = 111$  and 126), IS-spiked blood (2  $\mu\text{M}$ , at  $m/z = 114$  and 132) and non-spiked blood ( $m/z = 126$  and 132) are plotted in Figure 2.1.



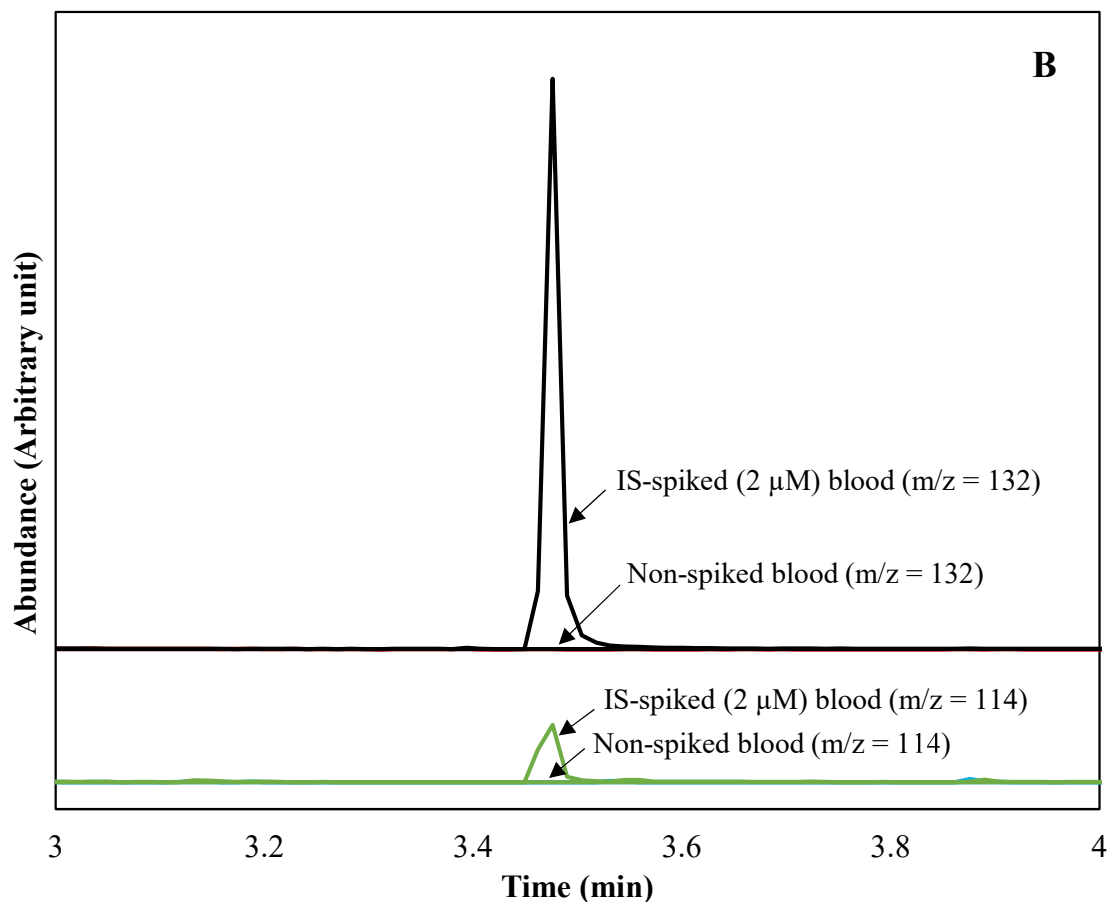


**Figure 2.1.** SIM mode GC-MS chromatograms of A) DMTS-spiked blood (0.5  $\mu\text{M}$ ) and non-spiked blood at  $m/z$  of 126 (quantification ion, *upper trace*) and  $m/z$  of 111 (qualification ion, *lower trace*), and B) IS-spiked blood (2  $\mu\text{M}$ ) and non-spiked blood at  $m/z$  of 132 (quantification ion, *upper trace*) and at  $m/z$  of 114 (qualification ion, *lower trace*).

As shown in Figure 2.1, the method produced good selectivity, with DMTS and IS eluting at approximately 3.50 min and the blank containing no coeluting peaks at this time. The closest consistent peaks of DMTS-spiked blood eluted at about 3.40 ( $m/z = 126$ ) and 3.55 ( $m/z = 111$ ) min, producing resolutions ( $R_s$ ) of 2.38 and 1.22, respectively. The peak shapes for both DMTS and IS were sharp and symmetrical with peak asymmetry factors of  $<1.3$  and  $<1.2$ , respectively.

Table 2.1 shows the analytical description of each previously published method for DMTS analysis from biological matrices as compared to the current method.

**Table 2.1:** Comparison of some important features of published and the current method for the analysis of DMTS from biological matrices.

Study	Analytical technique	Sample	Sample volume required ( $\mu\text{L}$ )	Sample preparation time (min)	LOD ( $\mu\text{M}$ )	LLOQ ( $\mu\text{M}$ )	ULOQ ( $\mu\text{M}$ )
Kiss et al. [104]	HS-SPME-GC-MS	Brain	588	30 <sup>a</sup>	1.49	4.51 <sup>b</sup>	38.0 <sup>b</sup>
	HPLC-UV	Blood	495	25 <sup>a</sup>	11.6	35.2 <sup>c</sup>	396 <sup>c</sup>
Manandhar et al. [45]	SBSE-GC-MS	Blood	450	70	0.06	0.5	100
Current method	DHS-GC-MS	Blood	450 <sup>d</sup> 50 <sup>e</sup>	10	0.04 <sup>d</sup> 0.06 <sup>e</sup>	0.2	50

<sup>a</sup>Total estimated sample preparation time

<sup>b</sup>Reported as 645 – 5435 ng<sub>DMTS</sub>/g<sub>brain</sub>

<sup>c</sup>Reported as 4.45 – 50  $\mu\text{g/mL}$

<sup>d</sup>Large volume technique

<sup>e</sup>Small volume technique

The main advantages of the current method are: 1) rapid and simple sample preparation, 2) sensitivity, 3) small required sample volume, and 4) minimal consumable use. First, the overall sample preparation time is only 10 min, with chromatographic analysis lasting approximately 12 min. Therefore, using the current method, roughly 72 parallel samples could be processed and analyzed in a 24-h period. Quick blood sample preparation is vital for DMTS to minimize its unwanted loss, and the reported sample preparation time (i.e., 10 min) is the shortest time necessary for any published method. Second, the current method is extremely sensitive, allowing detection and quantification as low as 0.04 and 0.2  $\mu\text{M}$  for the large and small volume approaches, respectively. This is the lowest LLOQ for the current methods by at least 2.5 times. Third, the required

volume of blood for the method presented here is only 50  $\mu\text{L}$  (as described in ‘small’ volume technique), which is the smallest blood volume required for any of the current DMTS analysis methods (Table 2.1). Fourth, the current approach uses one TD tube (Tenax<sup>®</sup> TA) for the extraction of DMTS for the entirety study, which makes the extraction process more consistent and less demanding than that of the other methods in Table 2.1. The need for multiple stir bars and SPME fibers makes the SBSE and SPME methods more costly since the Tenax<sup>®</sup> tube and a single stir bar or SPME fiber are approximately the same cost. Moreover, compared with the stir bars and SPME fibers, the Tenax<sup>®</sup> does not directly contact the biological samples, allowing greater longevity. Therefore, the Tenax<sup>®</sup> tube can be reused many more times than the stir bars or SPME fibers before it degrades (e.g., a single Tenax<sup>®</sup> sorbent tube was used for every sample in the current study with no observed loss in performance). Besides these main advantages, the DHS technique requires no organic solvent, whereas the HPLC technique requires extraction with acetonitrile, and mobile phase constitutes of water and acetonitrile in the ratio of 35 : 65 v/v.

#### ***2.4.2. Dynamic range, limit of detection, and sensitivity***

Initially, the linearity of the method was evaluated in the range of 0.2 - 200  $\mu\text{M}$  in blood. Multiple calibration curves were constructed to analyze the calibration behavior of DMTS by plotting the concentration of DMTS versus the signal ratio (i.e., peak area of DMTS at  $m/z$  126 divided by the corresponding peak area of IS at  $m/z$  132) as linear and log-log regressions over multiple calibration ranges. We confirmed that the calibration behavior of DMTS was best described by a log-log relationship. Manandhar et al. [45] also showed similar behavior of DMTS, which was explained by increased formation of the 126

(m/z) fragment at higher concentrations of DMTS in the ionization chamber (i.e., enhancement of MS ionization process at higher DMTS concentrations), independent of the sample preparation process. The largest two calibration standards (100 and 200  $\mu\text{M}$ ) did not meet the accuracy and/or precision inclusion criteria, resulting in a quantification range of 0.2  $\mu\text{M}$  (LLOQ) to 50  $\mu\text{M}$  (ULOQ). This linear range spanned over two orders of magnitude, as is desired for analysis of biological samples [77, 110]. Moreover, the LLOQ (0.2  $\mu\text{M}$ ) was much lower than the LLOQs for the HS-SPME-GC-MS and HPLC-UV methods reported by Kiss et al. [104], and is 2.5 times lower than the SBSE-GC-MS method of Manandhar et al. [45] (see Table 2.1).

Table 2.2 shows the calibration curve equations of three separate calibration curves prepared over a 3-day period with their corresponding  $R^2$  and PRA values. All three calibration curves were found to be highly stable in terms of slope,  $R^2$ , PRA, accuracy, and precision.

**Table 2.2:** Curve equations and related values.

Day	Equation	m	PRA	$R^2$	Accuracy (%)	Precision (%RSD)
Day-1	$\log y = 1.07 \log x - 0.76$	1.07	90.0	0.9962	100 $\pm$ 14.9	<9.3
Day-2	$\log y = 1.13 \log x - 0.80$	1.13	95.8	0.9989	100 $\pm$ 11.8	<7.5
Day-3	$\log y = 1.15 \log x - 0.83$	1.15	90.0	0.9965	100 $\pm$ 14.6	<9.3

The LOD of DMTS for the current method was 0.04  $\mu\text{M}$  (large volume technique), which is 1.5 times lower than that of the Manandhar et al. [45] method, and significantly better than the reported LODs of Kiss et al. (1.49 and 11.56  $\mu\text{M}$  [104]). The LOD was selected based on the concentration producing a signal-to-noise ratio of 3:1. This high

sensitivity is very important to accurately quantify DMTS in blood samples at typical doses of DMTS [111].

### 2.4.3. Accuracy and Precision

Although DMTS is very unstable and volatile in nature, the accuracy and precision, reported in Table 2.3, were excellent relative to other methods of DMTS analysis from blood. To perform the study, three QC standards (0.75, 7.5 and 35  $\mu\text{M}$ ) were analyzed in quintuplicate on three different days within six calendar days. FDA method validation guidelines were followed to evaluate the results [106, 112, 113] and the obtained intraassay accuracy ( $100 \pm 8\text{-}15\%$ ) and precision ( $<10\%$  RSD), and inter-assay accuracy ( $100 \pm 9\%$ ) and precision ( $<9\%$  RSD), were remarkable.

**Table 2.3:** Intra- and inter-assay accuracy and precision for analysis of DMTS in spiked rabbit blood.

Conc ( $\mu\text{M}$ )	Intra-assay						Inter-assay	
	Accuracy (%) <sup>a</sup>			Precision (%RSD) <sup>a</sup>			Accuracy (%) <sup>b</sup>	Precision (%RSD) <sup>b</sup>
	Day 1	Day 2	Day 3	Day 1	Day 2	Day 3		
0.75	100 $\pm$ 7.8	100 $\pm$ 11.1	100 $\pm$ 2.9	5.9	3.7	6.1	100 $\pm$ 5.4	8.3
7.5	100 $\pm$ 1.6	100 $\pm$ 14.1	100 $\pm$ 13.5	3.8	2.9	2.7	100 $\pm$ 8.7	8.6
35	100 $\pm$ 5.4	100 $\pm$ 5.8	100 $\pm$ 1.7	6.5	6.0	9.0	100 $\pm$ 3.2	7.9

<sup>a</sup>QC method validation (n = 5).

<sup>b</sup>Average of three different days of QC method validation (n = 15).

### 2.4.4. Matrix effect and storage stability

To evaluate the matrix effect, two types of calibration curves were constructed (non-IS corrected and IS-corrected curves) in both blood and in aqueous samples. The ratio of slopes ( $m_{\text{blood}}/m_{\text{aq}}$ ) was 0.90 (Table 2.4), indicating only a minor matrix effect for the analysis of DMTS in blood. Moreover, the IS-corrected slope ratio ( $m_{\text{blood}}/m_{\text{aq}}$ ) was 0.98,

revealing the importance of IS for correcting for any loss of analyte signal during DMTS analysis process.

**Table 2.4:** Slopes obtained from non-IS corrected and IS-corrected calibration curves of DMTS.

Calibration curve	$m_{\text{blood}}$	$m_{\text{aq}}$	$m_{\text{blood}}/m_{\text{aq}}$	Remark
Non-IS corrected	0.98	1.09	0.90	Minor matrix effect
IS-corrected	1.13	1.15	0.98	Corrected matrix effect

The short-term stability of DMTS in blood was evaluated in the autosampler over 24 h at ambient temperature and under multiple FT cycles. Results obtained from the autosampler stability showed that both QC concentrations of DMTS were unstable during the investigated time period. Without IS correction, the loss of DMTS signals from both QCs were approximately 50% of time zero after 10 h, which was expected, and likely caused mainly by the rapid enzymatic degradation of DMTS in blood. After 24 h, signal loss was exacerbated, with only about 16% of DMTS signal from both QCs recovered. Although the raw DMTS signals were unstable, the IS-corrected signals showed the necessary stability ( $\geq 90\%$ ) over the entire 24 h. Therefore, we recommended leaving prepared samples on the autosampler for periods of time not longer than 10 h, but if necessary, the IS correction can provide accurate quantification of DMTS over 24 h of storage on the autosampler. The FT stability test showed that DMTS is lost with each FT cycle, with almost 40% of DMTS signal loss after the first FT cycle. Similar outcomes were also reported by Manandhar et al. [45], reasoning that this is due to complex enzymatic activity. So, thawing and re-freezing blood samples should be avoided, but if it

is necessary, then IS should be added during sample preparation to correct the loss of DMTS signal during thawing process.

For long-term stability investigations, low and high QCs of DMTS spiked blood with IS were stored at  $-80\text{ }^{\circ}\text{C}$ , and the samples were analyzed periodically for 90 days. The purpose of this study was to evaluate the effectiveness of the storage protocol recommended by Manandhar et al. [45], where acid is used to denature blood proteins, IS is added to correct for loss of DMTS signal, and blood is flash frozen and stored at  $-80\text{ }^{\circ}\text{C}$ . Our results showed that the DMTS signal loss (without IS correction) from both QCs was about 40% over 60 days, which was in agreement with the findings from our FT stability. Over the next 30-day period the non-IS-corrected signal loss was drastic (i.e., almost 90% loss compared with Day “0”). However, IS-corrected DMTS signals were consistent ( $100\pm 10\%$  of Day 0), again showing to value of the IS to provide accurate DMTS concentrations during storage.

Considering the storage stability results in aggregate, similar to Manandhar et al. [45], we recommend immediate acid denaturation of biological samples, addition of DMTS- $d_6$  IS, snap freezing of the mixture and storage at  $-80\text{ }^{\circ}\text{C}$ . These frozen samples are stable for 60 days with IS correction. Multiple thawing and refreezing of samples should be avoided, and prepared samples should be stored on the autosampler  $\leq 10$  h.

#### ***2.4.5. Pharmacokinetic study of DMTS-treated animals***

The validated DHS-GC-MS method was applied to the analysis of blood samples from a pharmacokinetic study of DMTS in treated rats. Figure 2.2 shows the chromatograms of treated and untreated rat blood. DMTS was detected at 3.65 min,

whereas no peak was found at the retention time of DMTS in the blood of untreated rats. This slight shift in retention time is due to the installation of a new column before the analysis of pharmacokinetic study samples.

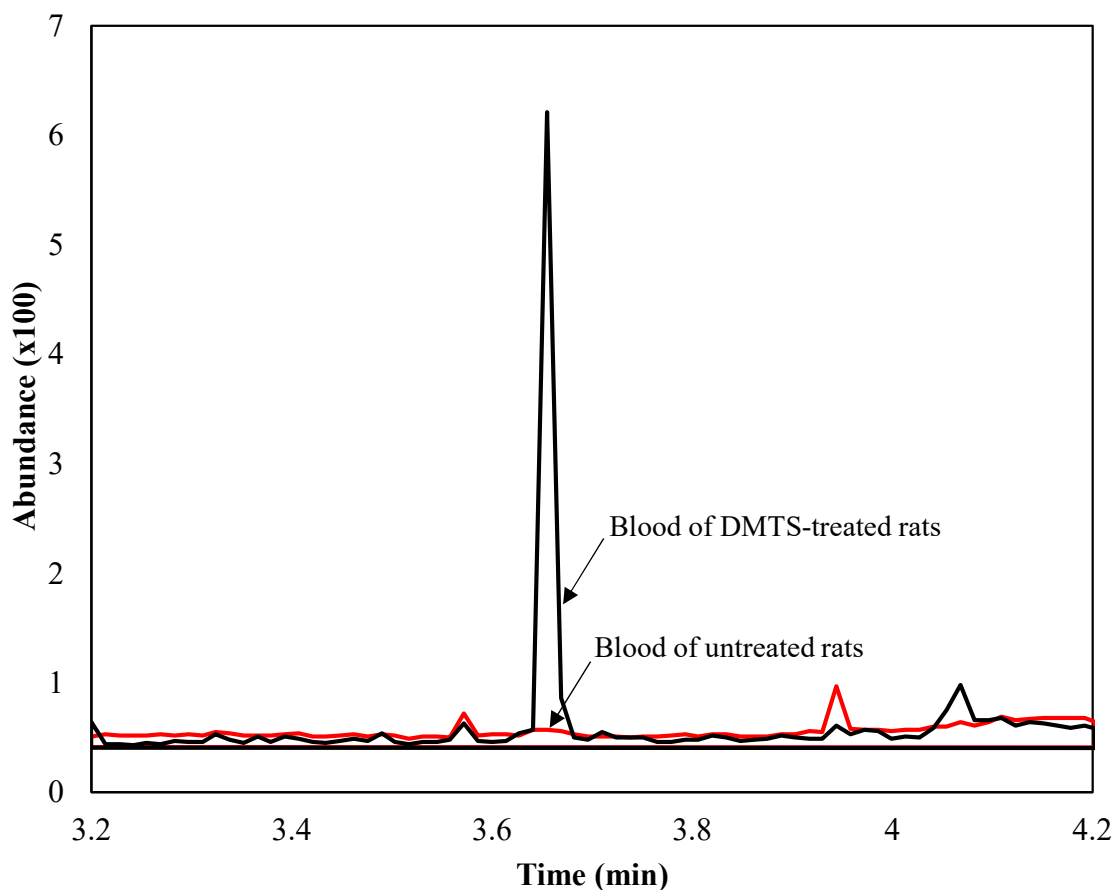


**Figure 2.2.** Representative GC-MS chromatograms of the blood of DMTS-treated and untreated rats ( $m/z$  126).

Figure 2.3 shows the plasma concentration-time curve of DMTS pharmacokinetics in rats. In terms of the DHS-GC-MS analysis of DMTS, the relatively low DMTS concentrations found in the blood of IM-treated rats mean that both the HPLC-UV and SPME-GC-MS techniques (Table 2.1) would not allow quantification of DMTS-spiked blood concentrations, even at  $C_{\max}$ , without extensive modification. Also, while it is a

possibility that the SBSE-GC-MS method may allow quantification of DMTS, the current method would need to be modified to allow analysis of lower volumes of blood.

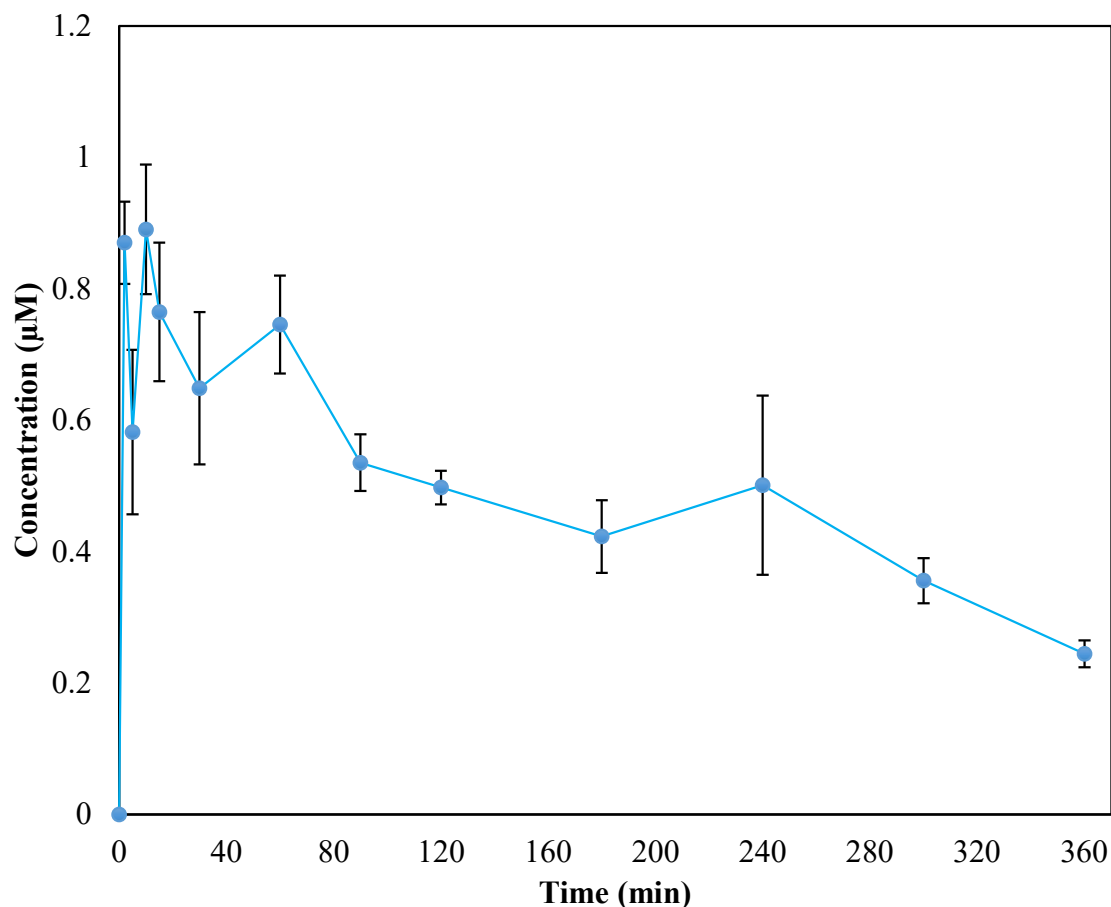


**Figure 2.3.** Blood concentration-time behavior of DMTS following IM administration of DMTS solution to rats. Each value is expressed as mean  $\pm$  SEM ( $n = 5$ ).

The pharmacokinetic results, although preliminary, reveal that DMTS is absorbed and distributed very quickly with a  $C_{\max}$  (the maximum concentration of a drug achieved in the plasma following dose administration) and  $t_{\max}$  (the time at which  $C_{\max}$  is attained) of  $0.89 \pm 0.09 \mu\text{M}$  and 10 min, respectively. Moreover, the blood DMTS concentration at the earliest time point (2 min) ( $0.87 \pm 0.06 \mu\text{M}$ ) was not significantly different from maximum concentration. This quick distribution of DMTS from intermuscular

administration is promising, in that it should allow fast treatment of cyanide throughout the body by untrained personnel. Additionally, DMTS showed a long elimination half-life ( $t_{1/2} = 630$  min or 10.5 h), with an estimated elimination rate constant ( $k_E$ ) of  $0.0011 \text{ min}^{-1}$ . This behavior allows early and continuous protection for long periods of time after DMTS treatment. Overall, this preliminary pharmacokinetic data showed impressive behavior of DMTS, most notably quick onset of action and slow elimination.

## 2.5. Conclusions

A simple, relatively affordable, and highly sensitive DHS-GC-MS method for the rapid analysis of DMTS in blood was developed. When considered in aggregate this validated method is superior to other published approaches in terms of its ability to detect and quantify low concentrations of DMTS (0.04 and 0.2  $\mu\text{M}$ , respectively), its simple and rapid sample preparation scheme (<10 min), and the low required blood volume (50  $\mu\text{L}$ ). Relative to other methods of DMTS analysis from blood, the method presented here produced consistently good recovery, high sensitivity, excellent accuracy, outstanding precision, and minimal matrix effect. Moreover, the recommended storage procedure allows analysis of blood samples for DMTS up to 60 days following collection. Because of its advantages, this method should be considered the current “gold-standard” method for the analysis of DMTS blood concentrations from drug development studies of DMTS.

## 2.6. Acknowledgement

The research described was supported by interagency agreements (AOD16026-001-00000/A120-B.P2016-01 and AOD18015-001-00000/MRICD-IAA-18-0129-00)

between the NIH Office of the Director (OD) and the U.S. Army Medical Research Institute of Chemical Defense under the oversight of the Chemical Countermeasures Research Program (CCRP) within the Office of Biodefense Research (OBRS) at the National Institute of Allergy and Infectious Diseases (NIAID/NIH). Any opinions, findings and conclusions or recommendations expressed in this material are solely those of the authors and do not necessarily represent the official views of the CCRP, NIAID, NIH, HHS, USAMRAA, USAMRICD or DoD.

### **Chapter 3. Analysis of the Soil Fumigant, Dimethyl Disulfide, in Swine Blood by Dynamic Headspace Gas Chromatography–Mass Spectroscopy**

#### **3.1. Abstract**

Plant parasites and soilborne pathogens directly reduce the overall yield of crops, vegetables, and fruits, negatively impacting the market demand for these products and their net profitability. While preplant soil fumigation helps maintain the consistent production quality of high-value cash crops, most soil fumigants are toxic to off-target species, including humans. Dimethyl disulfide (DMDS) has recently been introduced as a relatively low toxicity soil fumigant. Although DMDS exhibits low toxicity compared to other soil fumigants, it is volatile and exposure can cause eye, nasal, and upper respiratory tract irritation, skin irritation, nausea, dizziness, headache, and fatigue. While there is one analysis method available for DMDS from biological matrices, it has significant disadvantages. Hence, in this study, a dynamic headspace gas chromatography–mass spectroscopy (DHS-GC-MS) method was developed for the analysis of DMDS in swine whole blood. This method is highly sensitive and requires only three steps: 1) acid denaturation, 2) addition of internal standard, and 3) DHS-GC-MS analysis. The method produced a wide linear range from 0.1 – 200  $\mu\text{M}$  with an excellent limit of detection of 30 nM. Intra- and interassay accuracy ( $100\pm 14\%$  and  $100\pm 11\%$ , respectively) and precision ( $<5\%$  and  $<6\%$  relative standard deviation, respectively) were also excellent. The method worked well to quantify the DMDS level in the blood of dimethyl trisulfide (DMTS)-treated swine (i.e., DMDS is a byproduct of DMTS treatment) with no interfering substances at or around the retention time of DMDS (i.e., 2.7 min). This simple, rapid, and

extremely sensitive method can be used for the quantification of DMDS levels in blood to verify exposure to DMDS or to monitor levels of DMDS following DMTS treatment (e.g., for cyanide poisoning).

### **3.2. Introduction**

Preplant soil fumigation is the most direct and effective way to guarantee crop output and quality by controlling plant-parasitic nematodes, soilborne pathogens, and weeds [114, 115]. It is a popular process for high-value cash crops, including blueberries, cranberries, strawberries, vegetables (e.g., tomatoes), cucurbit crops (e.g., squash), nursery crops, fruit trees, forest nurseries and ornamental plants [116-118]. Its effectiveness, environmental impacts and human health risks are mostly dependent on the chemical used, the method of delivery, soil type and condition, and meteorological conditions [119]. While application of soil fumigants is popular, all soil fumigants are volatile, leading to an abundance of mobile toxic compounds in the air and creating human inhalation health hazards. These substances may also act as potential precursors for photochemical smog formed by the reaction of volatile organic chemicals (VOCs) with nitrogen oxides [119, 120]. While measures can be adopted to minimize human exposure (e.g., posting warning signs, entry restriction, on-site supervision, use of respiratory protection, tarp and buffer zone consideration), it is difficult to decrease the risk of exposure to negligible levels [117, 121]. Among the commercially available preplant soil fumigants, methyl bromide, metam sodium or potassium, dazomet, chloropicrin, 1,3-dichloropropene and dimethyl disulfide (DMDS) are commonly used [122].

Methyl bromide was the preferred preplant soil fumigant in the USA since its registration in 1961 until it was internationally banned in 2015. It is a colorless and nonflammable gas with a half-life in soil of about 55 days at 25 °C. Although it is a highly effective fumigant, it is acutely toxic to humans, producing headache, dizziness, nausea, eye, nose and throat irritation, chest and abdominal pain, delayed pulmonary edema, shortness of breath, and nervous system dysfunction if exposure is long term [123]. Additionally, it has been shown to have a role in depleting stratospheric ozone [116, 117].

Metam sodium, metam potassium, and dazomet are methyl isothiocyanate (MITC) generating fumigants, forming MITC as a breakdown product in soil, which kills nematodes, weeds, plant pathogens and insects. While MITC generators are considered more toxic than methyl bromide, they have short residence times in soil, dissipating at a rate of about 20% per day at 25 °C. MITC is a powerful lachrymator and has horseradish like odor. Short-term and prolonged exposure to MITC produces similar symptoms to methyl bromide [123, 124].

Chloropicrin, which has been used for decades to control soilborne fungi and nematodes, was first approved in the USA as a soil fumigant in 1975 [120]. It can be used alone or in combination with 1,3-dichloropropene or DMDS to broaden its effectiveness to pest control [123]. Because of its high vapor pressure (3.2 kPa at 25 °C), it disperses through the soil mainly as a gas and is nonpersistent in the soil, requiring tarps or adequate irrigation after application. Low level exposure causes eye and upper respiratory tract inflammation, but severe exposure can cause damage in the respiratory tract system and life-threatening pulmonary edema [123, 125].

1,3-Dichloropropene has been used as a preplant soil fumigant to control nematodes since the early 1950s. Like chloropicrin, it also has a low boiling point (104 °C), is slightly soluble in water, has low persistence in the soil, and requires tarps or adequate irrigation after application. The toxic effects of 1,3-dichloropropene include severe eye and respiratory irritation, kidney damage, and carcinogenic effects [120, 126]. In 1990, 1,3-dichloropropene was banned in California based on its kidney damaging behavior. It has also been banned as a pesticide in the European Union. Moreover, it was listed by the EPA as “likely to be carcinogenic to humans” [120, 123].

Because of the disadvantages associated with current soil fumigants, the search for a more environment friendly, less toxic, economically feasible alternative is of great significance. DMDS is a recently approved soil fumigant that is used alone or in combination with chloropicrin to control soilborne pathogens, bacteria, fungi, and weeds. It was introduced in the US in 2010 and is now used worldwide. DMDS is a transparent, pale yellowish liquid with a half-life in air of about one hour [127, 128]. It evaporates readily from soil and does not persist or accumulate in the air or water. Because of its high vapor pressure, application of high-barrier tarps is necessary immediately after fumigation with DMDS and a buffer zone is also required to minimize unwanted exposure and to improve efficacy of the fumigant [117, 127]. DMDS has a strong garlic-like pungent odor that humans can detect at a very low concentrations (7-12 ppb) [129], therefore, humans can generally avoid high dose inhalation exposure to DMDS [130]. Three products containing DMDS are registered for use in the US (Table 3.1).

**Table 3.1:** List of approved DMDS containing soil fumigants.

<b>Product name</b>	<b>EPA registration number</b>	<b>First registered date</b>	<b>% DMDS</b>	<b>Applicable crops</b>
Paladin	55050-4	July 09, 2010	98.8	Blueberry, Caneberry, Cucumber, Eggplant, Forest nursery, Melon, Ornamental plant, Pepper, Squash, Strawberry, Tomato
Paladin EC	55050-5	July 09, 2010	93.8	Blueberry, Cucumber, Eggplant, Forest nursery, Fruit tree, Irrigation system, Melon, Nursery crop, Ornamental plant, Pepper, Squash, Strawberry, Tomato, Vegetable crop
Paladin Pic-21	55050-7	June 14, 2016	78.1*	Blueberry, Cucumber, Eggplant, Forest nursery, Melon, Ornamental plant (field), Ornamental plant, Pepper, Squash, Strawberry, Tomato

\*Also contains Chloropicrin (20.9%)

Two of them, Paladin (98.8% DMDS) and Paladin EC (93.8% DMDS), were first registered in 2010. The third product, Paladin Pic-21, was approved for use in 2016, and is a mixture of 78.1% DMDS and 20.9% chloropicrin [117]. The addition of chloropicrin to DMDS fumigants broadens the pest control spectrum by significantly increasing the soil persistence of the combination fumigant [131, 132], but it also increases the overall toxicity. Although DMDS exhibits relatively low toxicity, it is a potential eye and skin irritant and can affect the central nervous system during acute exposure [127]. Exposure to large concentrations may cause nausea, headache, dizziness, and irritation of the upper respiratory tract. This leads to sneezing, coughing, sore throat, dyspnea, chest tightness, and a feeling of suffocation. Besides use as a soil fumigant, DMDS is also used as a food additive and as a sulfiding agent in the petrochemical industry [127, 133]. Moreover, it is

a breakdown product of dimethyl trisulfide (DMTS), a promising next generation cyanide antidote [17, 45, 134].

Although DMDS has been reported to cause acute illness [127, 135], there is no sensitive method available to determine the low level of exposure of DMDS in biological samples. One analytical method is available featuring a headspace gas chromatography-flame ionization detector (HS-GC-FID) screening technique [136], which has significant disadvantages. The main disadvantage of this method is that it is very insensitive, reporting an LOD of approximately 530  $\mu\text{M}$  (reported as 0.05 mg/mL). Additionally, the method can only quantify extremely high blood concentrations of DMDS (1.06 – 8.49 mM; reported as 0.1 – 0.8 mg/mL). The insensitivity of the method makes it suitable for only very high dose exposures to DMDS.

Because of the interest in DMDS as a fumigant and for other purposes, especially to evaluate DMDS concentrations in drug development studies of DMTS as a possible cyanide countermeasure, there is a critical need for a more sensitive method of analysis for DMDS from biological matrices. The objective of this study was to develop and validate an effective dynamic headspace (DHS) gas chromatography-mass spectrometry (GC-MS) analysis technique for the detection of DMDS in swine whole blood. The usefulness of the method was tested by determining DMDS levels produced in swine treated with DMTS.

### 3.3. Experimental

*Caution: Besides toxicity associated with DMDS, it and its deuterated internal standard (DMDS- $d_6$ ), both compounds are flammable liquids (i.e., flashpoints below 23 °C, “Category 2”) that are prone to ignite at normal working temperatures. Therefore,*

*DMDS was handled utilizing appropriate safeguards, including storage of DMDS solutions in a flammable material storage refrigerator and completing all sample preparation in a well-ventilated hood.*

### **3.3.1. Materials**

All reagents were high-performance liquid chromatographic (HPLC) grade unless otherwise noted. Methanol and sulfuric acid (certified ACS plus) were obtained from Fisher Scientific (Fair Lawn, NJ, USA). Reverse-osmosis water was purified to a resistivity of 18.2 M $\Omega$ -cm by passing through Lab Pro polishing unit from Labconco Corporation (Kansas City, KS, USA). DMDS and internal standard (IS), DMDS-d<sub>6</sub>, were purchased from Alfa Aesar (Heysham, Lancs, UK) and Toronto Research Chemicals (North York, ON, Canada), respectively, and stored in a flammable material storage refrigerator for future use. For each experiment, a freshly prepared working solution of DMDS (200 mM in methanol) was used to create calibrators and quality-control (QCs) samples. The stock solution of IS (5 mM) was prepared in methanol. This stock solution was further diluted to 500  $\mu$ M in DI water for each analysis and kept in a refrigerator. A thermal desorption (TD) tube filled with Tenax<sup>®</sup> TA sorptive material was purchased from Gerstel Inc. (Linthicum, MD, USA) and conditioned at 315 °C for 8 h under ultra-high purity nitrogen gas (Grade 5.0 from A-OX Welding Supply Co., Sioux Falls, SD, USA) flow (68 psi) using a tube conditioner (TC 2) and Gerstel Aux-controller 163 (Linthicum, MD, USA). One TD tube was used for the entire study, including method development and biological sample analysis.

### ***3.3.2. Biological samples***

For method development and validation, swine whole blood (non-sterile with sodium EDTA) was purchased from Pel-Freez Biologicals (Rogers, AR, USA) and kept in a  $-80^{\circ}\text{C}$  freezer (Thermo scientific, NJ, USA) until use. The whole blood was thawed and spiked with DMDS, where appropriate, for method development and validation.

Following validation, the effectiveness of the method was evaluated by analyzing the concentration of DMDS in the blood of DMTS-treated swine. This study was performed at University of Colorado Anschutz Medical Campus. All experiments were approved by the University of Colorado's Institutional Animal Care and Use Committee (IACUC) and complied with the regulations and guidelines of the Animal Welfare Act and the American Association for Accreditation of Laboratory Animal Care. Female Yorkshire swine (45-50 kg) were used for this study, and a detailed animal samples preparation process has been reported elsewhere [89]. In short, swine were anesthetized with ketamine and inhaled isoflurane. Following induction of anesthesia, animals were intubated, and sedation was maintained. Animals were instrumented for monitoring and recording of physiological parameters throughout the experiment. Following instrumentation, isoflurane was weaned until the animal was breathing spontaneously. Sedation was maintained with isoflurane throughout the experimental procedure to minimize pain and discomfort. After a 10-min acclimation period, animals were randomized into one of two treatment groups: IM DMTS or IM saline control. Potassium cyanide was then diluted in saline and delivered into the right jugular vein until 5 min after apnea occurred. At 5 min following apnea, animals were treated with either DMTS or saline control and the cyanide infusion was terminated. The DMTS treatment arm received 10 mg/kg DMTS injected into

the left gluteal muscle. Control animals received an equivalent volume of saline injected into the left gluteal muscle. Prior to cyanide exposure and administration of DMTS, baseline blood samples were collected. Following DMTS administration, blood samples were collected at 0.5, 1, 2, 5, 10, 20, 30, 40, 50, 60, 70, 80 and 90 min for evaluation of DMDS formation over time. Animals were observed and blood was drawn up to 90 min post-treatment or until death occurred, defined as a mean arterial pressure (MAP) of less than 30 mmHg for 10 min.

For each blood sample obtained from the animal study, 500  $\mu\text{L}$  of blood was withdrawn and transferred to a 2-mL centrifuge tube along with sulfuric acid (1 mL of 0.4% w/v in DI water) with mixing. IS (25  $\mu\text{L}$  of 42  $\mu\text{M}$ ) was immediately added and mixed well. All the prepared samples were then flash frozen and shipped (overnight) on dry ice to South Dakota State University (Brookings, SD, USA) for analysis. Upon receipt, the blood samples were stored in a  $-80\text{ }^{\circ}\text{C}$  freezer until analysis.

### ***3.3.3. Sample preparation for DHS-GC-MS analysis***

For method development and validation, standards were prepared by transferring 475  $\mu\text{L}$  of swine whole blood and 1 mL of aqueous sulfuric acid (0.4%) to a 4 mL glass screw-top vial. The mixture was then vortexed briefly (10 s) at 3000 rpm ( $252 \times g$ ) to ensure protein precipitation and enzyme denaturation. *Note that DMDS is unstable in non-denatured blood, therefore, sample preparation in acid denatured blood is a crucial step to minimize its rapid enzymatic degradation in blood.* Then, a 1:1 mixture of DMDS:IS solution (50  $\mu\text{L}$ ) was spiked into the acidified blood. The IS final concentration was 2  $\mu\text{M}$ . The standard was vortexed for 10 s at 3000 rpm ( $252 \times g$ ), and an aliquot (100  $\mu\text{L}$ ) of the

mixture was transferred to a 20-mL headspace (HS) vial with a polytetrafluoroethylene (PTFE) lined septum for analysis.

As indicated above, for samples obtained from DMTS-treated animals, acidification was performed immediately after withdrawing the blood. Subsequently, IS (2  $\mu$ M final concentration) was then quickly added, the samples were mixed and then flash frozen, and stored at -80 °C until immediately prior to analysis. At the time of analysis, the blood samples were thawed by running ambient tap water over the sample until the sample was completely thawed. An aliquot (100  $\mu$ L) of the acidified blood was transferred to a 20 mL headspace (HS) vial with a polytetrafluoroethylene (PTFE) lined septum for analysis.

#### ***3.3.4. DHS-GC-MS analysis***

DHS extraction was performed using a Gerstel automated DHS station via a MultiPurpose Sampler (MPS) (Linthicum, MD, USA). Sample analysis was accomplished via an Agilent GC-MS system (Wilmington, DE, USA) consisting of a gas chromatograph (6890N series) and mass selective detector (5975 series). Initially, the HS vial was incubated in the DHS station for 1 min at 40 °C, then the PTFE septum was punctured automatically by a dual needle assembly. Ultra-high purity nitrogen gas (Grade 5.0) was delivered through the needle at a rate of 30 mL/min for 10 min to purge the headspace of the sample vial to trap the DMDS on the Tenax<sup>®</sup> TA adsorptive material. The trapping, incubation and transfer heater temperatures were set at 28, 40 and 75 °C, respectively. After trapping, the TD tube was transferred to the thermal desorption unit (TDU) and heated from 30 °C to 280 °C at a rate of 720 °C/min to transfer DMDS to a cooled injection system (CIS) programmable temperature vaporization (PVT) type inlet, where a CIS liner trapped

the DMDS at -100 °C. Splitless desorption mode was used, and the TDU transfer heater temperature was maintained at 275 °C. To transfer the DMDS from the CIS to the GC column, the CIS temperature was increased to 275 °C at a rate of 12 °C/s before returning to its initial temperature.

For chromatographic separation, a DB5-MS bonded-phase column (30 m length × 0.25 mm inner diameter, 0.25 μm film thickness) purchased from J & W Scientific (Folsom, CA, USA) was used with helium (Ultra high purity, grade 5.0 from A-OX Welding Supply Co., Sioux Falls, SD, USA) as the carrier gas. The mobile phase flow rate was 1.0 mL/min and the column head pressure was 10.0 psi. The initial GC oven temperature was set at 30 °C for 1 min, then increased at 120 °C/min to 250 °C and held constant for 2 min, before returning to the initial temperature. An MS detector using electron ionization (EI) with an electron energy of 70 eV was used in selective ion monitoring (SIM) mode to monitor the quantification and identification ions of DMDS (m/z of 94 [CH<sub>3</sub>-S-S-CH<sub>3</sub>]<sup>+</sup> and 79 [CH<sub>3</sub>-S-S]<sup>+</sup>, respectively) and IS (m/z of 100 [CD<sub>3</sub>-S-S-CD<sub>3</sub>]<sup>+</sup> and 82 [CD<sub>3</sub>-S-S]<sup>+</sup>, respectively). The retention times for both DMDS and IS were about 2.7 min.

### ***3.3.5. Calibration, quantification, and limit of detection***

The method validation was performed by generally following the Food and Drug Administration (FDA) bioanalytical method validation guidelines [106, 107, 137]. The calibration behavior of DMDS was evaluated by constructing six calibration curves over the preliminary dynamic range (i.e., 0.1 – 200 μM). Weighted and unweighted linear ( $y = mx + c$ ) and unweighted log-log ( $\log y = m \log x + \log c$ ) regression models were evaluated

to determine the best fit model for analysis of DMDS. To quantify the goodness-of-fit (GoF) of the calibration models, percent residual accuracy (PRA, [108]) was used. For log-based calibration, the PRA was based on the linear values of the nominal and calculated concentrations by taking the anti-log of the logarithmic calculated and nominal concentrations for comparison. Because it is commonly used for evaluating GoF, the coefficient of determination ( $R^2$ ) was also calculated, but its value is predominantly based on the GoF of the highest concentration 2 or 3 calibrators and does not typically accurately quantify GoF throughout the calibration range [108]. Furthermore, the disadvantages of  $R^2$  are exacerbated when using a geometric series of concentrations for calibration standards and when calibration curves span 2–3 orders of magnitude, as in this study. In order to set the calibration range, the lower and upper limit of quantification (LLOQ and ULOQ, respectively) were required to satisfy the inclusion criteria of <10% relative standard deviation (RSD, as a measure of precision) and  $\pm 15\%$  percent deviation back-calculated from the nominal concentration (as a measure of accuracy). The limit of detection (LOD) was calculated by analyzing multiple concentrations of DMDS below the LLOQ and determining the lowest DMDS concentration which reproducibly produced a signal-to-noise (S/N) ratio of at least 3.

### ***3.3.6. Accuracy and precision***

For evaluation of intra- and inter-day method performance, the stock solution of DMDS (200 mM in methanol) was diluted in DI water to prepare calibration standards (0.1, 0.2, 0.5, 1, 2, 5, 10, 20, 50, 100 and 200  $\mu\text{M}$ ) and quality control (QC) standards (0.35, 7.5 and 75  $\mu\text{M}$ ) in acid-denatured swine blood. All QC standards (0.35, 7.5 and 75  $\mu\text{M}$ )

were prepared in quintuplicate and run in parallel with the calibration standards each day for three days. IS (2  $\mu\text{M}$ ) was spiked into blanks, calibrators, and QCs to correct for multiple sample-to-sample errors. Following analysis, calibration curves were constructed by plotting the log of the average peak-area signal ratios of DMDS to IS as a function of the log blood DMDS concentrations. The intraassay (calculated from each day's analysis) and interassay (calculated by comparing data obtained over three separate days, within five calendar days) accuracy and precision were quantified, with accuracy calculated as the percent difference of the calculated and nominal DMDS concentration of the QCs and precision quantified as the %RSD of the QCs. Precision and accuracy requirements were set at  $100 \pm 15\%$  and  $\leq 10\%$  RSD, respectively. Agilent ChemStation software (Santa Clara, CA, USA) was used to calculate the peak areas of both DMDS and IS.

### ***3.3.7. Recovery and matrix effect***

The recovery of DMDS was determined by comparing the signals of triplicates of low (0.35  $\mu\text{M}$ ), medium (7.5  $\mu\text{M}$ ) and high (75  $\mu\text{M}$ ) aqueous QCs with the equivalent concentration QCs in swine blood. Recovery (which was calculated as a percentage) was determined by dividing the peak area of DMDS signal in blood by the peak area of the equivalent concentration aqueous QC. The recovery obtained this way may not reflect true recovery because of the possible interaction (i.e., matrix effect) between DMDS and the blood matrix. Therefore, to evaluate the matrix effect, two calibration curves (abundance vs. concentration) of DMDS were prepared – one was prepared in DI water, where blood was replaced by DI water during sample preparation, and another one was constructed in swine blood. The ratio of the slopes of the calibration curves (i.e.,  $m_{\text{blood}}/m_{\text{aq}}$ ), where  $m_{\text{blood}}$

is the slope of the calibration curve from calibrators in swine blood and  $m_{\text{aq}}$  is the slope based on aqueous calibrators, was used to quantify the matrix effect, which was obtained from the log-log plots for blood and aqueous calibration curves. A slope ratio of  $<1$  and  $>1$  represent suppression and enhancement effects, respectively, whereas a ratio of 1 indicates negligible matrix effect. To evaluate the effectiveness of the IS for correcting for matrix effects, two other calibration curves were also constructed by plotting the signal ratio of DMDS to IS versus the concentration of DMDS for both aqueous and blood calibrators and comparing the slopes (i.e.,  $m_{\text{blood(IS-corrected)}}/m_{\text{aq(IS-corrected)}}$ ). For an IS to be considered effective, the difference in slopes should be negligible.

### ***3.3.8. Selectivity and stability***

The selectivity of this method was determined by confirming the consistent absence of interfering peak(s) at or near the retention time of DMDS in the blank swine blood sample. As a measure of selectivity, the resolution ( $R_s$ ) was calculated between the DMDS peak and the peak which consistently eluted nearest the DMDS retention time (2.7 min).

The short- and long-term stabilities of DMDS were assessed by analyzing triplicates of low and high QCs of DMDS-spiked blood samples at different storage conditions over multiple predetermined time periods. For all stability experiments, the stability of DMDS was measured as a percentage of the “time 0” signal. DMDS was considered stable if the peak response from a stability standard was within  $\pm 10\%$  of the initial (time 0) response. Bench-top, autosampler and freeze-thaw stabilities were evaluated as a part of the short-term stability study. For bench-top stability, DMDS-spiked non-denatured blood for both QCs were kept at room temperature for 0, 2, 5, 10 and 24 h prior

to analysis. Samples were then analyzed in triplicate after spiking acid (1 mL 0.4% H<sub>2</sub>SO<sub>4</sub>) and IS (25 µL 42 µM) to each QC. To evaluate autosampler stability, triplicates of low and high QCs were placed at on the GC autosampler at ambient temperature and the samples were then analyzed at approximately 0, 2, 5, 10, and 24 h to confirm the integrity of DMDS during the period of analysis. Because DMDS showed rapid degradation in blood, the ability of the IS to correct for the loss of DMDS during analysis was evaluated by comparing the IS-corrected signal at time “t” and time “0”.

Freeze-thaw stability samples were prepared by spiking DMTS in swine blood and treating in three different ways: (a) in non-denatured blood followed by unassisted freezing in the storage condition, (b) in non-denatured blood followed by flash-freezing, and (c) in acid-denatured blood followed by flash-freezing in liquid nitrogen. A summary of the freeze-thaw stability sample preparation is presented in Table 3.2.

**Table 3.2:** Freeze-thaw sample preparation.

Sample	Before storage			Before analysis	
	Acid added	IS added	Flash-freezing	Acid added	IS added
Set “a”	No	No	No	Yes	Yes
Set “b”	No	No	Yes	Yes	Yes
Set “c”	Yes	No	Yes	No	Yes

Five sets of low and high QCs were prepared in triplicates for all three conditions without IS. One set of samples was analyzed on the same day (Day “0”) after adding acid and IS (for “a” and “b”) or only IS (for “c”, as acid was already spiked for blood denaturation process before flash-freezing). To evaluate loss of DMDS with and without flash freezing, stability standard set “a” was frozen, unassisted, at -80 °C and the standard sets “b” and “c” were flash-frozen before storing the samples in a freezer. After 24 hr, all

stored samples were thawed at room temperature by applying ambient tap water over the base of the vials containing sample mixture. Immediately after fully thawing the standards, acid and IS were added to one set of “a” and “b” and IS alone was spiked to sample “c”, with the remaining three sets of QCs returned to the -80 °C freezer for storage. Thawed samples for analysis were vortexed at  $252 \times g$  for 10 s and analyzed. The entire process was repeated three more times to evaluate four freeze-thaw cycles.

Long-term DMDS stability was evaluated by analyzing triplicates of low and high QCs at 4, -30 and -80 °C to check how long DMDS samples can be stored under different stability conditions. For this, both QCs were prepared in bulk for each temperature condition to minimize unwanted sample-to-sample variation. The QCs were analyzed after 0, 1, 2, 5, 30, 45, 70 and 90 days. From the bulk preparations, triplicates of eight sets of low and high QCs were prepared by transferring one sample volume of an acid-denatured and DMDS-spiked blood sample mixture (i.e., 1.525 mL) to a 4-mL glass screw-top vial for each replicate. One set of QCs (i.e., “Day 0” sample) was analyzed on the day the standards were prepared and the other seven sets of samples for each temperature condition were stored at 4, -30, or -80 °C. Another set of three of long-term stability samples were prepared at the same time by following the same protocol, but flash-freezing was performed prior to storing at -80 °C using liquid nitrogen. The flash frozen storage stability standards were designated as “flash-frozen”, whereas standards frozen unassisted by placing directly in the freezer were designated as “unassisted freezing”. To perform the “Day-1” (24 h) stability experiment, triplicates of QCs (frozen both unassisted and with liquid nitrogen) were removed from all three storage conditions, thawed by applying ambient tap water over the base of the vials, and then analyzed. The same procedure was

followed to analyze the rest of the samples at designated storage times. For freeze-thaw and long-term stability experiments, the stability of DMDS was calculated as a percentage of the “Day 0” signal. DMDS was considered stable if the signal from the stored sample was  $\pm 10\%$  of the initial signal.

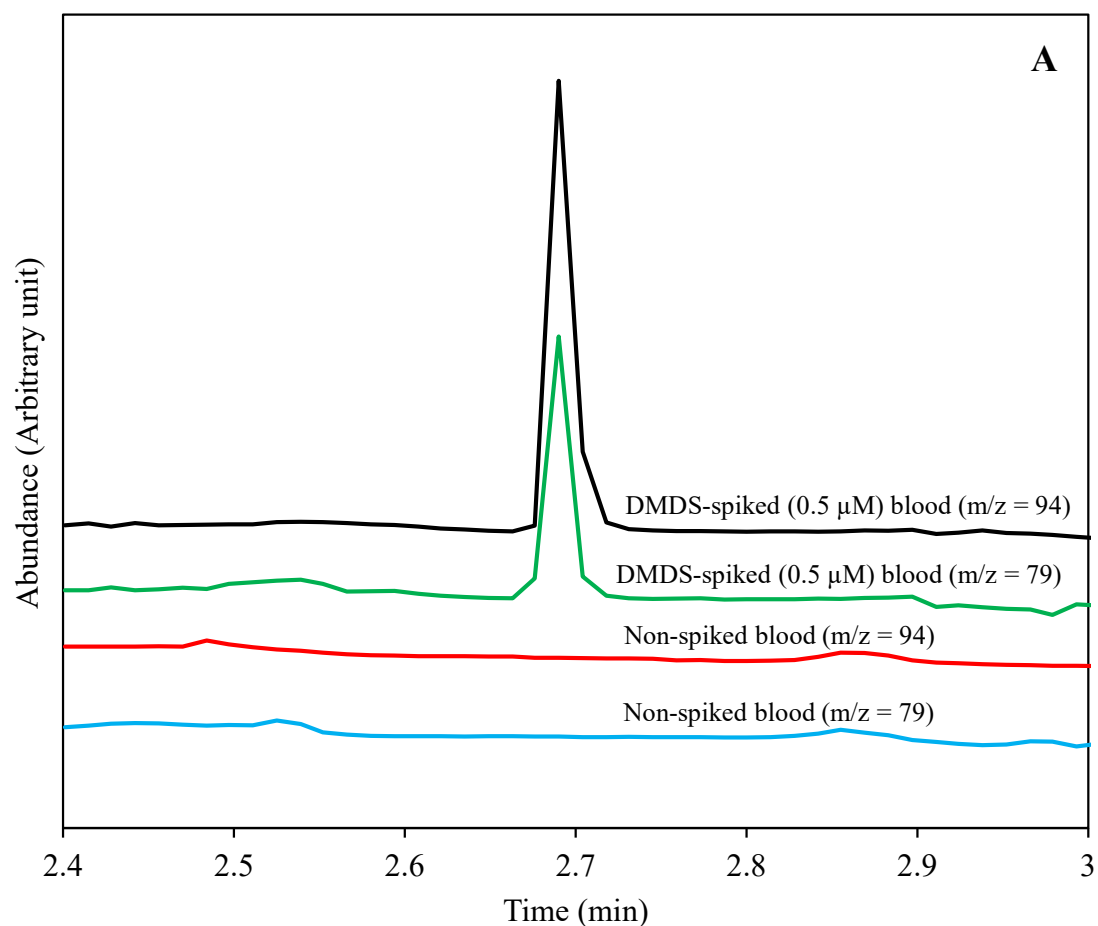
### **3.4. Results and discussion**

#### ***3.4.1. GC-MS analysis of DMDS***

The method proposed here is a sensitive analytical method for measurement of DMDS from a blood sample. The method features simple and rapid sample preparation from whole blood, requiring only three steps: 1) addition of sulfuric acid and IS, 2) mixing, and 3) analysis via DHS-GC-MS. This rapid sample preparation (<10 min) is vital for DMDS, as it minimizes the rapid degradation and unwanted evaporative loss of DMDS. A small volume of blood (100  $\mu\text{L}$ ) is required, and the method is environmentally friendly, requiring no organic solvents. With a sample preparation time of 10 min, and a total chromatographic analysis time (i.e., considering the DHS sample trapping time and CIS cooldown time) of about 12 min, the method can analyze 72 samples in parallel over a 24-h period. Moreover, the method requires minimal consumables and is more consistent than other related methods. The consistency of the method was aided by using one TD tube for the entirety of the study based on the robustness of the Tenax® sorbent and the fact that it does not directly contact the blood sample. Therefore, the DHS vials and caps and the pipette tips were the only consumables necessary for the method.

Figure 3.1 shows overlaid chromatograms of (A) DMDS-spiked blood (0.5  $\mu\text{M}$ ) and non-spiked blood (at  $m/z = 94$  and  $79$ ), and (B) IS-spiked blood (2  $\mu\text{M}$ ) and non-spiked

blood (at  $m/z = 100$  and  $82$ ). The peaks for both DMDS and the DMDS- $d_6$  eluted at about 2.7 min, with no interfering peaks observed at or near the retention time of DMDS. The resolution ( $R_s$ ) of DMDS and the closest consistently eluting peak (2.95 min) for the quantification ion ( $m/z$  of 94) was 4.76, indicating excellent selectivity. Moreover, both DMDS and its IS showed sharp and generally symmetrical peaks, with peak asymmetry factors ( $A_s$ ) of  $<1.4$  and  $<1.3$ , respectively, indicating only slight tailing. Tailing factors ( $T_f$ ) of 1.32 for DMDS and 1.23 for the IS, also indicate slight tailing and were well within the acceptable range ( $T_f < 2.0$ ). The number of theoretical plates ( $N$ ) was about  $2 \times 10^5$  (calculated based on DMDS), indicating excellent column efficiency.



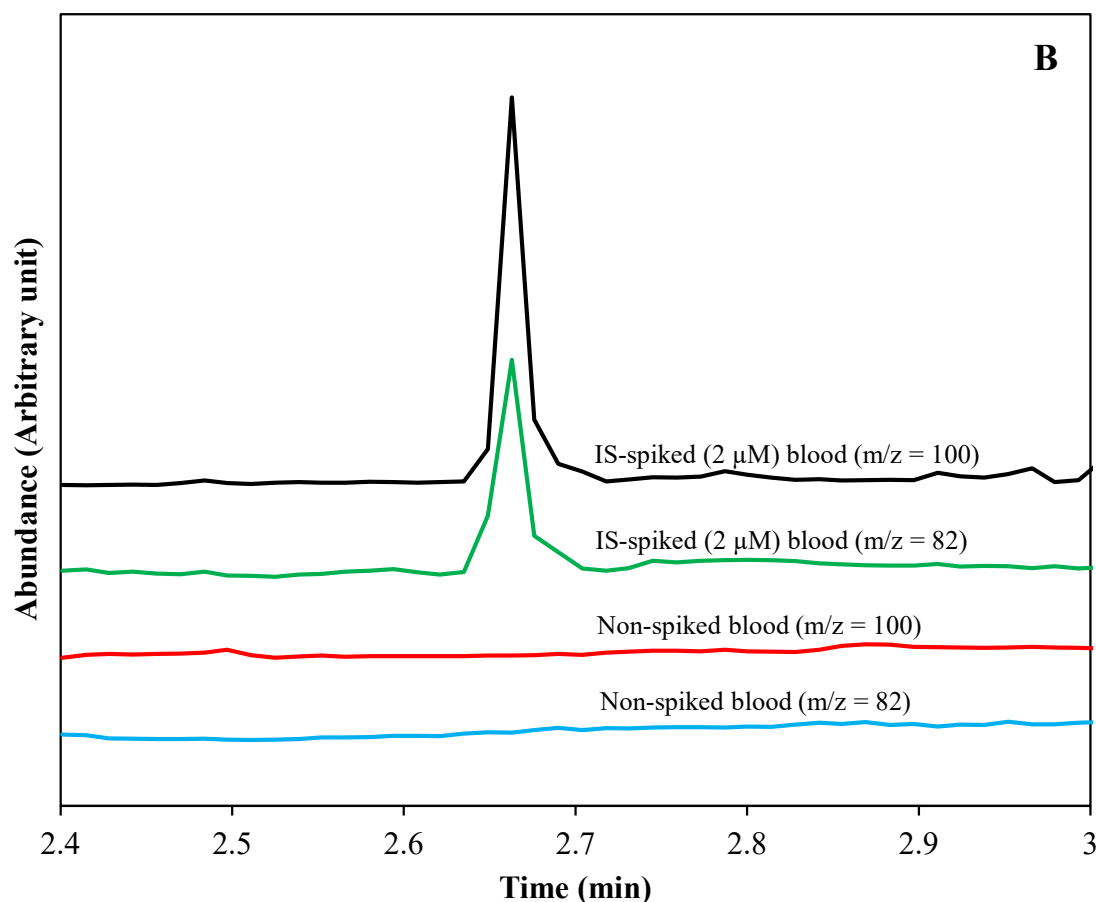


**Figure 3.1.** GC-MS chromatograms (in SIM mode) of A) DMDS-spiked ( $0.5 \mu\text{M}$ ) and non-spiked blood at  $m/z$  of 94 (quantification ion, *upper trace*) and  $m/z$  of 79 (qualification ion, *lower trace*), and B) IS-spiked ( $2 \mu\text{M}$ ) and non-spiked blood at  $m/z$  of 100 (quantification ion, *upper trace*) and at  $m/z$  of 82 (qualification ion, *lower trace*).

### 3.4.2. Dynamic range, limit of detection, and sensitivity

Calibration curves of DMDS in swine blood were initially evaluated in the range of  $0.02\text{-}200 \mu\text{M}$ . Both linear and log-log regression models were used over multiple calibration ranges to analyze the calibration behavior of DMDS. Both visual inspection and GoF parameters confirmed that a log-log regression model was the best fit model for DMDS calibration. This observation matched the calibration behavior of DMTS, which is structurally similar to DMDS (i.e., the only difference between DMDS and DMTS is a single sulfur atom) [17]. Once the calibration model was confirmed and the dynamic range

was set, the lowest two calibrators (i.e., 0.02 and 0.05  $\mu\text{M}$ ), fell outside of the linear range. Therefore, the dynamic range for DMDS was 0.1 to 200  $\mu\text{M}$  using a log-log regression model.

Table 3.3 shows the consistency of three separate calibration curves of DMDS prepared on three consecutive days. All three calibration curves showed consistent slopes (i.e., mean  $m_{\text{blood}} = 1.11$ , with a standard deviation of 0.02), intercepts (i.e., average  $b_{\text{blood}} = 0.32$ , with a standard deviation of 0.04), PRA ( $\geq 90\%$ ) and  $R^2$  ( $\geq 0.990$ ) values. The PRA values for all the calibration curves ( $\geq 90\%$ ) indicated an excellent fit of all the data over the calibration range [108].

**Table 3.3:** Calibration curve equations and goodness-of-fit analysis.

Day	Equation	PRA	$R^2$
Day-1	$\log y = 1.13 \log x - 0.36$	91.4	0.9984
Day-2	$\log y = 1.11 \log x - 0.29$	90.5	0.9982
Day-3	$\log y = 1.09 \log x - 0.32$	92.5	0.9987

The current method produced an excellent LOD of 30 nM. This high sensitivity is important to detect low level exposure to DMDS, in turn helping to identify the extent of community exposure in any unwanted or accidental release of DMDS, such as the mass DMDS exposure event in Florida in 2016 [127].

### 3.4.3. Accuracy and Precision

Three QCs (0.35, 7.5 and 75  $\mu\text{M}$ ) were analyzed in quintuplicate on three separate days to evaluate the accuracy and precision of the method. The experiment was performed on three different days over a period of five calendar days and the results were evaluated

following FDA method validation guidelines [137]. Although DMDS is very unstable in blood, excellent intraassay accuracy ( $100 \pm 8$ -14%) and precision (<5% RSD), and interassay accuracy ( $100 \pm 11$ %) and precision (<6% RSD) were observed, as shown in Table 3.4.

**Table 3.4:** Intra- and interassay accuracy and precision for analysis of DMDS in spiked swine blood.

Conc ( $\mu$ M)	Intraassay						Interassay	
	Accuracy (%) <sup>a</sup>			Precision (%RSD) <sup>a</sup>			Accuracy (%) <sup>b</sup>	Precision (%RSD) <sup>b</sup>
	Day 1	Day 2	Day 3	Day 1	Day 2	Day 3		
0.35	100 $\pm$ 12.8	100 $\pm$ 8.6	100 $\pm$ 4.0	3.4	4.5	4.2	100 $\pm$ 8.5	5.2
7.5	100 $\pm$ 12.8	100 $\pm$ 6.4	100 $\pm$ 12.8	0.9	3.9	4.0	100 $\pm$ 10.6	4.2
75	100 $\pm$ 12.9	100 $\pm$ 6.9	100 $\pm$ 13.3	1.3	3.6	4.2	100 $\pm$ 11.0	4.2

<sup>a</sup>Calculate from each day's analysis of high, medium, and low QCs (n = 5). Accuracy is measured as the percent difference of the calculated and nominal concentration of QCs, whereas precision is calculated as the %RSD of the calculated concentration of the QCs.

<sup>b</sup>Aggregate of three days of QC method validation (n = 15) over a period of five calendar days. Both accuracy and precision represent the maximum deviation from the nominal concentration of the QCs.

The excellent accuracy and precision were a function of the ability of the IS to correct for several potential errors, inconsistent recovery, and correction for matrix effect. Acid denaturation of the blood also helped provide consistency by minimizing DMDS degradation and potential protein binding.

#### **3.4.4. Matrix effect and recovery**

The matrix effect was assessed by constructing two DMDS calibration curves in DI water and blood, and comparing the slopes (i.e.,  $m_{\text{blood}}/m_{\text{aq}}$ ). Both non-IS-corrected (abundance vs. concentration) and IS-corrected (signal ratio vs. concentration) calibration

curves were evaluated to determine the importance of the IS. The ratio of slopes obtained from non-IS-corrected samples was 0.85, indicating a minor DMDS-blood matrix interaction. The minor signal suppression caused by the matrix was minimized when IS was incorporated, producing an IS-corrected slope ratio of 0.95.

The recoveries of DMDS in swine blood for low, medium, and high QCs were 98, 95, and 86%, respectively. The obtained recoveries of DMDS were very promising, considering its tendency to undergo rapid enzymatic degradation and evaporative loss in blood. While the high QC recovery was <90%, the IS readily corrected for this signal loss (as mentioned in the matrix effect), producing an IS-corrected signal recovery of 98%.

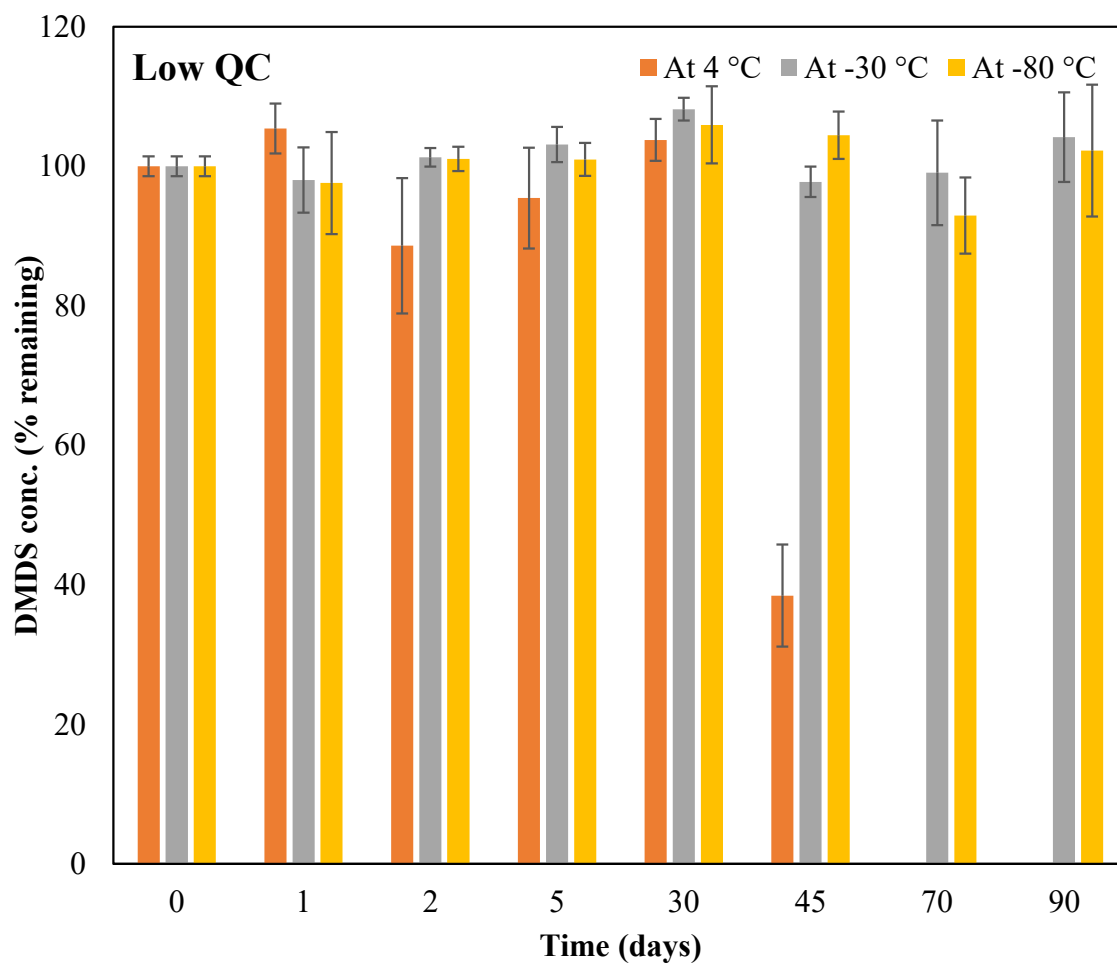
#### ***3.4.5. DMDS storage stability***

The short and long-term stability of DMDS were evaluated under multiple storage conditions. The bench-top and autosampler storage stabilities of DMDS were evaluated using high and low QCs. For the bench-top stability experiment, DMDS was very unstable in spiked non-denatured blood, even after 2 h, where the signal recoveries for the low and high QCs were only 7.26 and 11.13% of the original signal, respectively. DMDS was undetectable for the low and high QCs at 5 and 10 h, respectively. For autosampler stability, DMDS was stable ( $100\pm 10\%$  of the time "0" signal) for 5 and 10 h for the low and high QCs, respectively. While DMDS was considered unstable after 5-10 h on the autosampler, IS-corrected signals for both QCs were stable on the autosampler over the 24-h time period tested. The freeze-thaw (FT) stability of DMDS was tested over four FT cycles. The DMDS QCs showed gradual degradation of DMDS signals with each FT cycle for all three methods of preparation (Table 3.2). Maximum degradation was observed for non-

denatured and non-flash-frozen samples, producing only about 40% of the initial signal after the first FT cycle. DMDS spiked into acid-denatured blood followed by flash-freezing showed less degradation (about 70% signal recovery after first FT cycle), but DMDS was still considered unstable. This quick degradation was expected because DMDS showed rapid enzymatic degradation in non-denatured blood. Although both acid-denaturation and flash-freezing helped to minimize DMDS degradation for two sets of flash-frozen samples, the DMDS was still considered unstable during the FT process. Incomplete recoveries of DMDS in acid-denatured samples could be attributed to the evaporative loss during thawing process. Therefore, freezing and thawing of DMDS-spiked blood samples should be avoided and addition of IS prior to freezing is essential.

The long-term stability of DMDS was evaluated for up to 90 days for both low and high QCs, with IS, at 4, -30 and -80 °C. Two sets of frozen samples (i.e., the samples to be stored at -30 and -80 °C) were prepared and labeled as “flash-frozen” and “unassisted freezing” to further evaluate the effectiveness of flash freezing. Similar to the FT stability findings above, the flash frozen samples were much more stable than samples frozen unassisted. Specifically, DMDS signals recovered from unassisted freezing produced signals <90% of the original signal after only one day of storage. Figure 3.2 shows the results from the long-term stability experiment, considering only the flash frozen samples for storage at -30 and -80 °C. The IS-corrected signals for DMDS were consistent at all three temperature conditions until Day 30. After Day 30, samples stored at 4 °C showed visible changes (i.e., all started to coagulate and turn into non-uniform mixtures), and the IS-corrected signal loss was drastic (only 45% signal recovery at Day 30 compared with

Day "0"). Samples stored at -30 and -80 °C did not change in appearance and IS-corrected signals were stable throughout the study period.



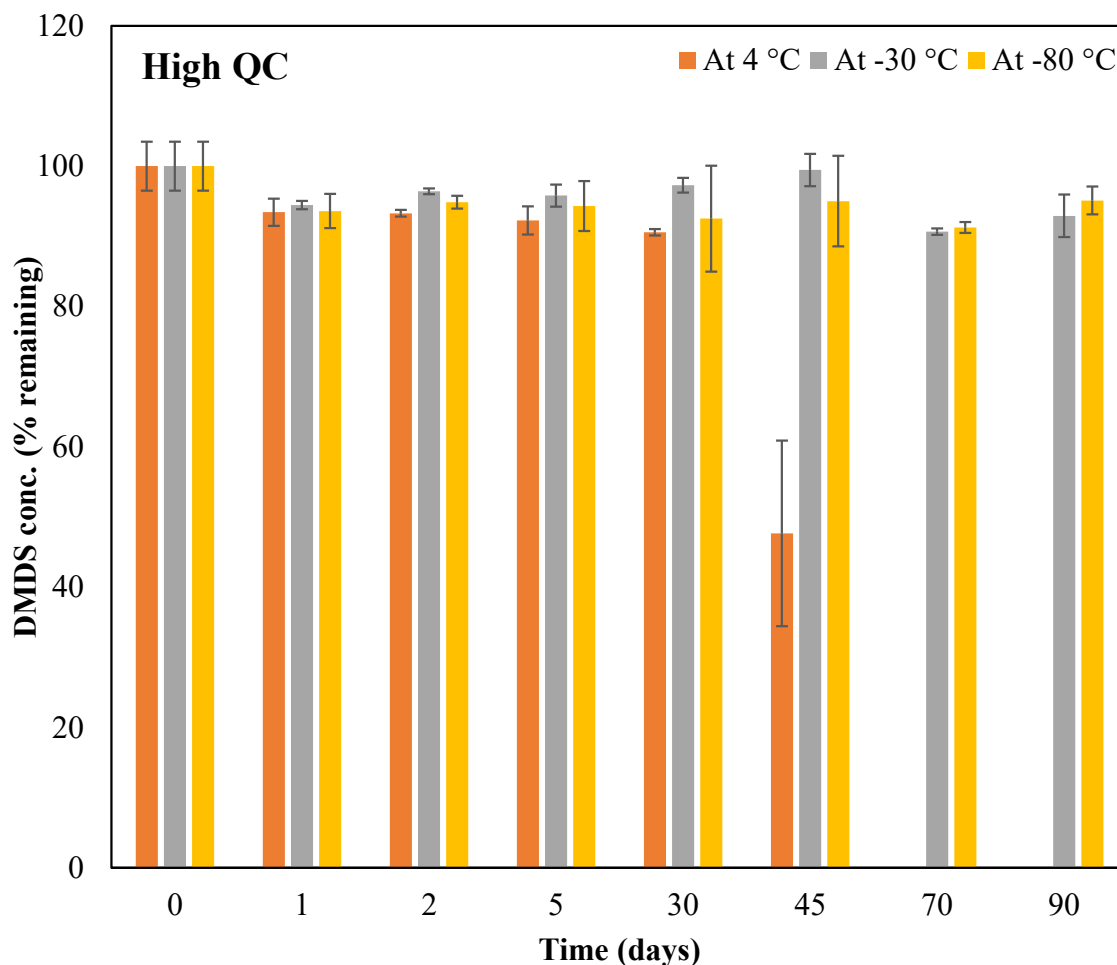


**Figure 3.2.** Evaluation of DMDS stability studies (with IS correction) during storage at 4, -30 and -80 °C, over 90-day period tested.

Based on aggregate storage stability results, three major observations can be drawn:

1) addition of IS before storing the sample is vital to obtain accurate DMDS concentrations following storage, 2) acid-denaturation followed by flash-freezing prior to storing the sample in the freezer helps minimize loss of DMDS, and 3) storage temperatures from 4 to -80 °C can be used to store blood samples for DMDS analysis for up to one month, but beyond that, it is recommended samples are stored at -30 or -80 °C. Overall, the best practice for storing blood samples for DMDS analysis is immediate acid denaturation of

the blood, addition of IS (DMDS-d<sub>6</sub>), flash-freezing of the sample and storage in a -80 °C freezer.

#### ***3.4.6. Analysis of DMDS in treated animals***

According to the United States Environmental Protection Agency, the DMDS vapor concentration of concern for human health is 55 ppb, based on a 24-hr acute rat inhalation study [138]. Considering this level of concern and that humans can smell very low levels of DMDS (7-12 ppb), humans can typically avoid high levels of inhalation exposure [127]. When considering the toxicity of DMDS in humans, there is very little information available. While there is no published study that describes the blood concentration of DMDS that is associated with DMDS toxicity, one report was published from China where a fatal volatile sulfur compound poisoning occurred at a bamboo pulp mill and the autopsy report revealed the presence of 3.1 mg/mL (32.9 mM) DMDS [136]. The DHS-GC-MS method reported here was used to analyze the blood concentration of DMDS generated from DMTS-treated pigs. Representative chromatograms were obtained (m/z of 94) by analyzing the blood from DMTS-treated and untreated pigs are shown in Figure 3.3. DMDS eluted at 2.70 min with no interfering peaks at the retention time of DMDS in untreated pigs and detectable levels of DMDS ranged from 0.1 – 11 μM. Therefore, the maximum concentration of DMDS in the swine blood was 3,000 times lower than the blood concentration of the victim of the volatile sulfur compound poisoning detailed above.

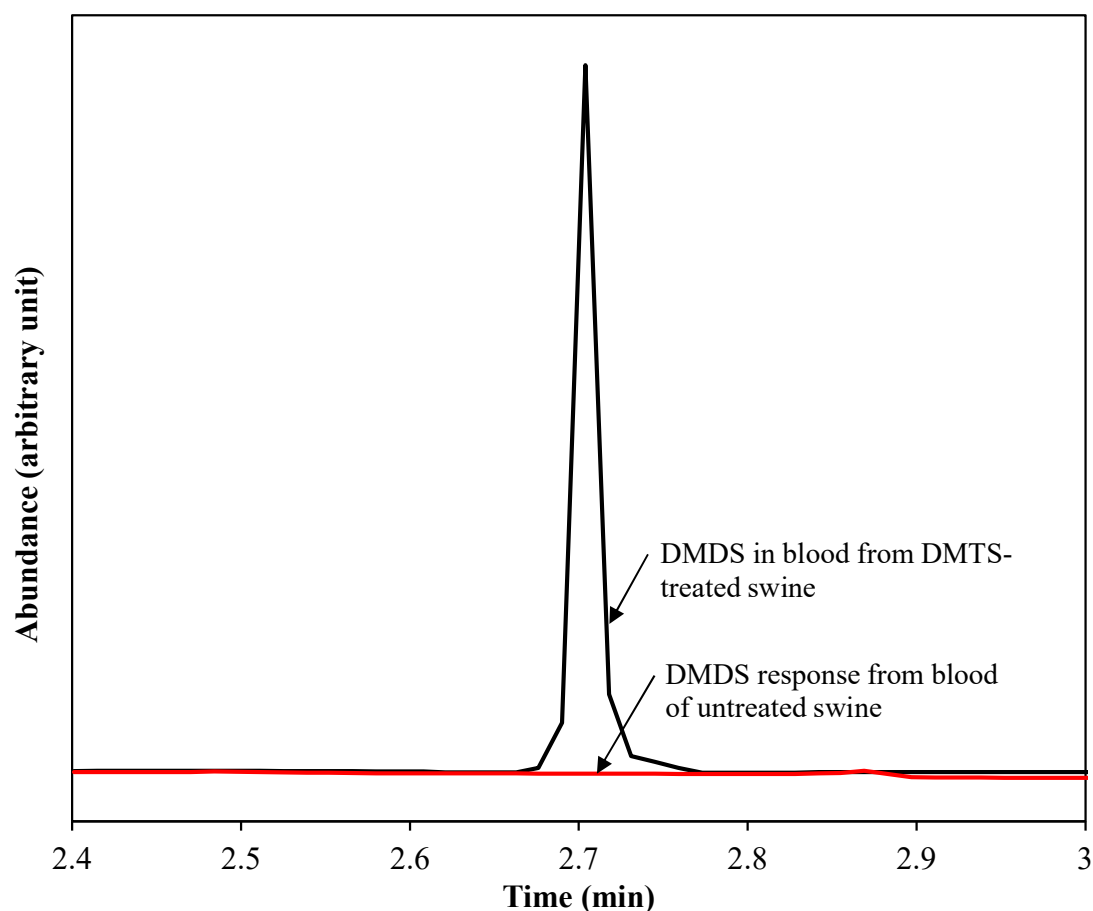


**Figure 3.3.** Representative GC–MS chromatograms of DMDS (10.46  $\mu\text{M}$ ) in the blood of DMTS-treated and untreated swine (m/z of 94).

To further evaluate how close DMDS production from DMTS treatment approaches toxic levels, we converted the known rat  $\text{LD}_{50}$  value for acute oral exposure to DMDS (i.e., 190 mg/kg [138]) to a swine  $\text{LD}_{50}$  (33.7 mg/kg) using standard human equivalent dose calculations [139]. Considering the swine were administered 10 mg/kg of DMTS and we have experimentally observed about 50% conversion of DMTS to DMDS in swine blood, we estimated the “dose” of DMDS as 5 mg/kg. Therefore, based on these assumptions and assuming equivalency of the oral and IM  $\text{LD}_{50}$  values, the estimated IM dose of DMDS in this study is about 6.7 times lower than the  $\text{LD}_{50}$  of DMDS. Because

large assumptions are necessary to complete this comparison since there is a paucity of toxicity information for DMDS, further evaluation of DMDS toxicity should be undertaken.

### **3.5. Conclusions**

A simple, highly sensitive, environment friendly and cost-effective DHS-GC-MS method was developed for the rapid analysis of DMDS in blood. This method is the first validated method for analysis of DMDS in a biological matrix that can investigate DMDS toxicity and the severity of community exposure during DMDS fumigation. This method does not require any toxic organic solvents for extraction and can detect and quantify as low as 30 and 100 nM of DMDS, respectively. Our recommended storage procedure allows accurate and reproducible analysis of DMDS blood samples up to 90 days following collection. The availability of this method now allows quantification of DMDS blood concentrations from toxicokinetic studies, occupational or accidental exposure and drug development studies.

### **3.6. Acknowledgement**

The research described was supported by interagency agreements (AOD16026-001-00000/A120-B.P2016-01 and AOD18015-001-00000/MRICD-IAA-18-0129-00) between the NIH Office of the Director (OD) and the U.S. Army Medical Research Institute of Chemical Defense under the oversight of the Chemical Countermeasures Research Program (CCRP) within the Office of Biodefense Research (OBRS) at the National Institute of Allergy and Infectious Diseases (NIAID/NIH). Any opinions, findings

and conclusions or recommendations expressed in this material are solely those of the authors and do not necessarily represent the official views of the CCRP, NIAID, NIH, HHS, USAMRAA, USAMRICD or DoD. Dennean S. Lippner and Jessica N. Winborn were supported in part by an appointment to the Research Participation Program for the U.S. Army Medical Research and Development Command administered by the Oak Ridge Institute for Science and Education through an agreement between the U.S. Department of Energy and the U.S. Medical Research and Development Command.

## **Chapter 4. Analysis of aminotetrazole cobinamide, a next-generation antidote for cyanide, hydrogen sulfide and methanethiol poisoning, in swine plasma by liquid chromatography-tandem mass spectrometry**

### **4.1. Abstract**

Cyanide and reduced sulfur compounds, especially hydrogen sulfide and methanethiol, are common toxic inhalation agents that inhibit mitochondrial cytochrome c oxidase and result in cellular hypoxia, cytotoxic anoxia, apnea, respiratory failure, cardiovascular collapse, seizure and potentially death. All are occupational gas exposure hazards and have the potential to cause mass casualties from industrial accidents or acts of terrorism, yet currently FDA-approved antidotes have major limitations, including difficult administration in mass-casualty settings. While aminotetrazole cobinamide (CbiAT) has recently gained attention because of its efficacy in treating each these metabolic poisons and its ability to address limitations of current antidotes, there is no method available for the analysis of CbiAT in any biological matrix. Hence, in this study, a simple and rapid liquid chromatography-tandem mass spectrometry (LC-MS/MS) method was developed and validated for the analysis of CbiAT in swine plasma. The method is extremely simple, consisting of protein precipitation, separation and drying of the supernatant, reconstitution in an aqueous solvent, and LC-MS/MS analysis. The method produced an LOD of 0.3  $\mu\text{M}$  with a wide dynamic range (2 – 500  $\mu\text{M}$ ). Inter- and intraassay accuracies ( $100\pm 12\%$  and  $100\pm 19\%$ , respectively) were acceptable and the precision ( $<12\%$  and  $<9\%$  relative standard deviation, respectively) was good. The developed method was used to analyze CbiAT from treated swine and the preliminary pharmacokinetic parameters showed

impressive antidotal behavior, most notably quick absorption and distribution ( $C_{\max}$  and  $t_{\max}$  of 44.7  $\mu\text{M}$  and 4 h, respectively) and slow elimination ( $t_{1/2} = 23.7$  h). This simple and rapid method can be used to facilitate the development of CbiAT as a therapeutic against toxic cyanide, hydrogen sulfide and methanethiol exposure.

## 4.2. Introduction

Exposure to cyanide ( $\text{CN}^-$  and HCN, inclusively represented as CN) and reduced sulfur compounds (RSCs, i.e., hydrogen sulfide ( $\text{H}_2\text{S}$ ) and methanethiol (MT)) occurs in a variety of settings, including occupational exposure and from acts of terrorism [22, 55, 93]. Although CN is extremely poisonous (e.g., rat  $\text{LC}_{50}$ , 5-min inhalation = 503 ppm [140, 141] and 50 mg can be lethal to humans [142]), it is still widely used in chemical industries to produce synthetic fibers and polymers, and for gold mining, electrolysis, electroplating, and pest control [17, 143]. Annual global production of CN is over 5.2 billion pounds [55]. Like CN, RSCs are extremely poisonous, with  $\text{LC}_{50}$  values in rats for 5-min of inhalation exposure of 444 and 675 ppm for  $\text{H}_2\text{S}$  and MT, respectively [71]. These compounds are commonly found in oil and gas industries, wastewater treatment facilities, plastic and paper mill industries, as well as in hot springs and volcanoes [68, 69].

CN,  $\text{H}_2\text{S}$  and MT each have similar mechanisms of toxicity. Once absorbed into the blood stream, these compounds inhibit mitochondrial cytochrome c oxidase, thereby terminating oxidative phosphorylation, interrupting the electron transport chain, reducing ATP production, and causing hyperlactatemia and metabolic acidosis [17, 20-22]. As a result, the common toxic outcomes include hypoxia, cytotoxic anoxia, cardiac arrhythmias, bronchospasm, respiratory paralysis, coma, and death [22, 36, 136]. These compounds

inhibit multiple other enzymes, including succinic dehydrogenase, carbonic anhydrase, and superoxide dismutase [26, 27]. Because the mechanisms of toxicity are similar, victims of CN, H<sub>2</sub>S and MT poisoning show essentially identical clinical symptoms. Therefore, it is desired to develop a single antidote that is effective against all of these poisons which can be administered by oral or intramuscular (IM) route, allowing more feasible administration during mass-exposure scenarios.

There are no currently Food and Drug Administration (FDA)-approved antidotes for either H<sub>2</sub>S or MT [22, 68] while there are effective FDA-approved antidotes for CN poisoning (i.e., hydroxocobalamin, as Cyanokit<sup>®</sup> and sodium nitrite/sodium thiosulfate, as Nithiodote<sup>®</sup>), each has major limitations [17]. Both the Cyanokit<sup>®</sup> and Nithiodote<sup>®</sup> require large doses and slow intravenous infusion, which necessitates trained medical personnel and specialized equipment [55, 56]. These antidotes are expensive and a second dose is sometimes required based on the severity of poisoning [44, 57]. These disadvantages limit their applicability in the event of an industrial accident, structural fire, or terrorist attack, where rapid administration of antidote in a short period of time is necessary [57, 76]. Patients may even require special medical attention for antidote-induced adverse effects, such as dizziness, blurred vision, confusion, vomiting, cardiac arrhythmia, tachycardia, hypotension, hypertension, and methemoglobinemia [57-59]. The limitations of CN antidotes have necessitated the search for a more effective countermeasure.

To address the absence or limitations of current metabolic poison antidotes, aminotetrazole cobinamide (CbiAT) was developed as a prodrug of cobinamide (Cbi). CbiAT is effective for treating multiple metabolic poisons and can be IM administered. [22, 68, 95]. While Cbi is similar to cobalamin (i.e., it is the penultimate precursor in the

biosynthesis of hydroxocobalamin [22], it can bind two ligands versus one for cobalamin. Moreover, Cbi does not suffer from the negative *trans* effect of dimethyl-benzimidazole group on the binding site (i.e., coordinating to the central cobalt atom in the lower axial position) [55, 96]. As a result, depending on the formulation, a 3-10 times higher dose of hydroxocobalamin is required to produce the same therapeutic effect of Cbi [56, 91]. Additionally, in aqueous solution, Cbi, as aquohydroxocobinamide (AHCbi), shows five times more water solubility than hydroxocobalamin [96], allowing a smaller volume to be administered to produce the desired therapeutic effect. Because of its effectiveness as an antidote for metabolic poisons, Cbi has recently gained attention as a potent next generation antidote for CN, H<sub>2</sub>S and MT poisoning [22, 90-95]. While Cbi is a promising antidote, some formulations have presented challenges. For example, AHCbi is not a good drug candidate for IM injection because it interacts with the macromolecules at the injection site, which limits its rate of absorption [97]. To address these challenges, multiple formulations have been evaluated [22, 144] and CbiAT was found to produce the most advantageous characteristics for treatment of metabolic poisons, allowing for quick absorption after IM administration, while retaining effective binding of CN, H<sub>2</sub>S and MT [22].

In spite of the potential advantages of CbiAT over other countermeasures, there is no currently available analytical approach for the quantification of CbiAT in any biological matrix. Therefore, the objective of this study was to develop and validate an effective liquid chromatography-tandem mass spectrometry (LC-MS/MS) technique for the analysis of CbiAT in plasma to allow for further development of CbiAT as a next-generation antidote for CN, H<sub>2</sub>S and MT poisoning.

### 4.3. Experimental

#### 4.3.1. Reagents and standards

Sodium hydroxide (NaOH), ammonium hydroxide (NH<sub>4</sub>OH, 29% by weight), acetonitrile (ACN) and sodium cyanide (NaCN) were obtained from Fisher Scientific (Fair Lawn, NJ, USA). Ammonium formate and 5-amino-1H-tetrazole monohydrate (ATM) were purchased from Fluka Analytical (Sigma-Aldrich, St. Louis, MO, USA) and Alfa Aesar (Tewksbury, MA, USA), respectively. Aquohydroxocobinamide (AHCbi) was provided by Dr. Gerry R. Boss, MD, Department of Medicine, University of California, San Diego, La Jolla, CA 92093, USA, following synthesis [96]. Deionized water (DI water) was purified to a resistivity of 18.2 MΩ-cm using a Lab Pro polishing unit from Labconco Corporation (Kansas City, KS, USA). All reagents used in this experiment were of high-performance liquid chromatography (HPLC) grade, unless otherwise noted.

Stock solutions of AHCbi (10 mM prepared in an amber vial) and ATM (20 mM, pH = 7.4) were prepared in DI water and stored at 4 °C. Calibration and quality control (QC) standards of CbiAT were prepared by mixing AHCbi and ATM at a 1:1 molar ratio, leaving on the benchtop for 10 min, diluting to the desired concentration via serial dilutions in DI water, and spiking the aqueous CbiAT into swine plasma (1:9 ratio). CbiAT spiked plasma mixtures were then mixed well at 3,000 rpm (252 × g) for 10 s before sample preparation.

For protein denaturation, 10% NH<sub>4</sub>OH in ACN solution was used. This solution was prepared by transferring 7.86 mL of NH<sub>4</sub>OH (29% by weight) in a 100-mL volumetric flask, followed by addition of ACN to the 100-mL mark, capping tightly, mixing well and storing at room temperature for future use.

### ***4.3.2 Biological samples***

For analytical method development and validation, swine plasma (with heparin as anticoagulant) was obtained from Pel-Freez Biologicals (Rogers, AR, USA) and stored at  $-80\text{ }^{\circ}\text{C}$  until used. To evaluate the method's ability to detect CbiAT for drug development studies, the method was utilized to analyze swine plasma from a CbiAT pharmacokinetic study performed at University of Colorado Anschutz Medical Campus (Aurora, CO, USA). This study was approved by the University of Colorado's Institutional Animal Care and Use Committee (IACUC) and complied with the regulations and guidelines of the Animal Welfare Act and the American Association for Accreditation of Laboratory Animal Care. One female Yorkshire cross swine, weighing about 50 kg, was used for this study. Anesthesia was induced with 10 mg/kg ketamine (MWI, Boise, ID) and sedation maintained with 1-3% isoflurane (MWI, Boise, ID) with an  $\text{FiO}_2$  of 21%. The animal was intubated with an 8.0 mm cuffed endotracheal tube (Teleflex, Morrisville, NC). Heart rate, arterial blood pressure, end tidal  $\text{CO}_2$ , oxygen saturation, and body temperature were monitored continuously throughout the study. The animal was treated intramuscularly with a dose of 75 mg/kg CbiAT, and blood was collected at 0 (baseline), 4, 24, 48, 72, 96, and 168 h post-injection. Collected blood was placed in lithium heparin tubes and centrifuged. Plasma was then transferred to 2-mL clean centrifuge tubes and shipped on ice (overnight) to South Dakota State University (Brookings, SD, USA) for the analysis. Upon receipt, the samples were stored at  $-80\text{ }^{\circ}\text{C}$  until analysis was performed with the validated CbiAT analysis technique.

#### ***4.3.3 Sample preparation for LC-MS/MS analysis***

CbiAT-spiked plasma (100  $\mu$ L) was first denatured by adding 700  $\mu$ L of 10%  $\text{NH}_4\text{OH}$  in ACN solution (see Section 2.1 for detailed preparation procedure). The mixture was then vortexed for 10 s at 3,000 rpm ( $252 \times g$ ) and cold centrifuged (at 8  $^\circ\text{C}$ ) for 20 min at 14,500 rpm ( $16,454 \times g$ ). Afterwards, 700  $\mu$ L of the supernatant was transferred into a 4-mL glass vial and dried with inert nitrogen gas for about 30 min at room temperature. The completely dried sample was then reconstituted with 100  $\mu$ L of 10% aqueous ACN solution, vortexed briefly ( $\sim 10$  s) at 3,000 rpm ( $252 \times g$ ), filtered using a 0.22  $\mu\text{m}$  tetrafluoropolyethylene membrane syringe filter, and the filtrate (100  $\mu$ L) was transferred into a glass insert assembled in a 2-mL HPLC vial for LC-MS/MS analysis.

#### ***4.3.4. LC-MS/MS analysis***

Liquid chromatographic analysis of CbiAT was conducted on a Shimadzu HPLC system (LC-20AD, Shimadzu Corp., Kyoto, Japan). A Phenomenex Synergi<sup>TM</sup> Fusion-RP column (50 mm length  $\times$  2 mm internal diameter, 4  $\mu\text{m}$  particle size and 80  $\text{Å}$  pore size) was used at ambient temperature for chromatographic separation. Ammonium formate (5 mM) in 10% ACN (mobile phase A) and ammonium formate (5 mM) in 90% ACN (mobile phase B) were used to separate CbiAT at a flow rate of 0.5 mL/min with a gradient of 0% B increased linearly to 100% over 0.5 min, held constant for 1.5 min, decreased to 0% B over 0.5 min, and held constant for 0.5 min to equilibrate between injections. A cooled autosampler (15  $^\circ\text{C}$ ) was used to store prepared samples, and the injection volume was set to 30  $\mu$ L. Mass spectroscopic analysis of CbiAT was performed by a tandem mass spectrometer (AB Sciex QTRAP 5500 MS, Framingham, MA, USA) using positive

polarity electrospray ionization (ESI). To identify abundant fragments, a standard solution of CbiAT was directly infused into mass spectrometer at a flow rate of 10  $\mu\text{L}/\text{min}$ . After infusion of CbiAT into the ESI, molecular ion (in the form of CbiAT dihydrate) of  $m/z$  1196.5 was identified ( $[\text{M} + \text{H}]^+$ ). Multiple reaction monitoring (MRM) transitions were identified based on most abundant product ions of CbiAT, and other parameters were optimized and are outlined in Table 4.1.

**Table 4.1:** MRM transitions, and optimized declustering potentials (DPs), entrance potentials (EPs), collision energies (CEs), and collision cell exit potentials (CXPs) for CbiAT analysis by LC-MS/MS.

Compound	Q1 ( $m/z$ )	Q3 ( $m/z$ )	Time (ms)	DP (V)	EP (V)	CE (V)	CXP (V)
CbiAT (Quantification)	1196.5	1028.6	100	177.47	3.44	57.97	18.23
CbiAT (Identification)	1196.5	989.7	100	159.11	7.16	76.49	12.85

For the method, CbiAT was analyzed in MRM mode and the data acquisition was performed using Analyst software (Applied Biosystems, Version 1.6.3). For the detection of CbiAT, nitrogen at a pressure of 40 psi was used as both curtain and nebulization gas. The ion spray voltage was set at 5,500 V with a source temperature of 500  $^{\circ}\text{C}$ . Nebulizer (GS1) and heater (GS2) gas pressures were 40 and 60 psi, respectively.

Carryover is a common problem with the analysis of Cbi species because it has a tendency to bind with the column and other LC-MS/MS components, including the autosampler syringe [56, 145]. A comprehensive cleaning protocol was devised by Dzisam et al. [56] to remove Cbi from LC-MS/MS systems. While this protocol eliminated carryover, it consisted of a large number of relatively complex steps, including separate

washing of (1) the LC system and (2) the column. According to this protocol, the LC system wash included three steps: (a) rinsing the system with DI water followed by aqueous ACN solutions (5% and 10%), (b) multiple injection of a diluted cyanide solution (100  $\mu\text{M}$ ,  $n = 50$ ), and (c) washing with aqueous ACN solutions (5% and 10%). The column wash required even longer times and three additional steps: (a) overnight washing with a mixture of  $\text{Na}_2\text{SO}_4$  (1 mM aqueous) and ACN (1:10 ratio), (b) washing of residual  $\text{Na}_2\text{SO}_4$  from the column for 4 h with 5% aqueous ACN solution followed by 2 h wash with 10% aqueous ACN solution, and (c) multiple injection of a dilute cyanide solution (100  $\mu\text{M}$ ,  $n=70$ ).

Unlike other species of Cbi, CbiAT complex does not bind strongly with the LC-MS/MS components. Therefore, we extensively modified the cleaning protocol and utilized ATM as a much less-toxic substitute for cyanide. The revised protocol consisted of the following two simple steps: (a) rinsing of the LC system (including the column) via much fewer injections of 200  $\mu\text{M}$  aqueous ATM ( $n = 5$ ) after analysis of each set of CbiAT, and (b) much fewer injection of aqueous NaCN (100  $\mu\text{M}$  in 10 mM NaOH,  $n = 10$ ) without column and periodically checking for the presence of  $\text{Cbi}(\text{CN})_2$  using the method developed by Dzisam et al. [56]. During CbiAT analysis, 200  $\mu\text{L}$  of 90% aqueous ACN solution was used to rinse the autosampler syringe between injections.

#### ***4.3.5. Calibration, quantification, and limit of detection***

The developed method was validated by following the FDA bioanalytical method validation guidelines [146]. To evaluate the calibration behavior of CbiAT, calibration standards (0.5, 1, 2, 5, 10, 20, 50, 100, 200, and 500  $\mu\text{M}$ ) were prepared in swine plasma in triplicate from the CbiAT stock solution (5 mM). Following analysis, the average peak

areas of CbiAT were plotted as a function of plasma CbiAT concentrations. Both weighted ( $1/x$  and  $1/x^2$ ) and unweighted linear ( $y = mx + c$ ) and unweighted log-log ( $\log y = m \log x + \log c$ ) regression models were constructed to evaluate the best fit model for CbiAT analysis. Percent residual accuracy (PRA) was considered and emphasized over the frequently used coefficient of determination ( $R^2$ ) to quantify the goodness-of-fit (GoF) of the calibration models as the current method used a geometric series of concentrations for calibration curve preparation. When calibration curves span 2-3 orders of magnitude,  $R^2$  is significantly limited, typically misrepresenting the GoF throughout the calibration range. PRA values of  $\geq 90\%$  are considered indicative of a good fit [17, 36, 108].

The upper and lower limit of quantification (ULOQ and LLOQ, respectively) were set based on the calibrator precision of  $<15\%$  relative standard deviation (RSD), and an accuracy of  $100 \pm 20\%$  of the nominal calibrator concentration back-calculated from the calibration curve. To calculate the limit of detection (LOD), multiple concentrations of CbiAT were prepared in plasma below the LLOQ and analyzed. The LOD was defined as the lowest CbiAT concentration which reproducibly produced a signal-to-noise (S/N) ratio of at least 3. Blank samples were analyzed to determine the noise as peak-to-peak noise over the elution time of CbiAT.

#### ***4.3.6. Accuracy and precision***

To calculate the intra- and interassay accuracies and precisions of the method, calibration standards ( $n = 3$ ) and quality control (QC) standards (7.5, 35, and 150  $\mu\text{M}$ ,  $n = 5$  each) were prepared in swine plasma and analyzed in parallel each day for three days (within five calendar days). The intraassay accuracy and precision were determined from

the QCs on each day's analysis, whereas the interassay accuracy and precision were calculated by comparing QCs over three separate days. The selection criteria for accuracy and precision were set at <15% RSD and  $100\pm 20\%$ , respectively.

#### ***4.3.7. Matrix effect and recovery***

To determine the matrix effect, calibration curves were prepared by spiking CbiAT in aqueous solution (where plasma was replaced by DI water during sample preparation) and plasma. The slopes of the resulting calibration curves were compared. A slope ratio (i.e.,  $m_{\text{plasma}}/m_{\text{aqueous}}$ ) of <1 and >1 indicate plasma matrix suppression and enhancement effects, respectively. The recovery of CbiAT was calculated by comparing the signals of triplicates of plasma QCs (7.5, 35, and 150  $\mu\text{M}$ ) with the equivalent concentration of QCs spiked in aqueous solution. Recovery was determined by dividing the average peak area of CbiAT in plasma by the average peak area of the equivalent concentration aqueous QC and multiplying by 100%.

#### ***4.3.8. Stability***

The short- and long-term stabilities of CbiAT were evaluated by analyzing triplicates of plasma spiked at low (7.5  $\mu\text{M}$ ) and high (150  $\mu\text{M}$ ) QC concentrations stored at different conditions for multiple time periods. CbiAT was considered stable in plasma if the signal from a stability standard was within  $\pm 10\%$  of the initial (time 0) signal. As a part of short-term stability study, bench-top and autosampler stabilities were assessed for 24 h, and freeze-thaw (FT) stability was performed for four FT cycles. For bench-top stability, CbiAT spiked non-denatured plasma for both QCs were left on the benchtop for 0, 1, 2, 5,

10 and 24 h at room temperature before analysis. To evaluate the autosampler stability, the prepared QCs were placed in the autosampler of the LC at 15 °C and were analyzed at 0, 1, 2, 5, 10 and 24 h. FT stability samples were prepared in two different ways before storing the CbiAT spiked non-denatured plasma samples at -80 °C: (a) unassisted freezing, and (b) flash-freezing in liquid nitrogen. Five sets of QC samples were prepared in triplicate, where one set of both QCs was analyzed on the same day (Day “0”), while the other four sets (for both “a” and “b”) were kept at -80 °C. After 24 h for 1 FT cycle, all stored samples were thawed at room temperature by leaving the vials undisturbed on the countertop for about 10 min. After fully thawing the samples, one set of QCs (for both unassisted and flash freezing) were analyzed following the necessary sample preparation steps, while the rest three sets were placed back at -80 °C. This procedure was repeated three more times to evaluate four FT cycles.

For evaluation of the long-term stability of CbiAT, the QC samples were prepared as with the FT stability study: (a) unassisted freezing, and (b) flash-freezing. These samples were analyzed after 0, 1, 2, 5, 15, and 30 days. For unassisted freezing, the CbiAT-spiked plasma samples were stored at 4, -20 and -80 °C, whereas flash frozen samples were first frozen in liquid nitrogen before storing in -20 and -80 °C freezers. Both QCs were prepared in bulk to minimize sample-to-sample variation. To correct for day-to-day instrument sensitivity, fresh QCs were prepared each day in triplicate. The average peak area signal ratio of the QC from the stability sample to the QC prepared fresh on the same day was used to evaluate the long-term stability of CbiAT. The stability of CbiAT was measured as a percentage of the “Day 0” signal ratio.

## 4.4. Results and Discussion

### 4.4.1. LC-MS/MS analysis of CbiAT

The LC-MS/MS method reported here is the first ever published technique for CbiAT analysis from any biological matrix. It features rapid and simple sample preparation of a small volume of plasma (100  $\mu$ L), consisting of plasma protein denaturing (with 10%  $\text{NH}_4\text{OH}$  in ACN), centrifugation ( $16,454 \times g$ ), transfer and drying of the supernatant (under inert nitrogen), reconstitution (10% aqueous ACN), and LC-MS/MS analysis. The overall sample preparation time was less than 1 h, with the chromatographic analysis time of only 3 min allowing an estimated 480 samples to be analyzed over a 24-h period. Figure 4.1 shows the mass spectrum of CbiAT produced by ESI(+)-MS with the CbiAT molecular ion structure ( $[\text{M} + \text{H}]^+$ ,  $m/z = 1196.5$ ) and its abundant ions inset. Transitions  $1196.5 \rightarrow 1028.6$  and  $1196.5 \rightarrow 989.7$  were used for quantification and identification, respectively. Figure 4.2 shows chromatograms of the quantification ( $1196.5/1028.6$   $m/z$ ) and identification ( $1196.5/989.7$   $m/z$ ) transitions from analysis of CbiAT-spiked and non-spiked plasma. The CbiAT peak eluted at 1.5 min. The selectivity of CbiAT was excellent as there was no significant peak, aside from CbiAT, in the blank or spiked samples eluting throughout the chromatographic run time. The CbiAT peak was quite symmetrical above a flat baseline, with an asymmetry factor ( $A_s$ ) of  $<1.3$  and a tailing factor ( $T_f$ ) of 1.15. The  $T_f$  and  $A_s$  indicate only slight tailing, but both values were well within generally accepted ranges (i.e.,  $A_s < 2.0$  and  $T_f < 2.0$ ).

The cleaning protocol devised for CbiAT was rapid ( $<1$  h) and easy to adopt compared with the protocol proposed by Dzisam et al. [56], which required over 24-h and either two LC systems or utilizing a single LC-MS/MS system for over 24-h. Moreover,

the use of ATM decreased the volume of cyanide solution necessary to clean and check for residual Cbi in the LC-MS/MS.

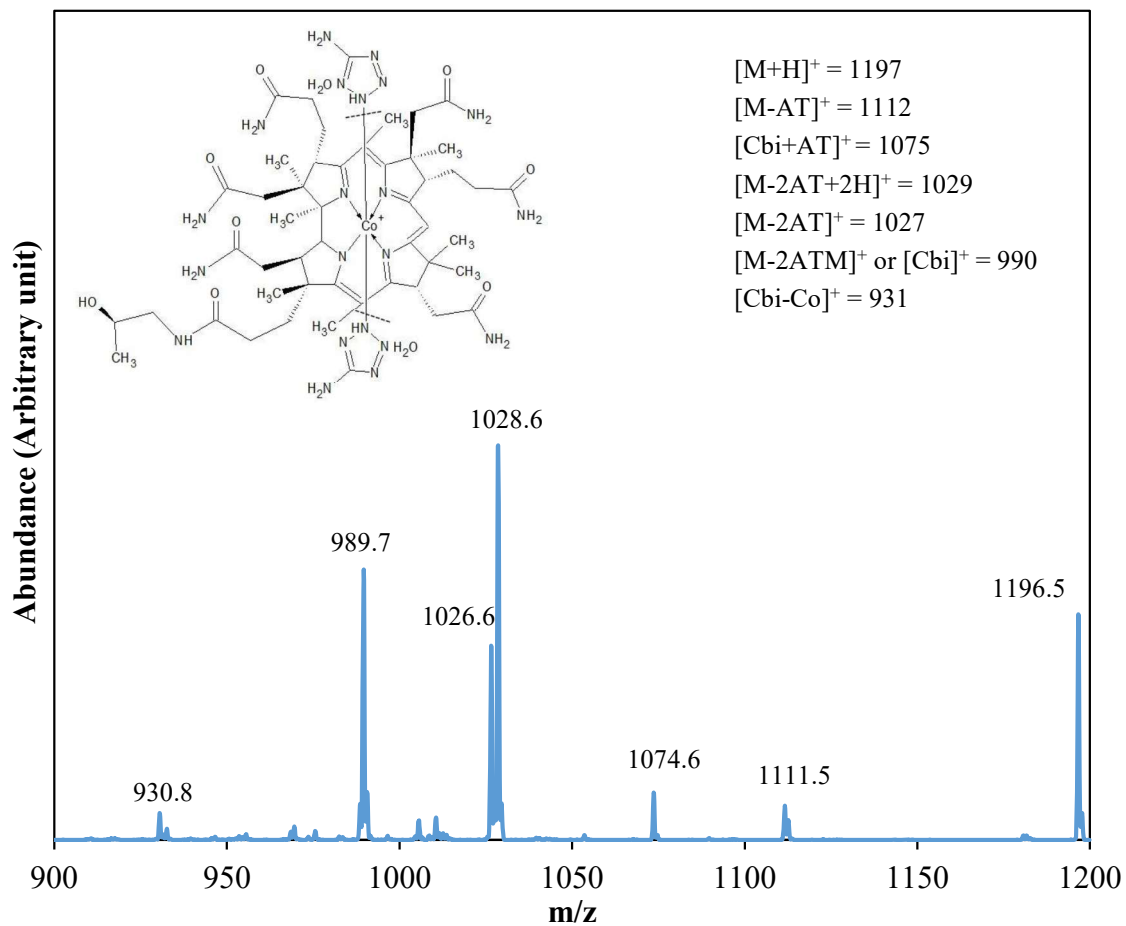


**Figure 4.1.** ESI(+) mass spectra of CbiAT with identification of the abundant ions. Inset: Structure of CbiAT with abundant fragments indicated. AT represents 5-amino-1H-tetrazole.

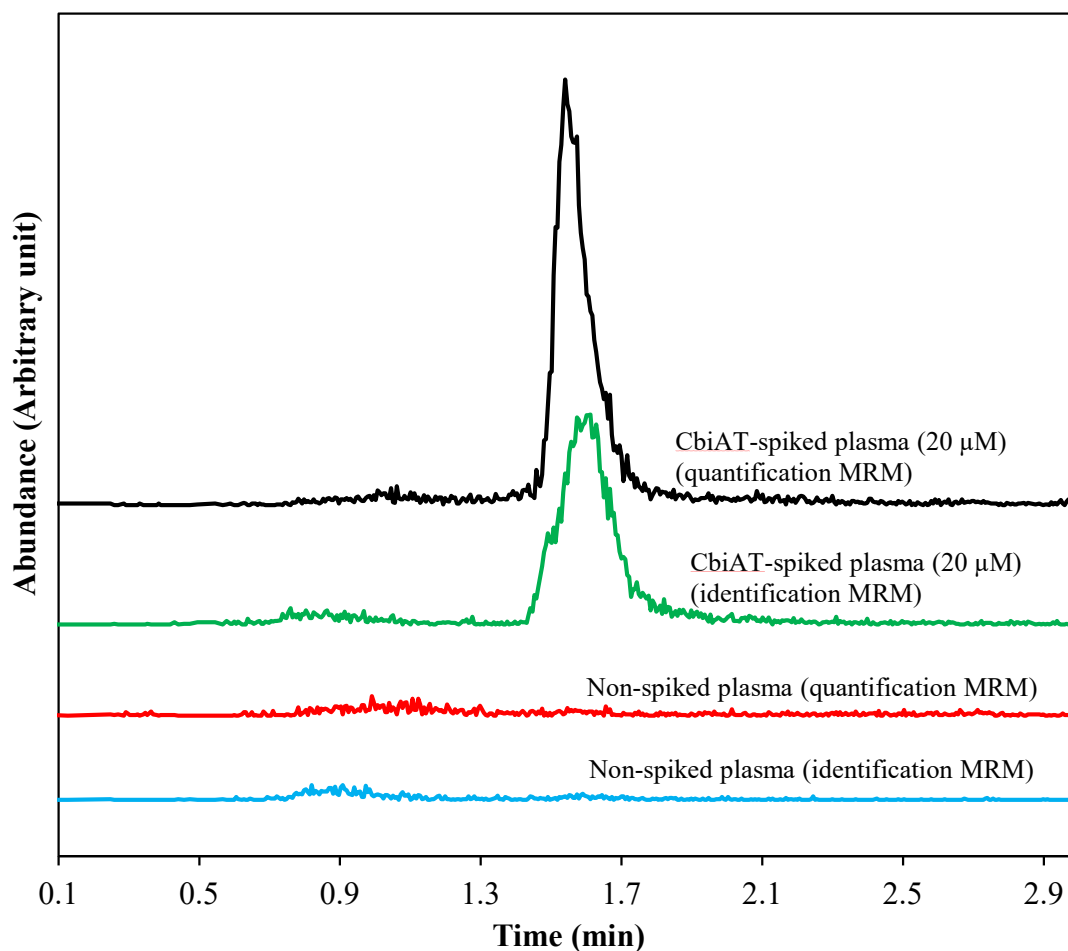


**Figure 4.2.** LC-MS-MS chromatogram of CbiAT-spiked plasma (20  $\mu\text{M}$ ) and non-spiked plasma. Transitions 1196.5/1028.6 and 1196.5/989.7 represent quantification and identification MRM, respectively.

#### 4.4.2. Dynamic range and limit of detection

The current method produced an excellent LOD of 0.3  $\mu\text{M}$  in plasma which is similar to the LODs of previous cyanoCbi [56] and total Cbi [143] methods, which was 0.2  $\mu\text{M}$  for both approaches. The low LOD is important because the method can be used to detect the presence of low levels of CbiAT for drug-development studies.

For dynamic range determination, calibration curves were evaluated over the concentration range of 0.5 – 500  $\mu\text{M}$ . Based on GoF parameters and visual inspection of

residuals for both linear and log-log regression models, we found 0.5 and 1  $\mu\text{M}$  were outside the calibration range and that a log-log regression model produced the best fit for the calibration data. Therefore, the dynamic range for CbiAT was 2 (LLOQ) to 500  $\mu\text{M}$  (ULOQ). This dynamic range is useful for drug-development studies where analysis of a wide concentration range is necessary. To test the consistency of the calibration, three calibration curves were prepared on three consecutive days. Consistent slopes (i.e., mean  $m_{\text{plasma}} = 1.66$  with a standard deviation of 0.02) and intercepts (i.e., mean  $m_{\text{plasma}} = 1.47$  with a standard deviation of 0.07) were found and all calibration curves showed acceptable PRA ( $\geq 93\%$ ) and  $R^2$  ( $\geq 0.993$ ) values, indicating an excellent fit of all the data over the calibration range. Table 4.2 shows the consistency of CbiAT calibration curves and goodness-of-fit analysis over 3 days.

**Table 4.2:** Calibration curve equations prepared on three consecutive days with related goodness-of-fit parameters.

Day	Calibration equation	PRA (%)	$R^2$
Day-1	$\log y = 1.64 \log x + 1.40$	94.2	0.9955
Day-2	$\log y = 1.65 \log x + 1.56$	93.8	0.9943
Day-3	$\log y = 1.69 \log x + 1.45$	93.4	0.9938

#### 4.4.3. Accuracy and Precision

Quintuplicate analysis of three QCs (7.5, 35, and 150  $\mu\text{M}$ ) was performed on three separate days to determine the accuracy and precision of the proposed method. As shown in Table 4.3, inter- and intraassay accuracies ( $100 \pm 12\%$  and  $100 \pm 19\%$ , respectively) and precisions ( $< 12\%$  and  $< 9\%$  RSD, respectively) were considered acceptable, according to the FDA method validation guidelines [146]. While future addition of an internal standard (IS) may theoretically help to improve the intraassay accuracy (i.e., it was close to the

selection criteria limit of  $100\pm 20\%$ ), an IS would likely be difficult to synthesize and may compete for ligands bound to the analyte. Therefore, it is likely that an IS structurally similar to CbiAT would be problematic.

**Table 4.3:** The intra- and interassay accuracies and precisions for analysis of CbiAT from spiked swine plasma.

Conc ( $\mu\text{M}$ )	Intraassay						Interassay	
	Accuracy (%) <sup>a</sup>			Precision (%RSD) <sup>a</sup>			Accuracy (%) <sup>b</sup>	Precision (%RSD) <sup>b</sup>
	Day 1	Day 2	Day 3	Day 1	Day 2	Day 3		
7.5	100 $\pm$ 8.1	100 $\pm$ 18.7	100 $\pm$ 8.1	3.8	4.1	8.7	100 $\pm$ 11.6	7.4
35	100 $\pm$ 4.8	100 $\pm$ 17.9	100 $\pm$ 17.0	5.3	4.4	8.8	100 $\pm$ 10.0	11.6
150	100 $\pm$ 19.4	100 $\pm$ 9.9	100 $\pm$ 6.1	0.2	1.1	1.2	100 $\pm$ 11.8	5.1

<sup>a</sup>Calculate from each day's QC analysis (n = 5).

<sup>b</sup>Aggregate of three days of QC method validation (n = 15).

#### 4.4.4. Matrix effect, recovery, and storage stability

The matrix effect was determined by comparing the slopes of plasma and aqueous calibration curves (i.e.,  $m_{\text{plasma}}/m_{\text{aqueous}}$ ). The ratio of the slopes obtained was 1.04, indicating essentially no matrix effect occurs from plasma. The percent recoveries for CbiAT in swine plasma for low, medium, and high QCs were 38, 33, and 32%, respectively. This low recovery is likely due to low extraction of CbiAT from plasma with 10%  $\text{NH}_4\text{OH}$  in ACN solution. While the recovery was low, it was very consistent and did not affect the ability to accurately analyze CbiAT.

For the bench-top stability study, CbiAT was unstable in spiked non-denatured plasma at room temperature. Even after 1 h, the signal recoveries for the low and high QCs were only 68.8 and 41.0% of the "time 0" signal, respectively. It is, therefore, recommended that samples should not be kept at room temperature for storage. In contrast,

autosampler and FT “flash-frozen” samples were stable throughout the time period investigated. When comparing the “unassisted freezing” samples to the flash frozen samples, the unassisted freezing samples showed about 30% signal loss after one FT cycle and then minimal loss after each subsequent FT cycle. This initial loss of CbiAT signal is likely because of the quick interaction of Cbi with other strong ligands (e.g., carbon monoxide (CO), cyanide (CN<sup>-</sup>) or nitrite (NO<sub>2</sub><sup>-</sup>)) available in plasma or interaction with plasma proteins, which was effectively minimized using liquid nitrogen immediately after spiking the CbiAT in plasma. The long-term stability of CbiAT was evaluated for 30 days and the stored samples were analyzed after 0, 1, 2, 5, 15, and 30 days. CbiAT was stable at both -20 and -80 °C for at least 30 days when the samples were flash-frozen prior to storage. “Unassisted freezing” samples stored at 4 °C showed degradation after 24 h and there was a visual change in appearance after Day-5. Unassisted freezing samples stored at -20 and -80 °C showed about 60 and 48% degradation, respectively, after 30 days of storage.

Based on the overall results from the evaluation of storage stability, the following major conclusions can be drawn: 1) flash-freezing prior to storage is vital to limit initial loss of CbiAT, 2) CbiAT is stable for at least 30 days in plasma when flash frozen and stored at -20 or -80 °C, 3) prepared samples placed in the autosampler are stable at least 24 h, and 4) flash frozen samples are stable for at least four FT cycles.

#### ***4.4.5. Method application and pharmacokinetics***

The validated LC-MS/MS method was applied to the analysis of swine plasma obtained from a CbiAT pharmacokinetic study. Figure 4.3 shows the chromatograms of plasma of swine treated with CbiAT and untreated swine plasma collected prior to

treatment. The CbiAT peak was observed at 1.5 min in the treated plasma samples, whereas the plasma sample prepared from non-treated swine showed no peak at the retention time of CbiAT. The outcome confirmed the selectivity and the applicability of the method to analyze CbiAT-treated animal samples.

A preliminary pharmacokinetic profile of CbiAT (75 mg/kg IM) in swine (n=1) is presented in Figure 4.4. As CbiAT is a new drug candidate and no prior animal experiment was performed using CbiAT, the current animal experiment considered a comparatively long time interval (up to 168 h) to evaluate the pharmacokinetics of IM-administered CbiAT. Although preliminary, the toxicokinetic behavior of CbiAT was best described by a one-compartment model [147], with a  $C_{\max}$  and  $t_{\max}$  of 44.7  $\mu\text{M}$  and 4 h, respectively, indicating quick CbiAT distribution and availability throughout the body. It should be noted that time intervals prior to 4-h must be evaluated to confirm one-compartment behavior of CbiAT. The elimination was somewhat slow, with a  $t_{1/2}$  of 23.7 h, and the area under the curve was large (i.e.,  $\text{AUC} = 855.01 \mu\text{M}\cdot\text{h}$ ) showing that a large amount of CbiAT is available at this dose. The quick distribution and slow elimination of CbiAT from IM administration is promising, in that it should allow both quick antidotal efficacy following treatment and longer duration of treatment in situations where multiple exposures or continuous exposure occurs. The favorable pharmacokinetic profile of CbiAT administered via IM injection should allow relatively simple on-site self-treatment or treatment by untrained personnel. Overall, this preliminary pharmacokinetic experiment revealed impressive pharmacokinetic behavior of CbiAT, most notably a quick onset of action and slow elimination, but this experiment must be repeated with a much larger n-value, analysis of earlier time points, and lower doses of CbiAT to verify these results.

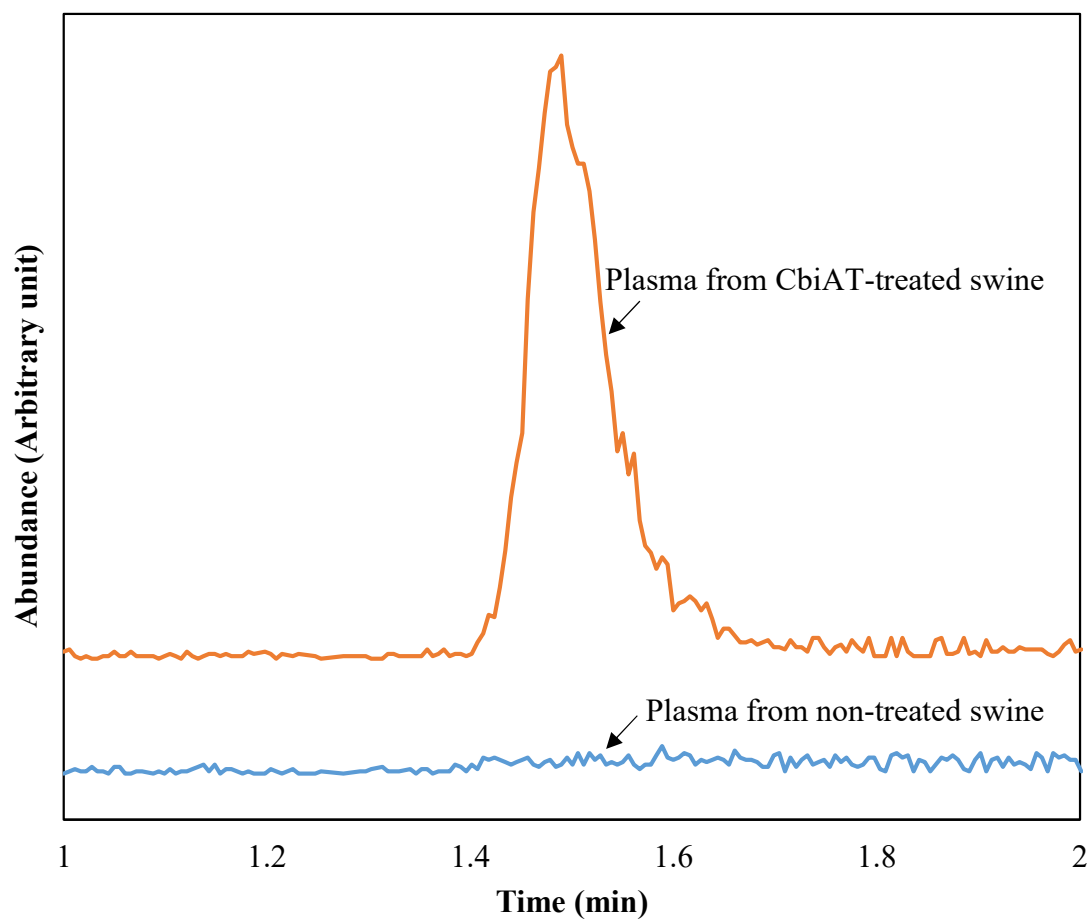


**Figure 4.3.** Representative LC-MS/MS chromatogram at an MRM transition of 1196.5/1028.6  $m/z$  (CbiAT quantification MRM transition) from the plasma of CbiAT-treated and untreated (prior to CbiAT treatment) swine.

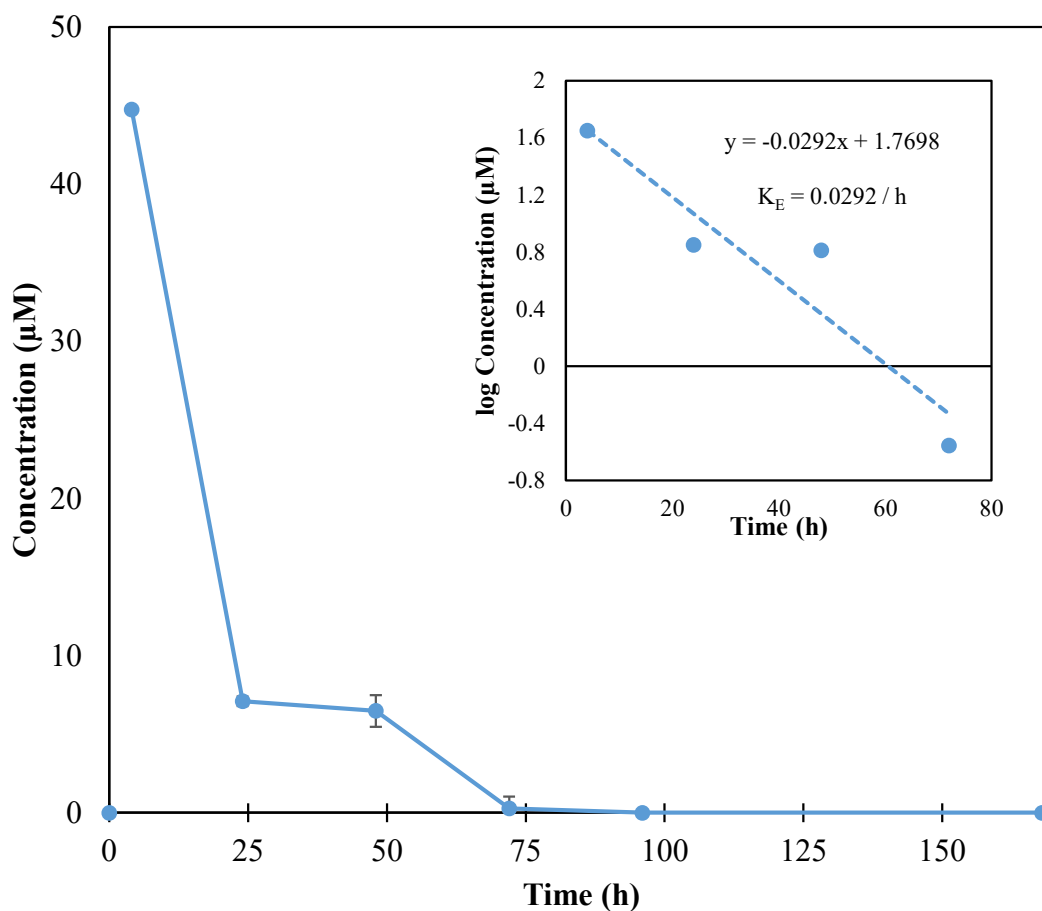


**Figure 4.4.** Plasma concentration-time behavior of CbiAT following IM administration of CbiAT to swine. Error bars represent standard error of the mean ( $n = 3$ ). Inset: Representation of CbiAT elimination constant ( $K_E$ ) by log concentration-time graph.

#### 4.5. Conclusions

A rapid and simple LC-MS/MS method was developed for the quantification of CbiAT in plasma. This method is the first ever validated method for the determination of CbiAT in any biological matrix. The applicability of this method was successfully tested by analyzing the plasma of swine treated with CbiAT and the preliminary results showed very promising pharmacokinetic profile following IM administration. The availability of

this method and the excellent pharmacokinetic behavior of CbiAT will allow further development of CbiAT as a potential countermeasure for CN, H<sub>2</sub>S and MT poisoning.

#### **4.6. Acknowledgments**

The research described was supported by interagency agreements (AOD16026-001-00000/A120B.P2016-01 and AOD18015-001-00000/MRICD-IAA-18-0129-00) between the NIH Office of the Director (OD) and the U.S. Army Medical Research Institute of Chemical Defense under the oversight of the Chemical Countermeasures Research Program (CCRP) within the Office of Biodefense Research (OBRS) at the National Institute of Allergy and Infectious Diseases (NIAID/NIH). We also gratefully acknowledge support from the CounterACT Program, National Institutes of Health Office of the Director, and the National Institute of Environmental Health Sciences (NIEHS), Grant number U54 ES027698 (CWW). The opinions or assertions contained herein are the private views of the authors and are not to be construed as official or as reflecting the views of the National Institutes of Health (including NIAID and the CounterACT Program), CCRP, Health and Human Service (HHS), United States Army Medical Research Acquisition Activity (USAMRAA), United States Army Medical Research Institute of Chemical Defense (USAMRICD) or Department of Defense (DoD).

## **Chapter 5. Conclusions, Broader Impacts, and Future Works**

### **5.1. Conclusions**

A rapid, cost effective, environmentally friendly, and highly sensitive DHS-GC-MS method was developed for the analysis of DMTS, a highly promising next generation CN antidote, in whole blood. This validated method was successfully applied to establish the pharmacokinetic profile of DMTS in animal blood, and the results obtained after analyzing DMTS pharmacokinetic study samples were highly promising. Another DHS-GC-MS method was developed and validated for the rapid analysis of DMDS in blood. This highly sensitive method was used to analyze the level of formation of DMDS following DMTS treatment in swine blood. Preliminary pharmacokinetic and toxicokinetic parameters of DMDS were also established, which will be helpful for DMTS drug-development studies. A simple and direct LC-MS/MS method was also developed for the quantification of CbiAT, a CN, H<sub>2</sub>S and MT countermeasure, in swine plasma. The applicability of this method was evaluated by analyzing CbiAT treated swine from pharmacokinetic study and the preliminary pharmacokinetic parameters of CbiAT in swine plasma were very promising for its use as an antidote for these poisons.

### **5.2. Broader impacts**

Although TIAs are extremely poisonous and can also be lethal, but they all have chemical, plastic, and pharmaceutical importance, therefore, most of the incidences and fatalities from TIs exposure happened in industrial settings. Hence, research to understand their toxicokinetic properties, designing quick detection technologies, development of

effective method to determine their level of exposure, and development of effective countermeasures are important to understand their behavior and defend against the adverse health effects of TIA exposure. The method reported here for the quantification of DMTS will allow for further development of DMTS as a promising next-generation antidote for CN exposure. In addition, the method developed for DMDS will help to understand the effectiveness of DMTS in detoxifying CN and will provide insight into the level of community exposure during DMDS fumigation. Furthermore, the method developed and reported here for the analysis of CbiAT will help further development of CbiAT as a potential antidote for CN, H<sub>2</sub>S and MT exposure.

### **5.3. Future work**

Future work should include more evaluation of DMTS effective dose and route of treatment based on pharmacokinetic and toxicokinetic profiles before extending the experiment its development towards clinical trials. The toxicokinetics of DMDS should be better evaluated in toxicological models of DMDS exposure to understand its behavior. As with DMTS, pharmacokinetic studies on CbiAT should also be performed in other animal models with more statistical significance as part of its development as a TIA antidote. Moreover, future work should identify and characterize the level of formation of DMTS and CbiAT degradation product(s) in biological matrices as well as in pharmaceutical preparations and evaluate their safety profiles. Lastly, the stabilities of DMTS and CbiAT formulations at different storage temperatures should also be monitored.

## References

- [1] M. Gorguner, M. Akgun, Acute inhalation injury, *The Eurasian journal of medicine*, 42 (2010) 28.
- [2] R.K. Albert, S.G. Spiro, J.R. Jett, *Clinical respiratory medicine*, Elsevier Health Sciences, 2008.
- [3] L. Rosenstock, M. Cullen, C. Brodtkin, C. Redlich, *Textbook of clinical occupational and environmental medicine*, (2004).
- [4] Agency for Toxic Substances and Disease Registry, in, U.S. Department of Health and Human Services, Atlanta, GA, 2021.
- [5] G.M. Wong-Chong, D.V. Nakles, R.G. Luthy, Manufacture and the use of cyanide, in: *Cyanide in Water and Soil*, CRC press, 2005, pp. 53-68.
- [6] P.S. Mehta, A.S. Mehta, S.J. Mehta, A.B. Makhijani, Bhopal tragedy's health effects: a review of methyl isocyanate toxicity, *Jama*, 264 (1990) 2781-2787.
- [7] R. Jackson, R.P. Oda, R.K. Bhandari, S.B. Mahon, M. Brenner, G.A. Rockwood, B.A. Logue, Development of a fluorescence-based sensor for rapid diagnosis of cyanide exposure, *Analytical chemistry*, 86 (2014) 1845-1852.
- [8] M. Greskevitch, G. Kullman, K.M. Bang, J.M. Mazurek, Respiratory disease in agricultural workers: mortality and morbidity statistics, *Journal of agromedicine*, 12 (2008) 5-10.
- [9] L. Rushton, Occupational causes of chronic obstructive pulmonary disease, *Reviews on environmental health*, 22 (2007) 195-212.
- [10] B.J. Lukey, J.A. Romano Jr, H. Salem, *Chemical warfare agents: biomedical and psychological effects, medical countermeasures, and emergency response*, CRC Press, 2019.
- [11] B. Bowonder, The Bhopal incident: Implications for developing countries, *Environmentalist*, 5 (1985) 89-103.
- [12] D. Layton, *Seductive poison: A Jonestown survivor's story of life and death in the Peoples Temple*, Anchor, 1999.
- [13] R. Cooke, PSU alumnus recalls 1982 Tylenol murders, *The Digital Collegian*, (2002).
- [14] H. Markel, How the Tylenol murders of 1982 changed the way we consume medication, (2014).
- [15] A.R. Lara, *Irritant Gas Inhalation Injury*, in, Merck & Co., Inc, Kenilworth, NJ, 2020.
- [16] K. Miller, A. Chang, Acute inhalation injury, *Emergency Medicine Clinics*, 21 (2003) 533-557.
- [17] S. Bhadra, Z. Zhang, W. Zhou, F. Ochieng, G.A. Rockwood, D. Lippner, B.A. Logue, Analysis of potential cyanide antidote, dimethyl trisulfide, in whole blood by dynamic headspace gas chromatography–mass spectroscopy, *Journal of Chromatography A*, 1591 (2019) 71-78.
- [18] D. Nowak, Chemosensory irritation and the lung, *International archives of occupational and environmental health*, 75 (2002) 326-331.
- [19] T.C. McCloud, Occupational lung disease, *Radiologic Clinics of North America*, 29 (1991) 931-941.
- [20] J. Jiang, A. Chan, S. Ali, A. Saha, K.J. Haushalter, W.-L.M. Lam, M. Glasheen, J. Parker, M. Brenner, S.B. Mahon, Hydrogen sulfide—mechanisms of toxicity and development of an antidote, *Scientific reports*, 6 (2016) 1-10.

- [21] P. Anantharam, D.-S. Kim, E.M. Whitley, B. Mahama, P. Imerman, P. Padhi, W.K. Rumbeiha, Midazolam efficacy against acute hydrogen sulfide-induced mortality and neurotoxicity, *Journal of medical toxicology*, 14 (2018) 79-90.
- [22] T.B. Hendry-Hofer, P.C. Ng, A.M. McGrath, D. Mukai, M. Brenner, S. Mahon, J.K. Maddry, G.R. Boss, V.S. Bebarta, Intramuscular aminotetrazole cobinamide as a treatment for inhaled hydrogen sulfide poisoning in a large swine model, *Annals of the New York Academy of Sciences*, (2020).
- [23] R.K. Bhandari, R.P. Oda, S.L. Youso, I. Petrikovics, V.S. Bebarta, G.A. Rockwood, B.A. Logue, Simultaneous determination of cyanide and thiocyanate in plasma by chemical ionization gas chromatography mass-spectrometry (CI-GC-MS), *Analytical and bioanalytical chemistry*, 404 (2012) 2287-2294.
- [24] I. Leybell, Cyanide Toxicity, in, *Medscape, Emergency Medicine*, 2018.
- [25] D. Beasley, W. Glass, Cyanide poisoning: pathophysiology and treatment recommendations, *Occupational Medicine*, 48 (1998) 427-431.
- [26] P.D. Bryson, *Comprehensive reviews in toxicology: for emergency clinicians*, CRC press, 1996.
- [27] J. Feeney, A.S. Burgen, E. Grell, Cyanide Binding to Carbonic Anhydrase: A <sup>13</sup>C-Nuclear-Magnetic-Resonance Study, *European journal of biochemistry*, 34 (1973) 107-111.
- [28] T.J. Henderson, I. Petrikovics, P. Kikilo, A.L. Ternay Jr, H. Salem, *Chemistries of Chemical Warfare Agents*, in: *Chemical Warfare Agents*, CRC Press, 2019, pp. 17-38.
- [29] F.P. Simeonova, L. Fishbein, W.H. Organization, *Hydrogen cyanide and cyanides: human health aspects*, World Health Organization, 2004.
- [30] A.P. Knight, R.G. Walter, *A guide to plant poisoning of animals in North America, A guide to plant poisoning of animals in North America.*, (2002).
- [31] F. Nartey, R. Smith, E. Bababumni, *Toxicological aspects of cyanogenesis in tropical foodstuffs*, *Toxicology in the Tropics*, (1980) 53-73.
- [32] E.E. Conn, Biosynthesis of cyanogenic glycosides, *Naturwissenschaften*, 66 (1979) 28-34.
- [33] A.E. Burns, J.H. Bradbury, T.R. Cavagnaro, R.M. Gleadow, Total cyanide content of cassava food products in Australia, *Journal of Food Composition and Analysis*, 25 (2012) 79-82.
- [34] R. Schnepf, Cyanide: sources, perceptions, and risks, *Journal of emergency nursing*, 32 (2006) S3-S7.
- [35] R.K. Bhandari, E. Manandhar, R.P. Oda, G.A. Rockwood, B.A. Logue, Simultaneous high-performance liquid chromatography-tandem mass spectrometry (HPLC-MS-MS) analysis of cyanide and thiocyanate from swine plasma, *Analytical and bioanalytical chemistry*, 406 (2014) 727-734.
- [36] S. Bhadra, V.S. Bebarta, T.B. Hendry-Hofer, D.S. Lippner, J.N. Winborn, G.A. Rockwood, B.A. Logue, Analysis of the Soil Fumigant, Dimethyl Disulfide, in Swine Blood by Dynamic Headspace Gas Chromatography–Mass Spectroscopy, *Journal of Chromatography A*, 1638 (2021) 461856.
- [37] E.P. Randviir, C.E. Banks, The latest developments in quantifying cyanide and hydrogen cyanide, *TrAC Trends in Analytical Chemistry*, 64 (2015) 75-85.

- [38] L.M. Cardoso, F.B. Mainier, J.A. Itabirano, Analysis Voltammetry of Cyanide and Process Electrolytic Removal of Cyanide in Effluents, *American Journal of Environmental Engineering*, 4 (2014) 182-188.
- [39] P. Longerich, *Holocaust: The Nazi persecution and murder of the Jews*, OUP Oxford, 2010.
- [40] P. Hayes, *From cooperation to complicity: Degussa in the Third Reich*, Cambridge University Press, 2007.
- [41] J. Judge, *The black hole of Guyana: The untold story of the Jonestown Massacre, Secret and suppressed: Banned ideas and hidden history*, (1993) 127-165.
- [42] F. Xu, J.P. Webb, Tianjin chemical clean-up after explosion, in, *Can Med Assoc*, 2015.
- [43] A. Jacobs, J.C. Hernández, C. Buckley, Behind deadly Tianjin blast, shortcuts and lax rules, *New York Times*, (2015).
- [44] J. Hamel, A review of acute cyanide poisoning with a treatment update, *Critical care nurse*, 31 (2011) 72-82.
- [45] E. Manandhar, N. Maslamani, I. Petrikovics, G.A. Rockwood, B.A. Logue, Determination of dimethyl trisulfide in rabbit blood using stir bar sorptive extraction gas chromatography-mass spectrometry, *Journal of Chromatography A*, 1461 (2016) 10-17.
- [46] N.V. Bhagavan, C.-E. Ha, *Essentials of medical biochemistry: with clinical cases*, Academic Press, 2011.
- [47] L.L. Pearce, E.L. Bominaar, B.C. Hill, J. Peterson, Reversal of Cyanide Inhibition of Cytochrome c Oxidase by the Auxiliary Substrate Nitric Oxide: An Endogenous Antidote to Cyanide Poisoning, *Journal of Biological Chemistry*, 278 (2003) 52139-52145.
- [48] Y. Yusim, D. Livingstone, A. Sidi, Blue dyes, blue people: the systemic effects of blue dyes when administered via different routes, *Journal of clinical anesthesia*, 19 (2007) 315-321.
- [49] M.A. Kirk, R. Gerace, K.W. Kulig, Cyanide and methemoglobin kinetics in smoke inhalation victims treated with the cyanide antidote kit, *Annals of emergency medicine*, 22 (1993) 1413-1418.
- [50] R. Gracia, G. Shepherd, Cyanide poisoning and its treatment, *Pharmacotherapy: The Journal of Human Pharmacology and Drug Therapy*, 24 (2004) 1358-1365.
- [51] S. Baskin, I. Petrikovics, J. Kurche, J. Nicholson, B. Logue, B. Maliner, G. Rockwood, Insights on cyanide toxicity and methods of treatment, *Pharmacological perspectives of toxic chemicals and their antidotes*, (2004) 105-146.
- [52] I. Petrikovics, M. Budai, K. Kovacs, D.E. Thompson, Past, present and future of cyanide antagonism research: From the early remedies to the current therapies, *World journal of methodology*, 5 (2015) 88.
- [53] L. Randaccio, S. Geremia, N. Demitri, J. Wuerges, Vitamin B12: unique metalorganic compounds and the most complex vitamins, *Molecules*, 15 (2010) 3228-3259.
- [54] C. Brunel, C. Widmer, M. Augsburger, F. Dussy, T. Fracasso, Antidote treatment for cyanide poisoning with hydroxocobalamin causes bright pink discoloration and chemical-analytical interferences, *Forensic science international*, 223 (2012) e10-e12.
- [55] M. Brenner, J.G. Kim, S.B. Mahon, J. Lee, K.A. Kreuter, W. Blackledge, D. Mukai, S. Patterson, O. Mohammad, V.S. Sharma, Intramuscular cobinamide sulfite in a rabbit model of sublethal cyanide toxicity, *Annals of emergency medicine*, 55 (2010) 352-363.

- [56] J.K. Dzisam, M. Brenner, S.B. Mahon, G.A. Rockwood, B.A. Logue, Determination of free cyano-cobinamide in swine and rabbit plasma by liquid chromatography tandem mass spectrometry, *Journal of Chromatography B*, 1124 (2019) 100-108.
- [57] T.B. Hendry-Hofer, C.C. Severance, S. Bhadra, P.C. Ng, K. Soules, D.S. Lippner, D.M. Hildenberger, M.O. Rhoomes, J.N. Winborn, B.A. Logue, Evaluation of aqueous dimethyl trisulfide as an antidote to a highly lethal cyanide poisoning in a large swine model, *Clinical Toxicology*, (2021) 1-7.
- [58] Cyanokit, in: Cyanokit (hydroxocobalamin for injection) drug, RxList, 2019.
- [59] Nithiodote, in: Nithiodote (sodium nitrite injection for intravenous infusion) drug, RxList, 2021.
- [60] N.N. Greenwood, A. Earnshaw, *Chemistry of the Elements*, Elsevier, 2012.
- [61] P. May, D. Batka, G. Hefter, E. Königsberger, D. Rowland, Goodbye to S 2- in aqueous solution, *Chemical communications*, 54 (2018) 1980-1983.
- [62] F. Pouliquen, C. Blanc, E. Arretz, I. Labat, J. Tournier-Lasserve, A. Ladousse, J. Nougayrede, G. Savin, R. Ivaldi, M. Nicolas, Hydrogen sulfide, *Ullmann's Encyclopedia of Industrial Chemistry*, (2000).
- [63] W.W. Burnett, E. King, M. Grace, W. Hall, Hydrogen sulfide poisoning: review of 5 years' experience, *Canadian Medical Association Journal*, 117 (1977) 1277.
- [64] I. Arnold, R.M. Dufresne, B.C. Alleyne, P. Stuart, Health implication of occupational exposures to hydrogen sulfide, *Journal of occupational medicine.: official publication of the Industrial Medical Association*, 27 (1985) 373-376.
- [65] K. Poulsen, Dangerous Japanese 'Detergent Suicide' Technique Creeps Into US, in, *WIRED*, 2009.
- [66] J. Lindenmann, V. Matzi, N. Neuboeck, B. Ratzenhofer-Komenda, A. Maier, F.-M. Smolle-Juettner, Severe hydrogen sulphide poisoning treated with 4-dimethylaminophenol and hyperbaric oxygen, *Diving Hyperb Med*, 40 (2010) 213-217.
- [67] D. Morii, Y. Miyagatani, N. Nakamae, M. Murao, K. Taniyama, Japanese experience of hydrogen sulfide: the suicide craze in 2008, *Journal of occupational medicine and toxicology*, 5 (2010) 1-3.
- [68] T.B. Hendry-Hofer, P.C. Ng, A.M. McGrath, K. Soules, D.S. Mukai, A. Chan, J.K. Maddy, C.W. White, J. Lee, S.B. Mahon, Intramuscular cobinamide as an antidote to methyl mercaptan poisoning, *Inhalation toxicology*, (2020) 1-8.
- [69] J. Fang, X. Xu, L. Jiang, J. Qiao, H. Zhou, K. Li, Preliminary results of toxicity studies in rats following low-dose and short-term exposure to methyl mercaptan, *Toxicology reports*, 6 (2019) 431-438.
- [70] R.E. Kirk, D.F. Othmer, M. Grayson, D. Eckroth, *Kirk-Othmer Concise encyclopedia of chemical technology*, Wiley, 1985.
- [71] S. Richard J. Lewis, *Sax's dangerous properties of industrial materials*, 11 ed., Jon Wiley & Sons, Inc., Hoboken, NJ, USA, 2012.
- [72] J. Kangas, P. Jäppinen, H. Savolainen, Exposure to hydrogen sulfide, mercaptans and sulfur dioxide in pulp industry, *American Industrial Hygiene Association Journal*, 45 (1984) 787-790.
- [73] J. Klingberg, A. Beviz, C.-G. Ohlson, R. Tenhunen, Disturbed iron metabolism among workers exposed to organic sulfides in a pulp plant, *Scandinavian journal of work, environment & health*, (1988) 17-20.

- [74] K. Torén, S. Hagberg, H. Westberg, Health effects of working in pulp and paper mills: exposure, obstructive airways diseases, hypersensitivity reactions, and cardiovascular diseases, *American journal of industrial medicine*, 29 (1996) 111-122.
- [75] C.D. Heaney, S. Wing, R.L. Campbell, D. Caldwell, B. Hopkins, D. Richardson, K. Yeatts, Relation between malodor, ambient hydrogen sulfide, and health in a community bordering a landfill, *Environmental research*, 111 (2011) 847-852.
- [76] A. Chan, J. Lee, S. Bhadra, N. Bortey-Sam, T.B. Hendry-Hofer, V.S. Bebart, S.B. Mahon, M. Brenner, B. Logue, R.B. Pilz, Development of sodium tetrathionate as a cyanide and methanethiol antidote, *Clinical Toxicology*, (2021) 1-10.
- [77] M.W. Stutelberg, C.V. Vinnakota, B.L. Mitchell, A.R. Monteil, S.E. Patterson, B.A. Logue, Determination of 3-mercaptopyruvate in rabbit plasma by high performance liquid chromatography tandem mass spectrometry, *Journal of Chromatography B*, 949 (2014) 94-98.
- [78] L. Kiss, A. Bocsik, F.R. Walter, J. Ross, D. Brown, B.A. Mendenhall, S.R. Crews, J. Lowry, V. Coronado, D.E. Thompson, From the Cover: In Vitro and In Vivo Blood-Brain Barrier Penetration Studies with the Novel Cyanide Antidote Candidate Dimethyl Trisulfide in Mice, *Toxicological Sciences*, 160 (2017) 398-407.
- [79] J. Lee, G. Rockwood, B. Logue, E. Manandhar, I. Petrikovics, C. Han, V. Bebart, S.B. Mahon, T. Burney, M. Brenner, Monitoring Dose Response of Cyanide Antidote Dimethyl Trisulfide in Rabbits Using Diffuse Optical Spectroscopy, *Journal of Medical Toxicology*, (2018) 1-11.
- [80] G.A. Rockwood, D.E. Thompson, I. Petrikovics, Dimethyl trisulfide: a novel cyanide countermeasure, *Toxicology and industrial health*, 32 (2016) 2009-2016.
- [81] H.T. Nagasawa, D.J. Goon, D.L. Crankshaw, R. Vince, S.E. Patterson, Novel, orally effective cyanide antidotes, *Journal of medicinal chemistry*, 50 (2007) 6462-6464.
- [82] N. Nagahara, T. Ito, H. Kitamura, T. Nishino, Tissue and subcellular distribution of mercaptopyruvate sulfurtransferase in the rat: confocal laser fluorescence and immunoelectron microscopic studies combined with biochemical analysis, *Histochemistry and cell biology*, 110 (1998) 243-250.
- [83] N. Nagahara, T. Ito, M. Minami, Invited Reviews-Mercaptopyruvate sulfurtransferase as a defense against cyanide toxication: Molecular properties and mode of detoxification, *Histology and histopathology*, 14 (1999) 1277-1286.
- [84] S.E. Patterson, A.R. Monteil, J.F. Cohen, D.L. Crankshaw, R. Vince, H.T. Nagasawa, Cyanide antidotes for mass casualties: water-soluble salts of the dithiane (sulfanegen) from 3-mercaptopyruvate for intramuscular administration, *Journal of medicinal chemistry*, 56 (2013) 1346-1349.
- [85] A. Spallarossa, F. Forlani, A. Carpen, A. Armirotti, S. Pagani, M. Bolognesi, D. Bordo, The "rhodanese" fold and catalytic mechanism of 3-mercaptopyruvate sulfurtransferases: crystal structure of SseA from *Escherichia coli*, *Journal of molecular biology*, 335 (2004) 583-593.
- [86] A. Chan, D.L. Crankshaw, A. Monteil, S.E. Patterson, H.T. Nagasawa, J.E. Briggs, J.A. Kozocas, S.B. Mahon, M. Brenner, R.B. Pilz, The combination of cobinamide and sulfanegen is highly effective in mouse models of cyanide poisoning, *Clinical Toxicology*, 49 (2011) 366-373.
- [87] Sulfanegen, in, PlexPage, 2020.

- [88] L. Binet, G. Wellers, J. Dubrisay, Value and mechanism of the antidote action of sodium tetrathionate in hydrocyanic poisoning, *La Presse medicale*, 59 (1951) 641-643.
- [89] T.B. Hendry-Hofer, A.E. Witeof, P.C. Ng, S.B. Mahon, M. Brenner, G.R. Boss, V.S. Bebarta, Intramuscular sodium tetrathionate as an antidote in a clinically relevant swine model of acute cyanide toxicity, *Clinical Toxicology*, 58 (2020) 29-35.
- [90] V.S. Bebarta, N. Garrett, M. Brenner, S.B. Mahon, J.K. Maddry, S. Boudreau, M. Castaneda, G.R. Boss, Efficacy of intravenous cobinamide versus hydroxocobalamin or saline for treatment of severe hydrogen sulfide toxicity in a swine (*Sus scrofa*) model, *Academic emergency medicine*, 24 (2017) 1088-1098.
- [91] V.S. Bebarta, D.A. Tanen, S. Boudreau, M. Castaneda, L.A. Zarzabal, T. Vargas, G.R. Boss, Intravenous cobinamide versus hydroxocobalamin for acute treatment of severe cyanide poisoning in a swine (*Sus scrofa*) model, *Annals of emergency medicine*, 64 (2014) 612-619.
- [92] A. Chan, J. Jiang, A. Fridman, L.T. Guo, G.D. Shelton, M.-T. Liu, C. Green, K.J. Haushalter, H.H. Patel, J. Lee, Nitrocobinamide, a new cyanide antidote that can be administered by intramuscular injection, *Journal of medicinal chemistry*, 58 (2015) 1750-1759.
- [93] J. Lee, S.B. Mahon, D. Mukai, T. Burney, B.S. Katebian, A. Chan, V.S. Bebarta, D. Yoon, G.R. Boss, M. Brenner, The vitamin B 12 analog cobinamide is an effective antidote for oral cyanide poisoning, *Journal of medical toxicology*, 12 (2016) 370-379.
- [94] P.C. Ng, T.B. Hendry-Hofer, N. Garrett, M. Brenner, S.B. Mahon, J.K. Maddry, P. Haouzi, G.R. Boss, T.F. Gibbons, A.A. Araña, Intramuscular cobinamide versus saline for treatment of severe hydrogen sulfide toxicity in swine, *Clinical Toxicology*, 57 (2019) 189-196.
- [95] P.C. Ng, T.B. Hendry-Hofer, A.E. Witeof, M. Brenner, S.B. Mahon, G.R. Boss, P. Haouzi, V.S. Bebarta, Hydrogen sulfide toxicity: mechanism of action, clinical presentation, and countermeasure development, *Journal of Medical Toxicology*, (2019) 1-8.
- [96] M. Brenner, S.B. Mahon, J. Lee, J.G. Kim, D.S. Mukai, S. Goodman, K.A. Kreuter, R. Ahdout, O. Mohammad, V.S. Sharma, Comparison of cobinamide to hydroxocobalamin in reversing cyanide physiologic effects in rabbits using diffuse optical spectroscopy monitoring, *Journal of biomedical optics*, 15 (2010) 017001.
- [97] J.W. Wassenaar, G.R. Boss, K.L. Christman, Decellularized skeletal muscle as an in vitro model for studying drug-extracellular matrix interactions, *Biomaterials*, 64 (2015) 108-114.
- [98] W. Fan, H. Shen, Y. Xu, Quantification of volatile compounds in Chinese soy sauce aroma type liquor by stir bar sorptive extraction and gas chromatography–mass spectrometry, *Journal of the Science of Food and Agriculture*, 91 (2011) 1187-1198.
- [99] L.D. Lawson, Z.-Y.J. Wang, B.G. Hughes, Identification and HPLC quantitation of the sulfides and dialk(en)yl thiosulfonates in commercial garlic products, *Planta medica*, 57 (1991) 363-370.
- [100] L. Frankenberg, Enzyme therapy in cyanide poisoning: effect of rhodanese and sulfur compounds, *Archives of toxicology*, 45 (1980) 315-323.
- [101] M.g. Iciek, L. Wlodek, Biosynthesis and biological properties of compounds containing highly reactive, reduced sulfane sulfur, *Polish journal of pharmacology*, 53 (2001) 215-226.

- [102] I. Petrikovics, G. Kuzmitcheva, D. Haines, M. Budai, J. Childress, A. Nagy, G. Rockwood, Encapsulated rhodanese with two new sulfur donors in cyanide antagonism, *Toxicology Letters*, 196 (2010) S144.
- [103] I.P. J.D. Downey, B.A. Logue, M. Brenner, G. Boss, S.B. Mahon, M.R. DeFreytas, D.A. Harris, L. Booker, K.A. Basi, A.R. Allen, and G.A. Rockwood, In vivo efficacy and optimization of novel cyanide countermeasures, in: NIH CounterACT 7th Annual Network Research Symposium, Washington, DC, USA, 2013.
- [104] L. Kiss, S. Holmes, C.-E. Chou, X. Dong, J. Ross, D. Brown, B. Mendenhall, V. Coronado, D. De Silva, G.A. Rockwood, Method development for detecting the novel cyanide antidote dimethyl trisulfide from blood and brain, and its interaction with blood, *Journal of Chromatography B*, 1044 (2017) 149-157.
- [105] Validation of Chromatographic Methods, in: C.f.D.E.a.R. (CDER) (Ed.), Reviewer Guidance, 1994, pp. 33.
- [106] V.P. Shah, K.K. Midha, J.W. Findlay, H.M. Hill, J.D. Hulse, I.J. McGilveray, G. McKay, K.J. Miller, R.N. Patnaik, M.L. Powell, Bioanalytical method validation—a revisit with a decade of progress, *Pharmaceutical research*, 17 (2000) 1551-1557.
- [107] G.A. Shabir, Validation of high-performance liquid chromatography methods for pharmaceutical analysis: Understanding the differences and similarities between validation requirements of the US Food and Drug Administration, the US Pharmacopeia and the International Conference on Harmonization, *Journal of chromatography A*, 987 (2003) 57-66.
- [108] B.A. Logue, E. Manandhar, Percent residual accuracy for quantifying goodness-of-fit of linear calibration curves, *Talanta*, 189 (2018) 527-533.
- [109] J. Gant, J. Dolan, L. Snyder, Systematic approach to optimizing resolution in reversed-phase liquid chromatography, with emphasis on the role of temperature, *Journal of Chromatography A*, 185 (1979) 153-177.
- [110] H.A. Schwertner, S. Valtier, V.S. Beberta, Liquid chromatographic mass spectrometric (LC/MS/MS) determination of plasma hydroxocobalamin and cyanocobalamin concentrations after hydroxocobalamin antidote treatment for cyanide poisoning, *Journal of Chromatography B*, 905 (2012) 10-16.
- [111] C. Fernandez, C. Martin, F. Gimenez, R. Farinotti, Clinical pharmacokinetics of zopiclone, *Clinical pharmacokinetics*, 29 (1995) 431-441.
- [112] Reviewer Guidance: Validation of Chromatographic Methods in: C.f.D.E.a.R. (CDER) (Ed.), Washington, 1994.
- [113] R.R. Kalakuntla, K.S. Kumar, Bioanalytical method validation: A quality assurance auditor view point, *Journal of Pharmaceutical Sciences and Research*, 1 (2009) 1-10.
- [114] D. Han, D. Yan, A. Cao, W. Fang, X. Wang, Z. Song, Y. Li, C. Ouyang, M. Guo, Q. Wang, Study on the hydrolysis kinetics of dimethyl disulfide, *Water, Air, & Soil Pollution*, 228 (2017) 234.
- [115] S.M. Schneider, E.N. Roskopf, J.G. Leesch, D.O. Chellemi, C.T. Bull, M. Mazzola, United States Department of Agriculture—Agricultural Research Service research on alternatives to methyl bromide: pre-plant and post-harvest, *Pest Management Science: formerly Pesticide Science*, 59 (2003) 814-826.
- [116] S. Gao, B. Hanson, D. Wang, G. Browne, R. Qin, H. Ajwa, S. Yates, Methods evaluated to minimize emissions from preplant soil fumigation, *California Agriculture*, 65 (2011) 41-46.

- [117] Soil Fumigant Labels - Dimethyl Disulfide (DMDS), in, United States Environmental Protection Agency, epa.gov, 2017.
- [118] G.X. Castillo, M. Ozores-Hampton, P.A.N. Gine, Effects of fluensulfone combined with soil fumigation on root-knot nematodes and fruit yield of drip-irrigated fresh-market tomatoes, *Crop Protection*, 98 (2017) 166-171.
- [119] G. Gilardi, M. Gullino, A. Garibaldi, Soil disinfection with dimethyl disulfide for management of *Fusarium* wilt on lettuce in Italy, *Journal of plant diseases and protection*, 124 (2017) 361-370.
- [120] S.R. Yates, D.J. Ashworth, W. Zheng, Q. Zhang, J. Knuteson, I.J. Van Wessenbeeck, Emissions of 1, 3-dichloropropene and chloropicrin after soil fumigation under field conditions, *Journal of agricultural and food chemistry*, 63 (2015) 5354-5363.
- [121] R. Reiss, J. Griffin, A probabilistic model for acute bystander exposure and risk assessment for soil fumigants, *Atmospheric Environment*, 40 (2006) 3548-3560.
- [122] Regulatory Status of Fumigants, in, EPA, United States Environmental Protection Agency, 2019.
- [123] S. Cohen, Field Fumigation, UCANR Publications.
- [124] H. Ajwa, W. Ntow, R. Qin, S. Gao, Chapter 9. Properties of soil fumigants and their fate in the environment, Hayes' Handbook of Pesticide Toxicology, 3rd ed.; Krieger, R., Ed, (2010) 315-330.
- [125] M. Pesonen, K. Vähäkangas, Chloropicrin-induced toxicity in the respiratory system, *Toxicology Letters*, 323 (2020) 10-18.
- [126] W. Stott, B. Gollapudi, 1, 3-Dichloropropene, in: Hayes' Handbook of Pesticide Toxicology, Elsevier, 2010, pp. 2281-2292.
- [127] P.R. Mulay, P. Cavicchia, S.M. Watkins, A. Tovar-Aguilar, M. Wiese, G.M. Calvert, Acute illness associated with exposure to a new soil fumigant containing dimethyl disulfide—Hillsborough County, Florida, 2014, *Journal of agromedicine*, 21 (2016) 373-379.
- [128] X. Wang, W. Fang, D. Yan, D. Han, B. Huang, Z. Ren, J. Liu, A. Cao, Q. Wang, Effect of films on dimethyl disulfide emissions, vertical distribution in soil and residues remaining after fumigation, *Ecotoxicology and environmental safety*, 163 (2018) 76-83.
- [129] J. Yu, S.M. Sharpe, G.E. Vallad, N.S. Boyd, Pest control with drip-applied dimethyl disulfide and chloropicrin in plastic-mulched tomato (*Solanum lycopersicum* L.), *Pest management science*, (2019).
- [130] M.C. Iliuta, F. Larachi, Solubility of total reduced sulfurs (hydrogen sulfide, methyl mercaptan, dimethyl sulfide, and dimethyl disulfide) in liquids, *Journal of Chemical & Engineering Data*, 52 (2007) 2-19.
- [131] M. Stevens, J. Freeman, Soil persistence of dimethyl disulfide combined with chloropicrin after repeated applications, *Crop Protection*, 98 (2017) 143-148.
- [132] M.A. Gómez-Tenorio, M.J. Zanón, M. de Cara, B. Lupión, J.C. Tello, Efficacy of dimethyl disulfide (DMDS) against *Meloidogyne* sp. and three formae speciales of *Fusarium oxysporum* under controlled conditions, *Crop Protection*, 78 (2015) 263-269.
- [133] N. Asasian, T. Kaghazchi, Comparison of dimethyl disulfide and carbon disulfide in sulfurization of activated carbons for producing mercury adsorbents, *Industrial & engineering chemistry research*, 51 (2012) 12046-12057.
- [134] I.K. Warnakula, A. Ebrahimpour, S.Y. Li, R.D. Gaspe Ralalage, C.C. Hewa-Rahinduwege, M.r. Kiss, C.T. Rios, K.D. Kelley, A.C. Whiteman, D.E. Thompson,

- Evaluation of the Long-Term Storage Stability of the Cyanide Antidote: Dimethyl Trisulfide and Degradation Product Identification, ACS Omega, (2020).
- [135] H. Kim, S. Lee, Y. Chung, C. Lim, I. Yu, S. Park, J. Shin, S. Kim, D. Shin, J. Kim, Evaluation of subchronic inhalation toxicity of dimethyl disulfide in rats, *Inhalation toxicology*, 18 (2006) 395-403.
- [136] P. Xiang, H. Qiang, B. Shen, M. Shen, Screening for volatile sulphur compounds in a fatal accident case, *Forensic sciences research*, 2 (2017) 192-197.
- [137] Reviewer Guidance: Validation of Chromatographic Methods in, Center for Drug Evaluation and Research (CDER), Washington, 1994, pp. 33.
- [138] Dimethyl Disulfide - Fact Sheet, in, United States Environmental Protection Agency US EPA, 2010, pp. 1-25.
- [139] A.B. Nair, S. Jacob, A simple practice guide for dose conversion between animals and human, *Journal of basic and clinical pharmacy*, 7 (2016) 27.
- [140] L. DiPasquale, H. Davis, The acute toxicity of brief exposures to hydrogen fluoride, hydrogen chloride, nitrogen dioxide, and hydrogen cyanide singly and in combination with carbon monoxide, in, Air Force Aerospace Medical Research Lab, Wright-Patterson AFB, OH, 1971.
- [141] J. Taylor, N. Roney, C. Harper, M. Fransen, S. Swarts, Toxicological profile for cyanide, in: Health Effects, Agency for Toxic Substances and Disease Registry, Atlanta, GA, 2006, pp. 322.
- [142] M.J. Ellenhorn, *Ellenhorn's Medical Toxicology: Diagnosis and Treatment of Human Poisoning*, 2nd ed., Williams and Wilkins, Baltimore, MD, 1997.
- [143] M.W. Stutelberg, J.K. Dzisam, A.R. Monteil, I. Petrikovics, G.R. Boss, S.E. Patterson, G.A. Rockwood, B.A. Logue, Simultaneous determination of 3-mercaptopyrivate and cobinamide in plasma by liquid chromatography–tandem mass spectrometry, *Journal of Chromatography B*, 1008 (2016) 181-188.
- [144] S.N. Fedosov, L. Berglund, E. Nexø, T.E. Petersen, Tetrazole derivatives and matrices as novel cobalamin coordinating compounds, *Journal of organometallic chemistry*, 692 (2007) 1234-1242.
- [145] B.A. McCracken, M.K. Brittain, High performance liquid chromatography tandem mass spectrometry assay for the determination of cobinamide in pig plasma, *Journal of Chromatography B*, 1006 (2015) 104-111.
- [146] M10 Bioanalytical Method Validation, in, Food and Drug Administration, Center for Drug Evaluation and Research, 2019, pp. 1-59.
- [147] S.S. Jambhekar, P.J. Breen, *Basic pharmacokinetics*, Pharmaceutical Press London, 2009.